THE SINGLE-PHASE INDUCTION MOTOR

- - - - -

A CRITICAL APPRAISAL OF THE ROTATING-FIELD AND CROSS-FIELD THEORIES WITH PARTICULAR REFERENCE TO SKIN EFFECT

A thesis submitted for the degree of

DOCTOR OF PHILOSOPHY

Supported by the major publication

'ELECTRICAL MACHINE THEORY'

(Morris Jevons, Blackie 1966)

MORRIS JOHN JEVONS

THE UNIVERSITY OF ASTON IN BIRMINGHAM

November 1966

SUMMARY

The purpose of this thesis is twofold: to examine the validity of the rotating-field and cross-field theories of the single-phase induction motor when applied to a cage rotor machine; and to examine the extent to which skin effect is likely to modify the characteristics of a cage rotor machine.

A mathematical analysis is presented for a single-phase induction motor in which the rotor parameters are modified by skin effect. Although this is based on the usual type of ideal machine, a new form of model rotor allows approximations for skin effect phenomena to be included as an integral part of the analysis. Performance equations appropriate to the rotating-field and cross-field theories are deduced, and the corresponding explanations for the steady-state mode of operation are critically examined. The evaluation of the winding currents and developed torque is simplified by the introduction of new dimensionless factors which are functions of the resistance/reactance ratios of the rotor and the speed. Tables of the factors are included for selected numerical values of the parameter ratios, and these are used to deduce typical operating characteristics for both cage and wound rotor machines.

It is shown that a qualitative explanation of the mode of operation of a cage rotor machine is obtained from either theory; but the operating characteristics must be deduced from the performance equations of the rotating-field theory, because of the restrictions on the values of the rotor parameters imposed by skin effect.

CONTENTS

CHAPTER I

THE SINGLE-PHASE INDUCTION MOTOR

CHAPTER I

THE SINGLE-PHASE INDUCTION MOTOR

1.1 General and Historical Note

In a conclusion to a paper on the theory of asynchronous motors in 1896, Heyland stated [1] *

> 'The characteristic of a monophase motor is identical with the characteristic of a polyphase motor with approximately twice the magnetizing current, twice the stray coefficient, and half the short-circuit resistance.' .

The monophase motor referred to is the familiar single-phase induction motor - an a.c. smooth air-gap rotating electrical machine having a single-phase distributed stator winding connected to a supply, and a distributed balanced short-circuited rotor winding in the form of either an actual winding similar to that of the stator or a squirrel cage. Although the principle of the machine was known to Ferraris, as a result of the experiments on rotating magnetic fields which produced the polyphase induction motor in 1888, the development of a practical machine was hampered by the absence of an inherent starting

---

* references shown ( ) are listed at the end of the thesis

---

torque [2], and the single-phase induction motor was commonly understood to be a polyphase motor operated with one stator phase winding open-circuited. As a result the performance was inferior to that of a polyphase motor of comparable rating.

The development of satisfactory methods of starting [3] brought a growing market in small industrial and domestic drives for which, notwithstanding the limitations in performance, the single-phase induction motor was ideally suited [4]. Modified polyphase machines were economically unsuited for these applications and new designs were formulated specifically for single-phase induction motors [5]. Operating experience with the new machines enabled empirical corrections to be introduced, and the improved design procedures [6] resulted in a much closer correlation between theory and practice. However some of these corrections were unnecessary, being indicative of an incomplete appreciation of the operating principles and a too rigid adherence to the rotating-field theory of the polyphase machine. In fact this practice encouraged many erronious ideas, as the following examples show:

(a) In 1897 Behrend demonstrated that the steady-state characteristic of the single-phase induction motor could be synthesized from the characteristics of two suitably connected

polyphase machines [7]. Although he argued correctly that the stator windings of the two machines must be connected in series, the reasons were not regarded as obvious by his contemporaries [8]. His suggestion that the demonstration directly verified the rotating-field theory was incorrect however, because the correlation was between the characteristics and this could be interpreted as a verification of any qualitative theory. For example, it applies equally to the cross-field theory (EMT, 185) * .

(b) In a hypothetical polyphase machine exhibiting only rotor copper-loss the per-unit efficiency is equal to S . By extension, the qualitative use of the rotating-field theory [9] for an ideal single-phase induction motor gives the efficiency as S^2 - i.e., if the full-load speed is 0.96, then the full-load efficiency cannot be greater than 92% . But the rotor copper-loss is not simply related to the shaft torque [10], and the limiting value of the efficiency is more likely to be 86% . With a cage rotor, 78% would be a better figure because skin effect in the bars cannot be ignored.

---

* the notation (EMT, 185) refers to page 185 of the book 'Electrical Machine Theory', Blackie 1966 by Morris Jevons

A basic tenet of the polyphase motor theory was that a rotating magnetic field was necessary for the operation of an a. c. machine with induction coupling between the stator and rotor windings. The adaptation of this principle to the single-phase induction motor, in a form which enabled the operating characteristics to be explained, gave rise to alternative theories.

(a) The rotating-field theory, in which the alternating magnetic flux set up by the stator winding was replaced by two contra-rotating 'fluxes' of constant amplitude. It was assumed that each flux acted separately, and that the single-phase machine could be likened to two coupled polyphase machines. In this way the zero starting torque and twin-frequency rotor current were simply explained.

(b) The cross-field theory, in which a rotating magnetic flux was assumed to result from the alternating stator/rotor flux along the axis of the stator winding and a 'speed dependent' flux along an axis at right angles. This provided a satisfactory explanation for the zero starting torque, but not (directly) for the twin-frequency rotor current.

Other theories have been forthcoming [11], but these are merely variants of the rotating-field and cross-field theories, which have remained the principal descriptions of the mode of

operation up to the present day.

Although the original theories of the single-phase induction motor have not been superseded, the same cannot be said for the approach to machine analysis in general. At the turn of the century, any new machine was analysed by first developing a physical description of the operation, consistent with observed phenomena, and then using this to decide the simplifying assumptions to be introduced in a mathematical theory. In particular with the single-phase induction motor, two analyses were developed corresponding to the alternative descriptions and the impression was given that the two sets of predicted characteristics were not necessarily the same. In fact many articles have been written on the equivalence of the characteristics, even though any other conclusion would be surprising with linear analyses [12].

At the present time an alternative approach to machine analysis is available, based on the experimental and analytic experience of more than half a century. The fundamental experimental laws which govern the operation of all types of electrical machine have been established, and it has been amply verified that, in theory at least, the performance equations can be derived from a single dynamical equation [13]. The machine to

be analysed is examined, and the importance of the various features gauged by comparison with machines of a similar type. Simplifying assumptions are then introduced to make the analysis tractable. The physical description of the mode of operation is based on the resulting performance equations, instead of the other way around, and it is frequently possible to use this as a qualitative check on the validity of the analysis and of the initial assumptions. Kron [14] has further standardized the analysis of rotating electrical machines with the introduction of a 'unified theory'. This enables the performance equations to be simply determined if, as in the case of the single-phase induction motor, the machine to be analysed can be compared with the Kron 'primitive machine'. Actually the basic equations of the unified theory may be developed by reference to a machine with a layout identical to that of an ideal single-phase induction motor (EMT, 39).

1.2 Outline of this thesis

The assumptions implicit in the use of the unified theory (EMT, 6) are intended to simplify the analysis without obscuring the fundamental principles of operation, and the performance equations so obtained refer to an ideal version of the actual machine. In this thesis, a new and significant improvement on the

Kron unified theory is the use of a more fundamental type of primitive machine, which is suggested by the analysis of the rotor current waveforms in the single-phase induction motor. The rotor in the Kron machine is replaced by a hypothetical slip-ring rotor with two, magnetically separate, frequency selective, balanced two-phase windings. This is introduced so that lumped-circuit approximations for the skin effect phenomenon in the rotor can be included as an integral part of the analysis, instead of being treated as a secondary effect.

1.2.1 Mathematical analysis

A mathematical analysis is given in Chapter II for the single-phase induction motor based on the modified form of primitive machine. Expressions are deduced for the energy stored in the magnetic fields and dissipated in copper-losses, in terms of the winding parameters and currents. These energy functions are then used with the Lagrange dynamical equation to obtain the performance equations. Although there are 4 rotor currents, corresponding to the separate frequency components of each winding, experimental evidence is used to show that only 2 of these are distinct, and that a definite relationship must exist between rotor currents of the same frequency in this machine.

The inductance coefficients in the performance equations are functions of the angular position of the rotor, because holonomic reference axes are used in the derivation. A transformation to stationary axes removes the angular dependent factors and the equations are further simplified to apply to steady-state conditions. The frequencies of the separate rotor variables are then equal to that of the supply. Advantage is taken of the relationship between the pairs of rotor currents to define new rotor variables; this results in a set of performance equations appropriate to the rotating-field theory and an alternative set in terms of the cross-field variables. The two sets of variables are related by a power-invariant transformation and the characteristics predicted by the use of either set of performance equations are necessarily equivalent. However the coefficients of the second set are not the same as those of the classical cross-field theory, because of the changes in the rotor parameters attributed to skin effect. Hence the characteristics predicted from the classical theories are not equivalent when skin effect is included in the analysis. An indication of the extent of the discrepancy is given in Chapter V.

It is shown in Chapter II that when skin effect is neglected, and the rotor parameters are assumed equal, there is

no difference between the performance equations of the present approach and those of the classical theories. The use of the Lagrange equation is unnecessary and the Kron unified theory can be used to write down the equations of the cross-field theory. A simple transformation then gives the equations of the rotating-field theory, and although these are identical in form with the equations in which skin effect is included, the use of different primitive machines precludes any equivalence of the physical interpretations.

1.2.2 Interpretation of the performance equations

When the principal theories were first developed, the physical descriptions of the operation preceded the derivation of the performance equations, but in the present thesis it is more satisfactory to reverse that approach. Hence performance equations appropriate to the principal theories are first deduced, and are then the subject of separate physical interpretations - Chapters III, IV. The scheme adopted in these middle chapters is to associate explanations with terms in the mathematical equations instead of with an actual machine. Inevitably the discussion of such topics as induced e.m.f., flux, or developed torque, tends to be philosophical because of the abstract concepts

involved, and the present day descriptions have been evolved rather than simply deduced: e.g., the original Ferraris' theory [15] referred to rotating magnetic flux waves, but Thomälen subsequently replaced these by rotating m.m.f. waves [16]. These descriptions of the mode of operation are critically examined and explanations are suggested, compatible with the performance equations, for the induced e.m.f.'s in the windings and the shaft torque. In addition, equivalent circuits are deduced and phasor diagrams drawn for both the rotating-field and cross-field theories. Although an attempt is made to 'parallel' the development of the theory in each chapter, a departure is evident with the phasor diagrams. In the rotating-field theory, the operation of the machine is related to an equivalent circuit and then a phasor diagram is drawn for this circuit; while in the cross-field theory, the phasor diagram is developed qualitatively from the physical explanations, and the equivalent circuit is deduced separately from the performance equations.

The evaluation of the winding currents and the developed torque is simplified by the introduction of a new set of dimensionless factors - ξ functions. These are functions of the resistance/reactance ratios of the rotor and the per-unit speed, and are particularly useful in simplifying the derivation of the

operating characteristics. Separate functions are defined for the two theories, but these become simply related when skin effect is neglected. Graphs are included in the text, while tables and graphical constructions are given in an appendix, to illustrate the variations of these functions over the speed range $0 \leqslant S \leqslant 1$ for several values of the resistance/reactance ratio.

1.2.3 Harmony of the two theories

Although an allowance for skin effect is included in the mathematical analysis, the phenomenon cannot be explained by the resulting theories: the rotating-field theory provides an explanation of why twin-frequency currents exist in the rotor, but not why the rotor parameters are frequency dependent; while the cross-field theory is based on the overall behaviour of the rotor referred to stationary axes, and the existence of a twin-frequency in the rotor current is masked. Apart from queries relating to the qualitative treatment of the rotor, the alternative descriptions of the mode of operation must be assumed equally valid, for these are consistent with the experimental laws and there is no way of knowing whether one is more 'correct' than the other, or if neither is correct. The extent to which these descriptions are complementary is discussed in the final chapter

and a harmony is shown to exist when they are associated with an actual machine instead of with the mathematical equations (as in Chapters III, IV) .

Graphical constructions are given to illustrate that either theory may be used to derive a locus for the resultant m.m.f. vector in the air-gap, and it is shown that in the single-phase induction motor, unlike the two-phase machine, the appearance of the magnetic field depends upon the choice of reference axis. When viewed from the stator the locus is an ellipse, but with a change of reference axis to the rotor the locus becomes a retrograde epicycle. The variations in the amplitude and angular velocity of the m.m.f. vector are used to explain similar variations which are observed in the shaft torque and speed. An examination is made of the magnetic field at a typical point near to the surface of a hypothetical smooth rotor, and it is shown that the B/H hysteresis loop for the point must include a number of recoil loops so that, even in an ideal machine, the rotor hysteresis loss would not be simply related to the area of the B/H loop.

Modifications are made to the equivalent circuits to enable approximate allowances to be made for core losses in the performance calculations, but it is suggested that a physical interpretation of these changes should not be included in a

description of the mode of operation of the machine. Unlike skin effect, core loss cannot be used as an argument to favour one or other of the principal theories, because it is a functional non-linearity and the principle of superposition is not valid. Hence the loss should be calculated from the total value of the m.m.f. acting in the various parts of the machine, and it is fortuitous if loss calculations based on one theory, rather than the other, give a closer correlation with practice [17].

An expression for the input current to the stator winding is derived from the performance equations, and the effect of varying the rotor resistance/reactance ratio on the current/speed characteristic is illustrated. It is shown that the locus of the current vector for variable speed is a quartic curve, but that this reduces to a circle for certain approximations for skin effect and when skin effect is neglected. There is a close similarity in the form of the loci, which can be misleading as the locations of corresponding points are quite different.

The curves of the stator current and the ξ functions are used to deduce the torque/speed characteristic of the machine, and the effect of varying the rotor parameter ratios is illustrated. Some of the differences with the corresponding two-phase characteristic are discussed:- e.g., in the single-phase

induction motor the value of the rotor resistance affects the no-load speed and the value of the maximum torque. The extent to which the characteristic is modified by skin effect is examined, and it is shown that although this slightly reduces the magnitude of the developed torque, the form of the curve is unaltered. However, skin effect has a more noticeable effect on the rotor copper-loss/rotor output ratio so that the theoretical value of the maximum efficiency is considerably reduced.

1.3 Skin effect

The extent to which skin effect modifies the performance of the single-phase induction motor is the cardinal theme in this thesis. It is shown that if skin effect is included in the analysis then the mode of operation can only be correctly described by the rotating-field theory, but it must first be shown that the changes in the parameters warrant the inclusion of the phenomenon as an integral part of the analysis.

The component frequencies in the waveform of the e.m.f. induced in the rotor at a speed S , are (1-S) and (1+S) times that of the supply, and the latter value is high enough for eddy current effects in the rotor bars to cause a noticeable distortion of the current density. This is further modified by other operating

conditions: e.g., proximity effect of the iron, and non-uniform current density in the end rings. As there is no simple expression for the current density distribution [18], since this is a function of the operating variables and the geometry of the machine, some approximations must be introduced to make the analysis tractable. In this thesis, therefore, it is assumed that the effective values of the rotor parameters are dependent on the frequency of the rotor current but independent of the magnitude.

In the analysis, the cage rotor is replaced by a two-phase double-wound rotor and an approximation for skin effect is introduced by changing the parameters of one winding. Some idea of the order of these parameter changes is obtained from a simplified field theory analysis [19] (Appendix I).

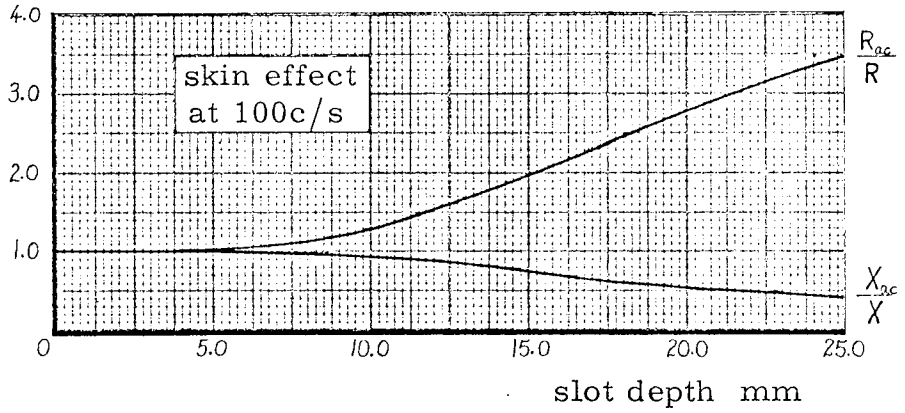

Fig. 1.1

The results, for copper bars of various depths, are illustrated in Fig. 1.1 . It is seen that for a slot depth of 10-15mm the backward

resistance at 100c/s is about 50% greater than the d.c. value. The corresponding values for aluminium bars are slightly less because of the increased resistivity of the aluminium. The graph also shows that the referred value of the cross-slot leakage reactance is reduced for the same conditions. In practice, however, this is likely to be masked by variations in the mutual reactance and by saturation effects.

Even though accurate values are not available, the general effect of the changes in the parameters can be gauged by the use of suitable approximations based on the above illustration. Two examples, which are limited to changes in the value of the 'backward' resistance, are used in the text:

(i) the backward resistance is equal to twice the d.c. value over the normal working range, and

(ii) the backward resistance is equal to (1+S) times the d.c. value.

In the second case the variation over the normal working range is small, but the performance equations are simplified as the referred value of the backward resistance is then independent of speed.

It is shown in the thesis, that if the parameters of a machine are actually modified to the extent suggested by these approximations, then skin effect must be included as an integral part of the analysis and cannot be regarded as a secondary phenomenon.

CHAPTER II

MATHEMATICAL ANALYSIS

CHAPTER II

MATHEMATICAL ANALYSIS

2.1 Chapter outline

A mathematical theory of the single-phase induction motor is presented in this chapter. The analysis is made tractable by defining an ideal version of the machine, having a simplified construction, but governed by the same experimental laws. The simplifications are justified because the resulting electrical and mechanical performance equations can be used to explain observed phenomena, and predicted characteristics are in reasonable agreement with those obtained in practice. An important feature of the present approach is the approximate allowance made at the outset for skin effect phenomena and retained throughout the analysis. The usual method is to regard skin effect as a secondary effect to be allowed for in the performance calculations.

Energy functions are formed from the lumped circuit parameters and the winding currents of the ideal machine, and then used with the Lagrange dynamical equation to deduce the performance equations. These are simplified by referring the rotor quantities to quasi-stationary axes, and modified to apply to steady-state conditions. A change of rotor variables leads to the

performance equations of the rotating-field theory, while an alternative change of variables results in a second set of performance equations. If the changes in the values of the rotor parameters attributed to skin effect are neglected, then this second set is identified with the cross-field theory. The various forms of the performance equations are discussed in detail in subsequent chapters.

It is shown that the operation of a wound rotor machine (in which skin effect is negligible) may be described by either the rotating-field or the cross-field theory, because the dependent variables of the two theories are related by a power-invariant transformation and the performance equations are equivalent. However, the cross-field theory cannot be used with a cage rotor machine, because there is no allowance for skin effect in the coefficients of the performance equations.

2.2 The ideal machine

The performance characteristics deduced from the analysis are those of an 'ideal' single-phase induction motor - i.e.,

> '.. a hypothetical model suitable for mathematical analysis and yet a fair representation of the practical machine.'
>
> (EMT, 7)

Its essential features are listed below.

(1) The stator is wound for two poles. If the rotor is wound this also has two poles.

(2) The variation of the air-gap permeance caused by stator and rotor teeth in relative motion is neglected, and the air-gap is assumed 'smooth'.

(3) The m.m.f.'s produced by the stator and rotor windings are sinusoidally distributed around the periphery of the air-gap. There is no variation in the axial direction due to the finite termination of the winding in the overhang.

(4) Straight slots are used on both the stator and rotor.

(5) There is a single winding (1d) on the stator connected to a sinusoidal constant voltage, constant frequency, source. The magnetic axis of the winding is coincident with the d axis.

(6) For the moment, it is assumed that there are two identical short-circuited rotor windings (2a, 2b) with axes in line with the a and b rotor axes respectively. Normally a cage rotor is used in the actual machine, and this is theoretically equivalent to an N-phase rotor with short-chorded windings, where N is equal to half the number of rotor bars. Since these hypothetical phase windings are balanced and short-circuited they may be replaced by an equivalent two-phase winding, which dissipates the same power and develops the

same fundamental components of m.m.f. .

(7) The equivalent turns-ratio between the stator and rotor windings is unity.

(8) The principle of superposition is valid - i.e., saturation, hysteresis, and other functional non-linearities, are not included in the analysis. The one exception is the skin effect phenomenon in the rotor bars.

(9) Iron losses are omitted.

****

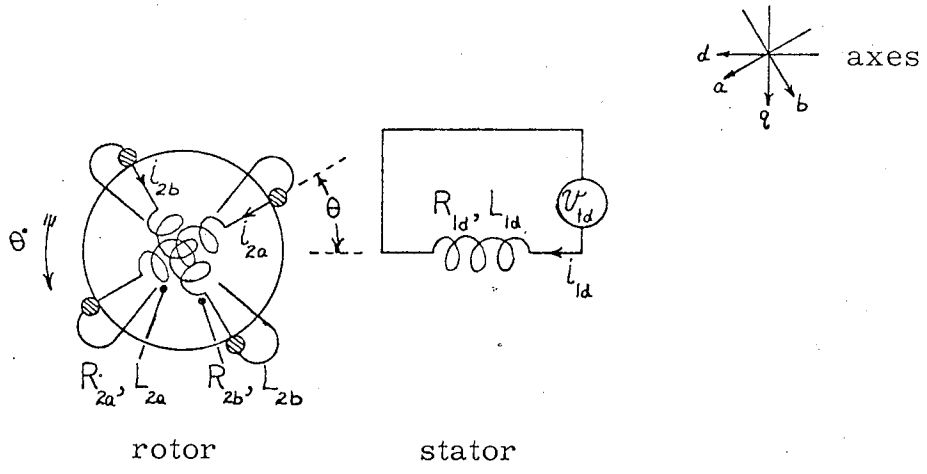

Fig. 2.1

The schematic layout of the ideal machine is illustrated in Fig. 2.1 . The subscripts refer to the three windings, and the applied voltages and currents are instantaneous values.

The sign convention adopted in the thesis is defined in reference (EMT, 5) .

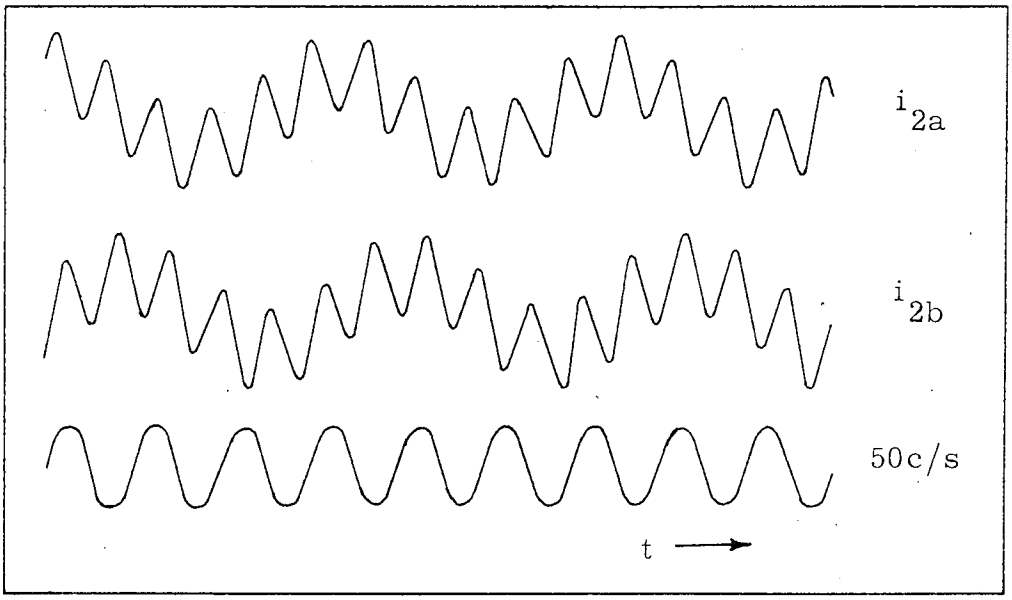

Fig. 2.2 The rotor current waveforms (S≃0.69)

2.2.1 The modified rotor

Experimental evidence (Fig. 2.2, above) shows that there are two dominant frequencies in the waveform of the rotor current:- (1-S)f, and (1+S)f. Therefore the rotor currents i_{2a} and i_{2b} may be expressed as the sum of two component currents of different frequencies

$$\begin{bmatrix} i_{2a} \\ i_{2b} \end{bmatrix} = \begin{array}{|c|c|c|c|} \hline i_{2af} & i_{2bf} & i_{2ab} & i_{2bb} \\ \hline 1 & & 1 & \\ \hline & 1 & & 1 \\ \hline \end{array} \qquad (2.1)$$

Now it is shown in section 1.3 that although the circuit parameters associated with the bars of a cage rotor are dependent on the operating conditions, restrictions have to be imposed on the type of non-linearity considered. Hence it is assumed that values of the parameters (i.e., R, L) are functions of frequency but are independent of the winding currents. This means that the action of the component currents (equation (2.1)) can be considered separately in the definition of the energy stored or dissipated in the rotor, e.g., the copper-loss for the 2a phase-winding is

$$W_{cu} = i_{2af}^2 R_{2af} + i_{2ab}^2 R_{2ab} \qquad (2.2)$$

The approximate replacement of a cage rotor by a wound rotor is described in section 2.2 (6). However the use of this rotor does not allow skin effect to be included as an integral part of the analysis, because the two-phase winding cannot exhibit the two distinct sets of parameters required by equation (2.2). This difficulty is overcome by the definition of a new type of double-wound model rotor having two separate winding layers, each layer comprising two identical short-circuited windings with axes in line with the a and b rotor axes respectively. It is implicit in the definition of the new rotor that

there is no magnetic coupling between the windings of the two layers because these are 'frequency selective', but that the magnetic coupling between the stator winding and the separate rotor phase windings in each layer is the same. Hence the circuit parameters of the two layers may be different and equation (2.2) can be realised.

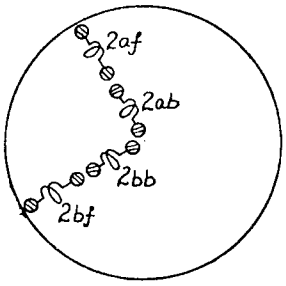

A schematic layout of the windings of the modified rotor is shown in the diagram above. Further subscripts f, b are added to the parameter symbols to distinguish between the two layers; f is associated with the low frequency component of the rotor current, while b is associated with the high frequency component.

The performance of the modified ideal machine is considered in the next section. The introductory transient analysis is not directly applicable to the single-phase machine because the substitution discussed above has been limited to steady-state conditions.

2.3 The performance equations of the ideal machine

2.3.1 The Lagrange equation

The performance of the ideal machine is described by the Lagrange equation

$$\frac{d}{dt}\left[\frac{\partial}{\partial \dot{i}_\rho}[\mathcal{L}]\right] - \left[\frac{\partial}{\partial q_\rho}[\mathcal{L}]\right] + \left[\frac{\partial}{\partial \dot{i}_\rho}[\mathcal{Y}]\right] = [f_\rho] \qquad (2.3)$$

.. where q, $\dot{i}$ are the generalized coordinates and velocities respectively, and ρ assumes as many values as there are degrees of freedom [1].

(i) The Lagrange function ($\mathcal{L}$) is the sum of the energy stored in the magnetic fields and the inertia of the rotor

$$[\mathcal{L}] = \tfrac{1}{2}\begin{bmatrix} i_{1d} & i_{2af} & i_{2bf} & i_{2ab} & i_{2bb} & \dot{\theta} \end{bmatrix}$$

i_{1d}	i_{2af}	i_{2bf}	i_{2ab}	i_{2bb}	$\dot{\theta}$
L_{1d}	$M_d\cos\theta$	$-M_d\sin\theta$	$M_d\cos\theta$	$-M_d\sin\theta$	
$M_d\cos\theta$	L_{2af}				
$-M_d\sin\theta$		L_{2bf}			
$M_d\cos\theta$			L_{2ab}		
$-M_d\sin\theta$				L_{2bb}	
					J

(2.4)

(ii) The Rayleigh dissipative function ($\mathcal{Y}$) is equal to one half the sum of the power losses in the winding resistances and the mechanical losses

$$\left[\mathcal{Y}\right] = \frac{1}{2}\begin{bmatrix} i_{1d} & i_{2af} & i_{2bf} & i_{2ab} & i_{2bb} & \dot{\theta} \end{bmatrix} \begin{array}{|c|c|c|c|c|c|} \hline R_{1d} & & & & & \\ \hline & R_{2af} & & & & \\ \hline & & R_{2bf} & & & \\ \hline & & & R_{2ab} & & \\ \hline & & & & R_{2bb} & \\ \hline & & & & & A \\ \hline \end{array} \begin{array}{c} i_{1d} \\ i_{2af} \\ i_{2bf} \\ i_{2ab} \\ i_{2bb} \\ \dot{\theta} \end{array} \tag{2.5}$$

(iii) The forcing function (f_ρ) is a column matrix formed from the electrical applied voltages and the mechanical applied torques, and is defined by

$$\left[f_\rho\right] = \left\{ v_{1d} \; 0 \; 0 \; 0 \; 0 \; -T_L \right\} \tag{2.6}$$

The performance equations for the machine are obtained by substituting equations (2.4), (2.5), (2.6) into equation (2.3) and putting (ρ) equal to 1d, 2af, 2bf, 2ab, 2bb, and θ.

The resulting performance equations are

$$\begin{bmatrix} v_{1d} \\ \\ \\ \\ \\ \end{bmatrix} = \begin{array}{c|ccccc} & i_{1d} & i_{2af} & i_{2bf} & i_{2ab} & i_{2bb} \\ \hline & R_{1d}+pL_{1d} & pM_d\cos\theta & -pM_d\sin\theta & pM_d\cos\theta & -pM_d\sin\theta \\ & pM_d\cos\theta & R_{2f}+pL_{2f} & & & \\ & -pM_d\sin\theta & & R_{2f}+pL_{2f} & & \\ & pM_d\cos\theta & & & R_{2b}+pL_{2b} & \\ & -pM_d\sin\theta & & & & R_{2b}+pL_{2b} \end{array} \qquad (2.7a)$$

$$-T_L = (A+pJ)\dot{\theta} + i_{1d}\left[(i_{2af}+i_{2ab})\sin\theta + (i_{2bf}+i_{2bb})\cos\theta\right]M_d \qquad (2.7b)$$

.. where it is assumed that $R_{2af} = R_{2bf} = R_{2f}$, $R_{2ab} = R_{2bb} = R_{2b}$,

and similarly $L_{2af} = L_{2bf} = L_{2f}$, $L_{2ab} = L_{2bb} = L_{2b}$.

Except for the additional rotor axes, these equations are identical in form to those of the simple three-winding machine illustrated in Fig. 2.1 (EMT, 41, 42).

2.3.1.1 The phase relations between the rotor currents

Experimental evidence suggests that if an ideal machine could be tested, there would be currents of line frequency only flowing in the stator windings. This enables the phase relations between the pairs of currents i_{2af}, i_{2ab} and i_{2bf}, i_{2bb} to be defined from equation (2.7a) because each row of this equation must be dimensionally correct with respect to frequency. The

actual rotor frequencies are (1-S)f and (1+S)f and the angular dependent terms in the impedance matrix represent the change in frequency of the currents as the 'air-gap' is crossed. To be consistent with the experimental evidence, the rotor currents must appear to be of line frequency only when referred across the air-gap to the stator. This is only possible if

$$i_{2bf} = -j\, i_{2af} \quad , \text{ and } \qquad i_{2bb} = j\, i_{2ab} \qquad (2.8)$$

- relationships which are confirmed experimentally (Fig. 2.2).

Initially it was assumed that the pairs of component currents in the rotor windings (defined by equation (2.1)) were unrelated, but if equations (2.1) and (2.8) are combined

$$\begin{bmatrix} i_{2a} \\ i_{2b} \end{bmatrix} = \begin{array}{c|cc} & i_{2af} & i_{2ab} \\ \hline & 1 & 1 \\ & -j & j \end{array} \qquad (2.9)$$

The currents i_{2a}, i_{2b} and i_{2af}, i_{2ab} are related by a connection matrix which is identical in form with the two-phase symmetrical-component transformation matrix [2]. However equation (2.9) is not part of a power-invariant transformation and it simply defines

---

* The notation here applies to the concept of rotating current vectors being used to define the instantaneous value.

---

an experimental relation between the variables. It would not be strictly correct to compare the component currents with sequence currents, because the frequencies of i_{2af} and i_{2ab} are not the same. Nevertheless some licence is permissible, since the two frequencies are the same with respect to stationary axes.

2.3.2 The transformation to stationary axes

The transcendental factors in equations (2.7a, b) are removed by a change of rotor variables, defined in the power-invariant transformation

$$\begin{bmatrix} i_{1d} \\ i_{2af} \\ i_{2bf} \\ i_{2ab} \\ i_{2bb} \end{bmatrix} = \begin{array}{|c|c|c|c|c|} \hline i_{1d} & i_{2df} & i_{2qf} & i_{2db} & i_{2qb} \\ \hline 1 & & & & \\ \hline & \cos\theta & \sin\theta & & \\ \hline & -\sin\theta & \cos\theta & & \\ \hline & & & \cos\theta & \sin\theta \\ \hline & & & -\sin\theta & \cos\theta \\ \hline \end{array} \qquad (2.10)$$

which in effect refers the rotor quantities to stationary reference axes. A physical interpretation of these rotor variables is included in subsequent chapters.

The modified forms of the performance equations are

$$\begin{bmatrix} v_{1d} \\ \\ \\ \\ \end{bmatrix} = \begin{array}{|c|c|c|c|c|} \hline i_{1d} & i_{2df} & i_{2qf} & i_{2db} & i_{2qb} \\ \hline R_{1d}+pL_{1d} & pM_d & & pM_d & \\ \hline pM_d & R_{2f}+pL_{2f} & L_{2f}\dot{\theta} & & \\ \hline -M_d\dot{\theta} & -L_{2f}\dot{\theta} & R_{2f}+pL_{2f} & & \\ \hline pM_d & & & R_{2b}+pL_{2b} & L_{2b}\dot{\theta} \\ \hline -M_d\dot{\theta} & & & -L_{2b}\dot{\theta} & R_{2b}+pL_{2b} \\ \hline \end{array} \qquad (2.11a)$$

$$-T_L = (A + pJ)\dot{\theta} + i_{1d}\,(i_{2qf} + i_{2qb})\,M_d \qquad (2.11b)$$

Although the mathematical description of the performance is simplified, rotor speed is introduced explicitly into the equations; in the general type of problem this is a variable and the solution of equations (2.11a, b) presents some difficulty. However as only steady-state conditions are considered in this thesis†, the performance equations are treated as a non-linear simultaneous set of ordinary equations and the currents (r.m.s. values) are evaluated in terms of the fixed winding parameters and the speed.

---

† The foregoing transient analysis applies to an ideal machine with a modified double-layer rotor. In the subsequent steady-state analysis the ideal machine is identified with the single-phase induction motor as a result of the development of section 2.2.1 which is based on the steady-state rotor current waveforms of Fig. 2.2 .

The steady-state performance equations are

$$\begin{bmatrix} V_{1d} \\ \\ \\ \\ \end{bmatrix} = \begin{array}{|c|c|c|c|c|} \hline I_{1d} & I_{2df} & I_{2qf} & I_{2db} & I_{2qb} \\ \hline R_{1d}+jX_{1d} & jX_d & & jX_d & \\ \hline jX_d & R_{2f}+jX_{2f} & SX_{2f} & & \\ \hline -SX_d & -SX_{2f} & R_{2f}+jX_{2f} & & \\ \hline jX_d & & & R_{2b}+jX_{2b} & SX_{2b} \\ \hline -SX_d & & & -SX_{2b} & R_{2b}+jX_{2b} \\ \hline \end{array} \qquad (2.12a)$$

$$-T_L = A\dot{\theta} - T_E \quad , \qquad T_E = -Re\,\frac{1}{\omega} I_{1d}\left(I^*_{2qf}+I^*_{2qb}\right)X_d \qquad (2.12b)$$

.. where T_E is the mean value of the developed torque.

2.3.2.1 The phase relations between the rotor currents

In section 2.3.1.1 it is shown that definite phase relations exist between the pairs of rotor currents i_{2af}, i_{2ab} and i_{2bf}, i_{2bb}. Using equation (2.8) with the transformation equation (2.10), it follows that the same relations must exist between the new rotor currents, i.e.,

$$i_{2qf} = -j\,i_{2df} \quad , \qquad \text{and} \qquad i_{2qb} = j\,i_{2db} \qquad (2.13a)$$

In terms of r.m.s. values these become

$$I_{2qf} = -j\,I_{2df} \quad , \qquad \text{and} \qquad I_{2qb} = j\,I_{2db} \qquad (2.13b)$$

These relations are used to effect further simplifications in the

performance equations.

2.4 The performance equations of the rotating-field theory

The fixed relations which exist between the pairs of rotor currents make it unnecessary to express the performance in terms of all of the rotor currents. Therefore two rotor axes are eliminated and the order of the performance equations is reduced by using equation (2.13b) as the basis for a power-invariant transformation

$$\begin{bmatrix} V_{2d}^{f} \\ V_{2d}^{b} \end{bmatrix} = \frac{1}{2} \begin{array}{|cccc|} \multicolumn{4}{c}{\overbrace{}} \\ V_{2df} & V_{2qf} & V_{2db} & V_{2qb} \\ \hline 1 & j & & \\ & & 1 & -j \\ \hline \end{array} \quad \text{and} \quad \begin{bmatrix} I_{2df} \\ I_{2qf} \\ I_{2db} \\ I_{2qb} \end{bmatrix} = \frac{1}{2} \begin{array}{|cc|} \multicolumn{2}{c}{\overbrace{}} \\ I_{2d}^{f} & I_{2d}^{b} \\ \hline 1 & \\ -j & \\ & 1 \\ & j \\ \hline \end{array} \qquad (2.14)$$

New rotor variables are necessary because the interpretation of equation (2.14) is that the performance can be expressed in terms of fewer variables, and not that two of the variables are redundant.

The modified performance equations are

$$\begin{bmatrix} V_{1d} \end{bmatrix} = \frac{1}{2} \begin{array}{|c|c|c|} \hline I_{1d} & I_{2d}^{f} & I_{2d}^{b} \\ \hline 2(R_{1d} + j X_{1d}) & j X_{d} & j X_{d} \\ \hline j(1-S) X_{d} & R_{2f} + j(1-S) X_{2f} & \\ \hline j(1+S) X_{d} & & R_{2b} + j(1+S) X_{2b} \\ \hline \end{array} \qquad (2.15a)$$

$$T_{E} = - Re \frac{1}{2\omega} I_{1d} \left(I_{2d}^{f*} - I_{2d}^{b*} \right) j X_{d} \qquad (2.15b)$$

The electrical performance equation is further simplified by dividing the second and third voltage-balance equations by (1-S) and (1+S) respectively, to obtain a symmetrical impedance matrix.

$$\begin{bmatrix} V_{1d} \end{bmatrix} = \frac{1}{2} \begin{array}{|c|c|c|} \hline I_{1d} & I_{2d}^{f} & I_{2d}^{b} \\ \hline 2(R_{1d} + j X_{1d}) & j X_{d} & j X_{d} \\ \hline j X_{d} & \frac{R_{2f}}{1-S} + j X_{2f} & \\ \hline j X_{d} & & \frac{R_{2b}}{1+S} + j X_{2b} \\ \hline \end{array} \qquad (2.16a)$$

$$T_{E} = - Re \frac{1}{2\omega} I_{1d} \left(I_{2d}^{f*} - I_{2d}^{b*} \right) j X_{d} \qquad (2.16b)$$

Equations (2.10) and (2.14) are used to derive the relations between the actual rotor currents and the variables I_{2d}^{f}, I_{2d}^{b} : reverting to instantaneous values

$$i_{2af} = \frac{1}{2} i_{2d}^{f} \exp(-j\theta), \text{ and } \qquad i_{2ab} = \frac{1}{2} i_{2d}^{b} \exp(j\theta). \qquad (2.17)$$

The description of the mode of operation of the single-phase induction motor in terms of equations (2.15a, b) and (2.16a, b)

is referred to as the rotating-field theory, and is considered in detail in Chapter III. No restriction has been placed on the values of the rotor parameters and, in particular, these may be modified in any manner to approximate for skin effect.

2.5 An alternative form of the performance equations

The currents in equations (2.11a, b) are of line frequency and the rotor variables may be correctly identified with sequence currents. These are artificial in the sense that the change of reference axis implicit in the use of equation (2.10) is devoid of reality in a slip-ring or cage rotor. Nevertheless, it is logical to reverse the 'symmetrical-component process' and examine the use of the hypothetical rotor currents I_{2d}, I_{2q} which are defined from the sequence currents.

Let new rotor variables be defined by

$$I_{2d} = I_{2df} + I_{2db} \qquad I_{2q} = I_{2qf} + I_{2qb} \tag{2.18}$$

Then using equation (2.13b): $I_{2q} = -j I_{2df} + j I_{2db}$

Hence

$$\begin{bmatrix} I_{2df} \\ I_{2qf} \\ I_{2db} \\ I_{2qb} \end{bmatrix} = \frac{1}{2} \begin{array}{|c|c|} \hline I_{2d} & I_{2q} \\ \hline 1 & j \\ \hline -j & 1 \\ \hline 1 & -j \\ \hline j & 1 \\ \hline \end{array} \tag{2.19a}$$

Similarly a voltage relation is defined by

$$\begin{bmatrix} V_{2d} \\ V_{2q} \end{bmatrix} = \frac{1}{2} \begin{array}{|c|c|c|c|} \hline V_{2df} & V_{2qf} & V_{2db} & V_{2qb} \\ \hline 1 & j & 1 & -j \\ \hline -j & 1 & j & 1 \\ \hline \end{array} \qquad (2.19b)$$

Equations (2.19a, b) are used as a power-invariant transformation with equations (2.12a, b) to deduce the performance equations for the machine in terms of the hypothetical rotor currents I_{2d}, I_{2q}.

The modified equations are

$$\begin{bmatrix} V_{1d} \\ \\ \end{bmatrix} = \begin{array}{|c|c|c|} \hline I_{1d} & I_{2d} & I_{2q} \\ \hline R_{1d} + jX_{1d} & jX_d & \\ \hline jX_d & \frac{1}{2}(Z'_{2f} + Z'_{2b}) & \frac{1}{2}j(Z'_{2f} - Z'_{2b}) \\ \hline -SX_d & -\frac{1}{2}j(Z'_{2f} - Z'_{2b}) & \frac{1}{2}(Z'_{2f} + Z'_{2b}) \\ \hline \end{array} \qquad (2.20a)$$

$$T_E = -Re\, \frac{1}{\omega} I_{1d} I^*_{2q} X_d \qquad (2.20b)$$

.. where $Z'_{2f} = R_{2f} + j(1-S)X_{2f}$, $Z'_{2b} = R_{2b} + j(1+S)X_{2b}$.

Equations (2.14) and (2.19a) are used to derive the relation between the variables of the alternative forms of the performance equations (equations (2.15a, b) and (2.20a, b)): i.e.,

$$\begin{bmatrix} I^f_{2d} \\ I^b_{2d} \end{bmatrix} = \begin{array}{|c|c|} \hline I_{2d} & I_{2q} \\ \hline 1 & j \\ \hline 1 & -j \\ \hline \end{array} \qquad (2.21)$$

Although equation (2.21) apparently identifies I_{2d}^{f}, I_{2d}^{b} as the sequence components of I_{2d}, I_{2q}, this interpretation is incorrect. The true sequence components are the winding currents of the model rotor as defined by equation (2.18).

2.5.1 The performance equations of the cross-field theory

The differences in the rotor parameters R_{2f}, L_{2f} and R_{2b}, L_{2b} depend upon the extent to which the corresponding d.c. values are modified by skin effect. If these differences are neglected so that $R_{2f} = R_{2b} = R_2$ and $L_{2f} = L_{2b} = L_2$, then equation (2.20a) reduces to

$$\begin{bmatrix} V_{ld} \\ \\ \end{bmatrix} = \begin{array}{|c|c|c|} \hline I_{ld} & I_{2d} & I_{2q} \\ \hline R_{ld} + j X_{ld} & j X_d & \\ \hline j X_d & R_2 + j X_2 & S X_2 \\ \hline -S X_d & -S X_2 & R_2 + j X_2 \\ \hline \end{array} \qquad (2.22)$$

A symmetrical form of this equation can be obtained by rearranging the rows of the impedance matrix (EMT, 184), but it is simpler to use equation (2.21) with equation (2.16a) and assume the values of the two sets of rotor parameters to be equal, when

$$\begin{bmatrix} V_{1d} \end{bmatrix} = \begin{array}{|c|c|c|} \hline I_{1d} & I_{2d} & -jI_{2q} \\ \hline R_{1d} + jX_{1d} & jX_d & \\ \hline jX_d & \frac{R_2}{1-S^2} + jX_2 & -\frac{SR_2}{1-S^2} \\ \hline & -\frac{SR_2}{1-S^2} & \frac{R_2}{1-S^2} + jX_2 \\ \hline \end{array} \qquad (2.23)$$

Equations (2.22) and (2.23) form the basis of the cross-field theory of the single-phase induction motor; the former equation provides a physical description of the mode of operation, while an equivalent circuit is deduced from the latter equation. The theory is considered in detail in Chapter IV .

2.5.2 The validity of the cross-field theory

The two sets of performance equations (equations (2.16a, b) and (2.20a, b)) form alternative mathematical descriptions of the machine, which are equally valid because the variables are related by a power-invariant transformation. The equations of the rotating-field theory permit a simple physical interpretation while the alternative set do not, otherwise there is little to choose between the equations since both are expressed in terms of rotor variables which do not actually exist.

In the present analysis a distinction is made between the electrical performance equation expressed in terms of the cross-field variables (equation (2.20a)) and the electrical performance equation of the cross-field theory (equation (2.22)). The rotor self-impedance and mutual coupling terms in these equations are different because a double-layer rotor winding is used to allow for skin effect. This is neglected in the transition from equation (2.20a) to equation (2.22) so that the circuit parameters of the two layers become identical and the latter equation applies equally to a machine with either a single- or a double-layer rotor winding. In fact the use of a special rotor is unnecessary and the equations appropriate to the cross-field theory may be derived directly from the equations of the Kron unified theory. It follows that for a cage rotor machine, the characteristics are only correctly predicted from the rotating-field theory as there is no allowance for skin effect in the performance equations of the cross-field theory; therefore the theories are not equivalent.

There is no inherent error in the use of the cross-field theory for the analysis of a wound rotor machine as it is then a valid alternative to the rotating-field theory and, like that theory, the performance equations permit a simple physical interpretation.

To draw attention to the different frequencies present in the rotor current waveform, the equations of the rotating-field theory are derived from those of the cross-field theory by using the relations defined in equation (2.21) [3]. The performance equations are identical in form with the corresponding equations in the text, but the explanations of the rotating-field theory cannot be extended to cover skin effect because the necessary modifications to the circuit parameters have no meaning with a single-layer winding. This difficulty is avoided in the present method because a double-layer winding is used and the modifications for skin effect are included in the initial analysis.

2.5.3 The Atkinson shunt commutator motor

The physical expression of a machine with stationary reference axes on the rotor and a performance described by equation (2.22) is obtained by substituting a commutator rotor for the wound slip-ring rotor of the single-phase induction motor. Two independent brush pairs are positioned on the commutator in the d and q axes respecively, and are short-circuited. This modified machine is an Atkinson shunt-connected commutator motor (EMT, 171).

The qualitative performance of the slip-ring and

commutator machines is the same and there is ample evidence to suggest that the characteristics of two ideal machines would be identical. Although the currents I_{2d}, I_{2q} do not have physical reality in the windings of either machine, the important conclusion drawn from these comparative tests is that the mathematical transformations defined in equation (2.10) can be simulated qualitatively with a commutator rotor. An exact equivalence of the m.m.f.'s in the two machines would require the use of specially shaped brushes, because the windings of the commutator rotor are uniformly distributed.

2.6 Comment

The steady-state operation of the single-phase induction motor may be described by alternative performance equations ((2.15a, b); (2.20b), (2.22)), but it is reasoned that the equations of the rotating-field theory are preferable because the analytic variables are directly related to the actual rotor currents and an allowance can be made for skin effect in the bars of a cage rotor.

If the rotor parameters are assumed equal, then the predicted characteristics resulting from either form of the performance equations must be the same, because of the invariant

nature of the transformation which connects the two equations. This is the principal reason why the operation of the machine may be explained by alternative theories of apparently equal merit. These theories are developed and examined in Chapters III and IV respectively, as physical interpretations of the two performance equations.

CHAPTER III

THE ROTATING-FIELD THEORY

CHAPTER III

THE ROTATING-FIELD THEORY

3.1 Chapter outline

The mode of operation of the single-phase induction motor may be described by alternative theories which stem from the two performance equations (2.15a) and (2.22). The rotating-field theory is associated with the former equation and is the subject of the present chapter.

In this theory the alternating magnetic field of the stator is resolved into two contra-rotating components, which are combined with the rotating magnetic fields of the rotor to form two resultant fields rotating in opposite directions around the 'air-gap'. The qualitative operation of the machine is discussed in terms of the separate action of these rotating fields, so that the characteristics of the two-phase induction motor (which are assumed to be known) may be used to deduce the salient operating features. These include a shunt-type torque/speed characteristic with zero torque at standstill, a no-load speed slightly less than the synchronous value, and a twin-frequency rotor current. It is shown that the retention in the theory of the actual rotating fields

of the rotor, enables the modifications in the operating characteristics due to skin effect to be easily assessed.

An equivalent circuit is deduced from the performance equations to give an added insight into the mode of operation, and also to illustrate the simplifications which are introduced into the performance calculations. The circuit is reduced to a simple series network by the elimination of the 'rotor' mesh currents, and the modified parameters are expressed in terms of speed dependent ξ functions. The variation of these functions with speed is examined and curves are included for several values of the rotor resistance/reactance ratios.

Approximations are introduced to allow for skin effect in the rotor bars and numerical values are used to examine the extent to which the rotor currents might be modified in practice. It is shown that quite large changes in the rotor resistance (due to skin effect) produce only relatively small changes in the values of the currents. Complete performance calculations are given in Appendix III.

3.2 The induced e.m.f.'s in the rotor

The instantaneous values of the induced e.m.f.'s in the open-circuited rotor windings are equal to the rates of change of

the flux-linkages between the stator and rotor windings. In the notation of equation (2.7a) these are expressed

$$e_{2a} = -p\, i_{1d} M_d \cos\theta \qquad e_{2b} = p\, i_{1d} M_d \sin\theta \tag{3.1}$$

If the stator current has the form $\hat{I}_{1d}\cos(\omega t + \phi_1)$, and the angular position of the rotor is given by $(\omega S t + \phi)$, then the e.m.f.'s are evaluated as

$$e_{2a} = -\tfrac{1}{2} p \hat{I}_{1d} M_d \left\{ \cos[(1-S)\omega t + \phi_1 - \phi] + \cos[(1+S)\omega t + \phi_1 + \phi] \right\} \tag{3.1a}$$

$$= -\tfrac{1}{2} j \hat{I}_{1d} X_d \left\{ (1-S)\cos[(1-S)\omega t + \phi_1 - \phi] + (1+S)\cos[(1+S)\omega t + \phi_1 + \phi] \right\} \tag{3.1b}$$

$$e_{2b} = -\tfrac{1}{2} p \hat{I}_{1d} M_d \left\{ \sin[(1-S)\omega t + \phi_1 - \phi] - \sin[(1+S)\omega t + \phi_1 + \phi] \right\} \tag{3.1c}$$

$$= -\tfrac{1}{2} \hat{I}_{1d} X_d \left\{ (1-S)\cos[(1-S)\omega t + \phi_1 - \phi] - (1+S)\cos[(1+S)\omega t + \phi_1 + \phi] \right\} \tag{3.1d}$$

The frequencies in the waveforms of the induced e.m.f.'s are $(1-S)f$ and $(1+S)f$ which are in agreement with test results. The e.m.f.'s vary sinusoidally with rotor position and can be represented by two vectors, pulsating in time and directed along the magnetic axes of the rotor windings. The resultants of these pairs of vectors appear to rotate in opposite directions through the windings with angular velocities $(1-S)\omega$ and $(1+S)\omega$ relative to the rotor conductors. This can be shown by rewriting equations (3.1b) and (3.1d) in the form

$$e_{2a} = e_{2a}^{+} + e_{2a}^{-}, \qquad e_{2b} = e_{2b}^{+} + e_{2b}^{-} = -j e_{2a}^{+} + j e_{2a}^{-}$$

where

$$e_{2a}^{+} = -\tfrac{1}{2} j (1-S) \hat{I}_{1d} X_d \cos[(1-S)\omega t + \phi_1 - \phi] = \tfrac{1}{2}(e_{2a} + j e_{2b}) = -\tfrac{1}{2} p\, i_{1d} M_d \exp(-j\theta)$$

$$e_{2a}^{-} = -\tfrac{1}{2} j (1+S) \hat{I}_{1d} X_d \cos[(1+S)\omega t + \phi_1 + \phi] = \tfrac{1}{2}(e_{2a} - j e_{2b}) = -\tfrac{1}{2} p\, i_{1d} M_d \exp(j\theta) \tag{3.2}$$

e^{+}_{2b} is a vector equal in magnitude to e^{+}_{2a}, but lagging 90° in time - the resultant e^{+}_{2} has a constant amplitude and appears to rotate (in space) with an angular velocity $(1-S)\omega$ relative to the rotor in the direction of rotation.

e^{-}_{2b} is a vector equal in magnitude to e^{-}_{2a}, but leading 90° in time - the resultant e^{-}_{2} has a constant amplitude and appears to rotate with an angular velocity $(1+S)\omega$ relative to the rotor in a direction opposite to that of rotation.

The corresponding equations referred to the stator axes (stationary axes), which appear to rotate backwards relative to the rotor, are defined by

$$\begin{aligned} e^{f}_{2d} &= e^{+}_{2a}\cos\theta - e^{+}_{2b}\sin\theta = e^{+}_{2a}\exp(j\theta) = -\tfrac{1}{2}j(1-S)\hat{I}_{1d}X_{d}\cos(\omega t+\phi_{1}) \\ e^{b}_{2d} &= e^{-}_{2a}\cos\theta - e^{-}_{2b}\sin\theta = e^{-}_{2a}\exp(-j\theta) = -\tfrac{1}{2}j(1+S)\hat{I}_{1d}X_{d}\cos(\omega t+\phi_{1}) \end{aligned} \qquad (3.3)$$

The steady-state values of the induced e.m.f.'s in equation (3.3) are represented as equivalent reactance voltages in equation (2.15a). In the derivation of the complete performance equations it is more convenient to introduce this change of reference axis (by means of the transformation equation (2.10)) prior to the consideration of the $2d^{f,b}$ components. A physical interpretation of the transformation is that the rotor of the ideal machine is replaced by a pseudo-stationary rotor [1] which develops the same components of m.m.f. and dissipates the same power. There are two winding

layers with each layer comprising two windings, the magnetic axes being directed along the d and q axes respectively. Since there is no magnetic coupling between any of the four windings and the induced e.m.f.'s and currents in the d and q axis windings are simply related, the mode of operation of the machine can be discussed by reference to the stator and rotor windings in the d axis. The induced e.m.f.'s e^{f}_{2d} and e^{b}_{2d} (equation (3.3)) in the rotor windings originate from two contra-rotating fields; the magnitudes are speed dependent, but the frequencies are the same as that of the supply when referred to stationary axes.

3.3 The rotating field

3.3.1 The various theories

The physical description of the mode of operation of the single-phase induction motor in terms of rotating vectors of m.m.f. and induced e.m.f. is referred to as the rotating-field theory. The precise form which the theory takes depends upon the mathematical treatment of the stator m.m.f. . In the above development the stator m.m.f. is represented by a single pulsating vector, and the use of rotating vectors is confined to rotor quantities as this is in line with the previous chapter. An alternative approach is to observe that identical flux-linkages

are obtained by representing the stator m.m.f. as two contra-rotating m.m.f. waves. This is the basis for the symmetrical-component and two-motor theories in which the operation of the machine is explained by reference to the somewhat simpler operation of the two-phase induction motor. In effect, the single-phase machine is 'replaced' by two magnetically separate, electrically connected, variable ratio transformers.

The ideas embodied in the two-motor theory are used in a qualitative discussion of the operation of the single-phase induction motor, but detailed reference to these other theories is omitted from the thesis.

3.3.2 The nature of the rotating field

There is ample experimental evidence to suggest that equation (3.1) correctly describes the terminal conditions of the machine. A single-phase m.m.f. vector exists in the real sense of a measured current flowing in actual conductors and giving a resultant sinusoidally distributed m.m.f., while the e.m.f. waveform may be observed on an oscilloscope. The component frequencies in the waveform are also explained by rearranging the mathematical expression for the stator m.m.f.

$$f_{ld} = \hat{F}_{ld} \cos\theta \cos(\omega t + \phi_1) = \tfrac{1}{2}\hat{F}_{ld}\left\{\cos(\omega t - \theta + \phi_1) + \cos(\omega t + \theta + \phi_1)\right\} \qquad (3.4)$$

but it does not follow either that the modified m.m.f. waveforms actually exist in the machine, or that the same e.m.f. would be induced in the rotor windings of a machine in which the m.m.f. waveforms are created separately.

The interpretation of the rearranged form of the m.m.f. in equation (3.4) is that the pulsating m.m.f. vector can be resolved into two contra-rotating m.m.f. vectors; and, equally, that a pulsating m.m.f. vector can be synthesized from two contra-rotating vectors. It is implicit that hypothetical windings are added in the q axis to give the impression of two superimposed two-phase stator windings which 'create' oppositely rotating m.m.f. waves. In each two-phase winding the resultant m.m.f.'s of the separate phases pulsate along fixed space axes, and the vector combination of the two resultants appears to rotate. The resultants may be assumed real in the sense defined above, but this does not impart a similar reality to the rotating vector. This is apparent in the failure of the experiments by Bretch [2] in which the practical aspects of this theory were examined.

The assumption that a rotating m.m.f. is intimately connected with the mathematical existence of two or more windings displaced in magnetic position around the air-gap periphery and carrying currents, stems from the interpretation of equation (3.4)

and not from the mathematical rearrangement of the terms. Suppose that θ is replaced by $S\omega t$ then the induced e.m.f. (equation (3.3)) results from transformer action, and it is apparently inconsistent to interpret equation (3.4) in terms of 'rotating m.m.f. waves'. To overcome this difficulty, the 'j' factor in the e.m.f. equation is associated with the currents $\pm jI_{1d}$ which flow in the hypothetical q axis windings. Similar explanations apply to the other reactive terms in the performance equations (2.15a).

The treatment of the stator and rotor m.m.f.'s in the rotating-field theory is summarized below..

(i) The resultant m.m.f. of the stator winding pulsates along the d axis and is resolved into contra-rotating m.m.f.'s having amplitudes equal to half the maximum amplitude of the resultant vector (equation (3.4)) .

(ii) The vector combination of the m.m.f.'s due to the currents in the bars of a cage rotor, appears to rotate and vary in amplitude. If space harmonics are neglected then the resultant rotating m.m.f. may be resolved into two oppositely rotating vectors of constant, but unequal, amplitude ($S \neq 0$) . The m.m.f.'s of a two-phase wound rotor are resolved in the same manner.

In the theory the rotating vectors are paired and only the interactions of vector quantities having the same rotation are discussed, i.e., the operation of the machine is related to the operation of the two-phase induction motor. This is given physical expression in the two-motor theory, where the oppositely rotating m.m.f.'s are 'created' in two separate two-phase machines. The operating characteristics of the composite machine are similar to those of the single-phase induction motor, but discrepancies do exist which confirm that the equivalence of the machines is only qualitative. For example, in the single-phase induction motor an oscillatory component is superimposed on the steady-state torque, but this is absent in the two-phase machine and in the combination of the two machines.

3.4 The developed torque

A schematic diagram of a cage rotor machine at standstill is shown in Fig. 3.1 (overleaf). The bars are associated in pairs to form 'independent' single-turn coils in which the induced e.m.f., and hence the current, is proportional to the flux-linkage of the coils with the stator flux. The currents vary harmonically around the rotor periphery, and the torque acts in opposite directions on each side to give zero resultant torque.

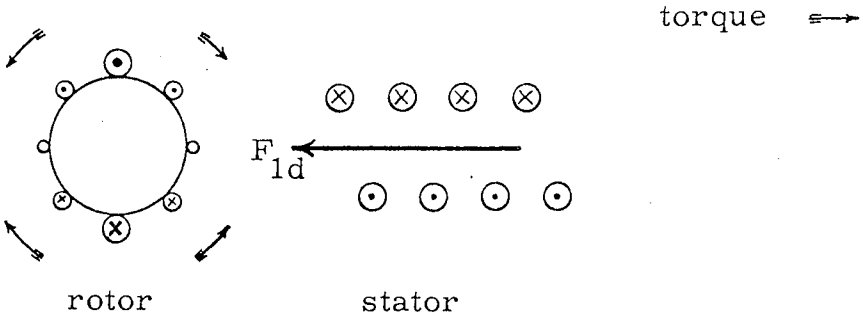

Fig. 3.1

Referring to the same diagram, suppose that the stator m.m.f. is resolved into contra-rotating m.m.f. waves then, as these are otherwise identical, any torque produced by the clockwise rotating wave is exactly balanced by an equal and opposite torque produced by the anticlockwise wave. Hence the single-phase induction motor has no inherent starting torque.

A simple method of starting the motor is to 'flick' the shaft by hand in the desired direction of rotation. Provided that there is no appreciable load torque the rotor increases speed until a stable operating point is reached. In some cases the slight movement of the rotor toward a minimum reluctance position, following the application of the supply, is sufficient to provide the necessary momentum. The onset of rotation causes a slight reduction in the rotor winding currents; the change in the magnitude of the forward component being larger than that of the backward component. However the effect on the phase angles of the currents

is such that a positive torque is developed. At low speeds the stator current remains almost constant and the torque is approximately proportional to speed; it is also proportional to the resistance of the rotor windings.

Theory confirms that the zero speed condition is one of unstable equilibrium [3] and that any slight disturbance causes a build up of speed until a stable operating point is reached. The same argument applies to operating points at low values of speed, formed as the intersection of the developed torque/speed curve and the load torque/speed curve, when the load torque is almost independent of speed.

The developed torque is dependent upon the currents in the rotor windings; in turn, these depend upon the relative velocity between the rotating m.m.f. wave and the rotor. If the backward wave were non-existent then, with zero load torque, the rotor speed would increase from standstill to the synchronous value. The relative velocity between the rotor conductors and the forward field is then zero, and the forward current is zero, and therefore the developed torque is zero. The presence of the backward m.m.f. reduces the available torque, but the operation is similar and the speed increases from standstill to a no-load value slightly lower than the synchronous speed. This is because a forward torque

must be developed to balance the small reverse torque due to the backward rotating field. In other words, even the no-load speed of an ideal single-phase induction motor can never equal the synchronous value.

Some idea of the effect of varying the standstill reactance/resistance ratio is obtained by evaluating the developed torque equation (2.15b) in terms of the stator current, as the latter is a monotonic decreasing function over the range $0 \leq S \leq 1$. Neglecting the change in the rotor parameters due to skin effect, the torque is expressed as

$$T_e = \frac{1}{\omega} \frac{X_d^2}{X_2} |I_{1d}|^2 R_2 \, \xi_{2q} \qquad (3.5)$$

.. where $\xi_{2q} = j S \Big/ \left\{ \left(2 - j \frac{R_2}{X_2}\right) + j \frac{X_2}{R_2} (1 - S^2) \right\}$ *

(The derivation of equation (3.5) is given in section 5.4.2 .)

The variation of the function $\mathrm{Re}\, \xi_{2q}$ with speed $(0 \leq S \leq 1)$ for 4 values of the ratio (X_2/R_2) is shown in Fig. 3.2 (overleaf) , while the corresponding stator current/speed characteristics are given by way of illustration in Fig. 3.3 †(these are considered in detail

---

* ξ functions are described in detail in sections 3.7 and 4.7 , and in Appendix II.

---

† The curves are calculated from equation (5.6) for the conditions:

$$V_{1d}/X_{1d} = 1.0 \,, \quad X_{1d} X_2 / X_d^2 = 1.1 \,, \quad R_{1d} = 0 \,.$$

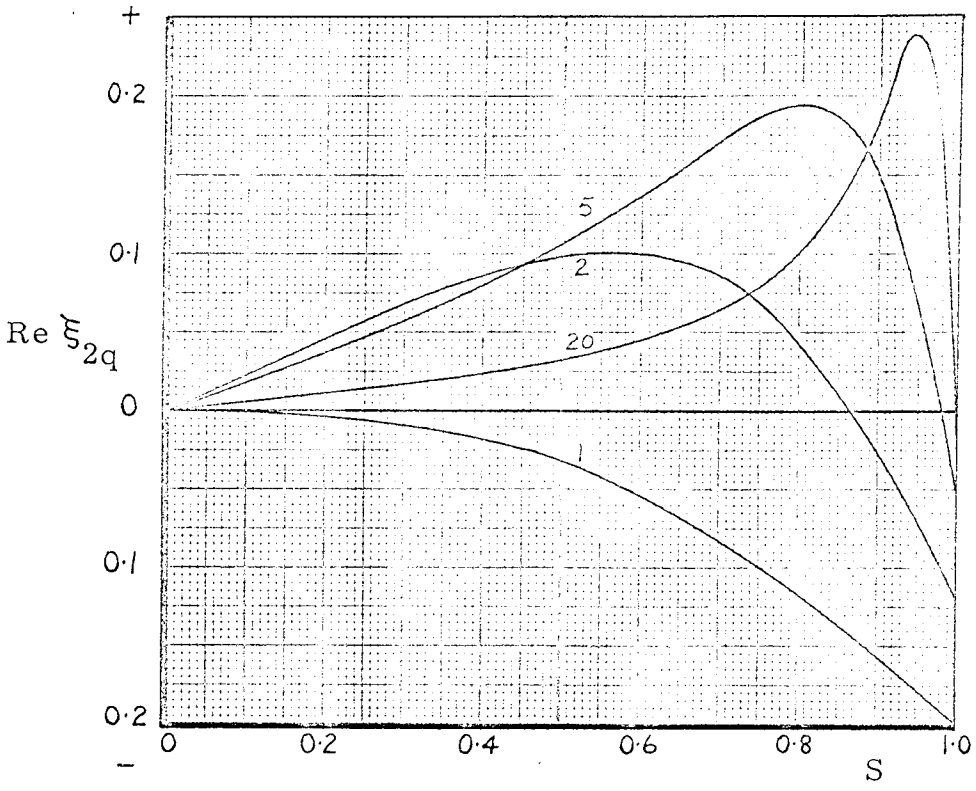

Fig. 3.2 Graph of the function Re ξ_{2q} to a base of speed for 4 values of the ratio X_2/R_2.

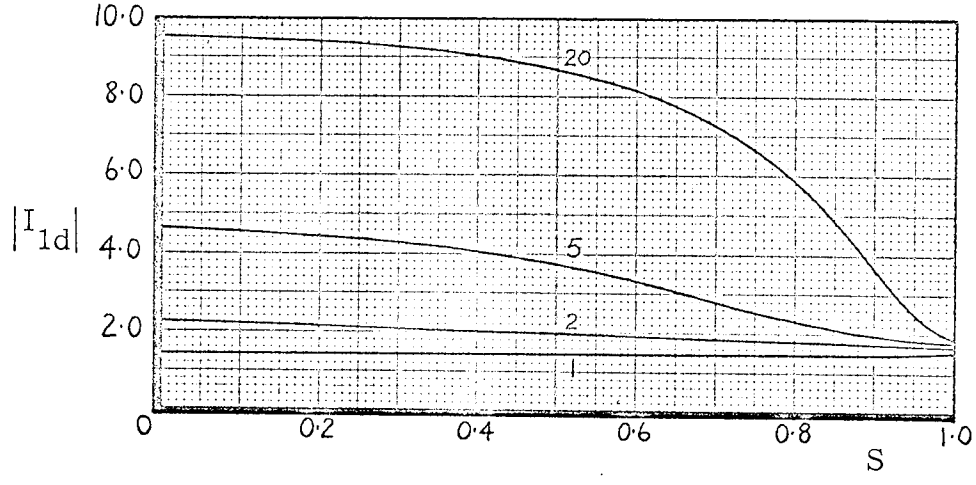

Fig. 3.3 Stator current/speed characteristic for 4 values of the ratio X_2/R_2.

in section 5.4.1) . It is clear from these characteristics that the factor $|I_{1d}|^2$ in equation (3.5) does not modify the form of the torque/speed characteristics and, in a qualitative discussion, can be treated as a constant which modifies the torque scale. Therefore the torque/speed characteristics are similar to Fig. 3.2; there is a stable and an unstable operating region and with normal loads the speed is near the synchronous value (EMT, 107) - the 'pull-out' speed is slightly lower than the value indicated from the maximum of the function $\mathrm{Re}\,\xi_{2q}$ because of the negative slope of $|I_{1d}|$ $(R_2 \neq X_2)$. In particular the zeros of the function are also the zeros of the torque/speed characteristic, and are given by

$$S_\infty = 0\,, \qquad \text{and} \qquad S_0 = \left\{1 - \left(\frac{R_2}{X_2}\right)^2\right\}^{\frac{1}{2}} \qquad (R_2 \neq X_2) \tag{3.6}$$

In most machines the ratio (X_2/R_2) is large and S_0 may be approximated with little error as

$$S_0 = 1 - \tfrac{1}{2}\left(\frac{R_2}{X_2}\right)^2, \qquad \text{first error term } -\tfrac{1}{8}\left(\frac{R_2}{X_2}\right)^4 \tag{3.7}$$

For this same condition the slope of the characteristic in the region of S_0 is almost constant for a given value of the ratio.

3.4.1 The instantaneous value of the developed torque

Referring to equation (2.11b), the developed torque is expressed as the product of two currents, both of which are at

line frequency. This means that although the mean value of the developed torque may be non-zero, the instantaneous value is oscillatory, with a frequency twice that of the supply, and is zero four times per cycle (with respect to line frequency). Therefore the mean value of the shaft speed has a superimposed double-frequency oscillation; the magnitude depends upon the combined moment of inertia of the rotor and the load and is normally quite small. The oscillatory torque is not apparent from the steady-state equations (e.g., (2.15b)) as these are expressed in terms of r.m.s. vector quantities.

****

The discussion of the torque/speed characteristics is continued in detail in section 5.4.2 .

3.5 Normal operation

The description of the steady-state operation of the machine is based on equation (2.15a), but in the treatment of the rotor reference is made to the twin-frequency currents in the actual windings.

In the stator winding the vector resultant of the applied voltage, and the self-induced 'transformer' e.m.f., causes a current I_{1d} and an m.m.f. defined by equation (3.4). The m.m.f.

is resolved into oppositely rotating components and it is assumed that these set up fluxes which act independently in the rotor; the 'forward' flux appears to rotate with a velocity $(1-S)\omega$ relative to the rotor and the changing flux-linkage induces a rotational e.m.f. in the short-circuited windings having a magnitude and frequency proportional to the relative velocity; the 'backward' flux behaves in a similar manner except that the relative velocity is $(1+S)\omega$. These induced e.m.f.'s in the rotor windings are exactly balanced by the self-induced transformer e.m.f.'s and the resistive voltage drops in the windings. The rotor currents set up oppositely rotating m.m.f.'s of unequal magnitude $(S \neq 0)$ and fluxes; the changing flux-linkage with the stator winding induces rotational e.m.f.'s of line frequency which modify the value of the stator current. A forward torque is developed from the interaction of the forward components of stator flux and rotor current, while a backward (retarding) torque results from the corresponding interaction of the backward components.

Over the normal operating range the backward torque has only a limited effect on the net value of the developed torque because the power associated with the backward field is small, and it may be assumed that the form of the torque/speed characteristic is determined from the forward torque and is linear from no-load to full-load. If the load torque is doubled the motor slows down

until the developed forward torque is doubled. The torque on each rotor conductor is proportional to the air-gap flux-density and the conductor current. The forward flux-density is almost constant for small values of rotor resistance, therefore to double the developed torque the forward component of the rotor current, and hence the induced e.m.f., must be doubled. But the induced e.m.f. is proportional to (1-S) so that this factor must be doubled. In other words the torque is linearly related to the speed. The foregoing argument is valid for speeds near to synchronous where the effect of the leakage reactance can be neglected when compared with the rotor resistance, but at speeds nearer to pull-out the leakage impedance causes a pronounced falling-off of the torque/speed characteristic.

3.6 The equivalent circuit

Equation (2.16a) is another form of the electrical performance equation for the rotating-field theory. The modified impedance matrix of the machine is symmetrical and applies equally to the stationary network shown in Fig. 3.4 (overleaf). The mesh currents may be identified with the pseudo-stationary winding currents and the elements of the network have a 1:1 correspondence with the winding parameters, i.e., the network is

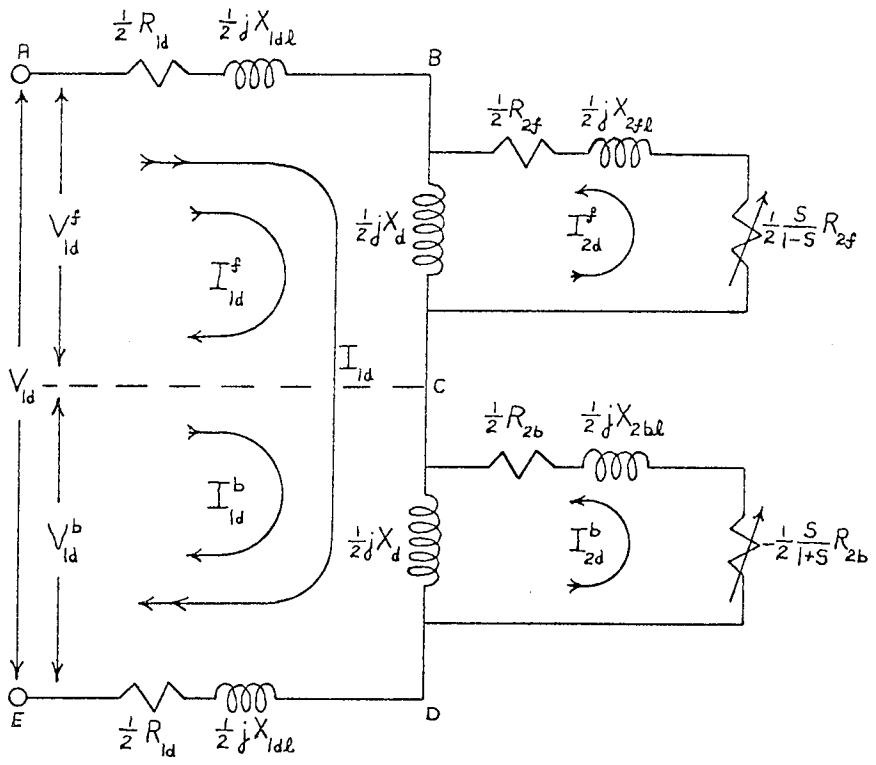

Fig. 3.4

an equivalent circuit for the machine. The usefulness of the diagram is extended by first resolving the stator current into sequence currents and then replacing these by $1d^{f,b}$ components (v. equation (2.14)), so that

$$I_{1d} = I^f_{1d} = I^b_{1d}$$

In addition, the stator leakage impedance is divided into equal impedances. The separation into $.^{f,b}$ components is depicted on the diagram by the dotted median line. This emphasizes the interaction between 'like' stator/rotor currents (m.m.f.'s) and also shows that it is possible to modify the network parameters to allow for skin effect phenomena in the actual machine.

The variations of the hypothetical voltages V_{1d}^{f}, V_{1d}^{b} for typical values of the winding parameters, are shown in Fig. 3.5 .

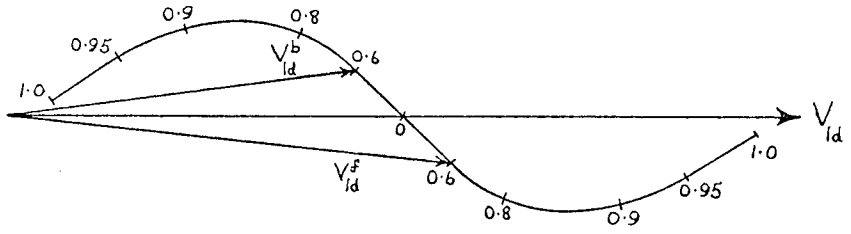

Fig. 3.5

Although the voltages are almost equal for low values of speed, over the normal working range V_{1d}^{b} falls rapidly and the phase angle between the two voltages changes noticeably.

As the overall variation of the speed in the normal working range is less than 10% (5% would be a more accurate figure for many machines), certain simplifying approximations may be made in a qualitative assessment of the performance: e. g. ,

(i) the forward rotor circuit is almost entirely resistive and the leakage reactance may be neglected, and

(ii) if the backward circuit is treated as an equivalent leakage impedance (of constant value) in series with the stator winding [4], then the performance is similar to that of a rather inferior two-phase machine.

Any of the network elements corresponding to the rotor leakage parameters may be modified as an approximation for skin

effect, but in this thesis only variations in the values of the backward circuit resistance ($R_{2b}/2$) are considered. These modifications are necessarily empirical, but the general effect on the performance can be gauged by the use of suitable values. In particular, two assumed variations are referred to in subsequent discussions:

(i) the backward resistance is equal to twice the d.c. value over the normal working range, and

(ii) the backward resistance is equal to (1+S) times the d.c. value.

In the second case the variation over the normal working range is small, but the performance equations are simplified as the parameters of the backward circuit are then independent of speed.

Although the equivalent circuit may be used for the evaluation of the winding currents (because of the correspondence between the currents of the network and the machine) it does not constitute a basis for a description of the operation of the actual machine. Two objections to this are the result of the mathematical division of the voltage-balance equations by the speed dependent factors.

(i) The reactance voltage drops are equivalent to induced e.m.f.'s but the speed of the rotor windings relative to the forward and backward fields is not included in the new terms, and it must

be assumed that the e.m.f.'s in the machine are induced by transformer action only.

(ii) A new concept is introduced - that the apparent rotor resistance is dependent upon speed. This is irrespective of variations due to skin effect.

In both cases the inferred conclusions are contrary to physical reasoning and experimental evidence.

3.6.1 The phasor diagram

A phasor diagram appropriate to speeds in the normal working range is shown in Fig. 3.6, being based on the equivalent circuit and therefore on the symmetrical form of the electrical performance equation. For the conditions shown, the rotor currents are of the same order of magnitude but are displaced in phase, with the result that the magnetizing current of the forward field is large compared with that of the backward field, and similarly the forward torque is large compared with the backward torque. The developed torque is proportional to

$$(-j\,I_{1d})\,I_{2d}^{f}\cos\phi_{f} \;+\; (j\,I_{1d})\,I_{2d}^{b}\cos\phi_{b} \qquad (3.8)$$

The phase angle ϕ_b is slightly greater than $\pi/2$, therefore the second term is small and negative.

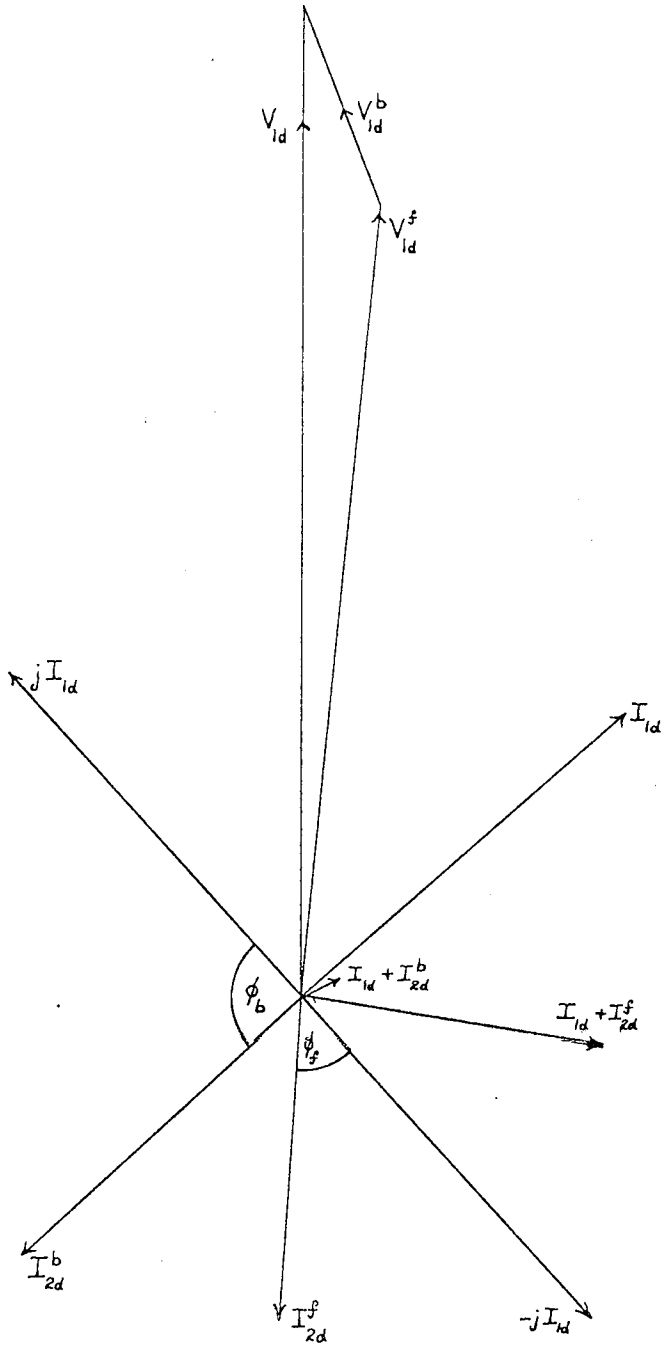

(a) general diagram

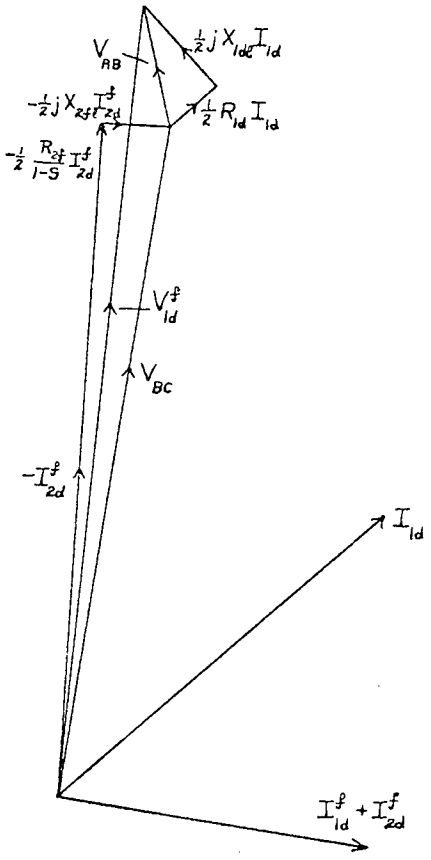

(b) forward circuit

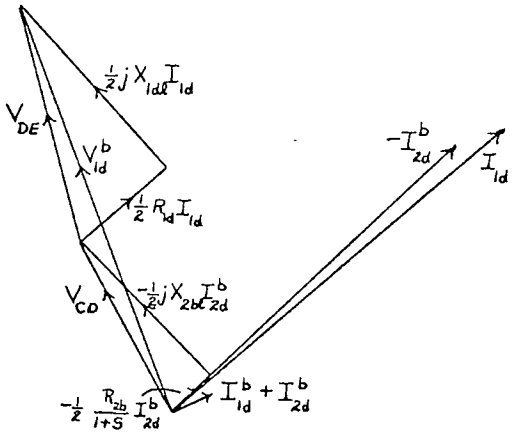

(c) backward circuit

(voltage phasors twice normal size)

Fig. 3.6 Phasor diagrams based on the equivalent circuit

3.6.2 The developed torque

The developed torque may be determined directly from the equivalent circuit as the ratio of the total power in the 'variable resistance loads' and the per-unit speed. This may be verified from a power-balance equation for the rotor of the actual machine.

Let T be the torque of the rotating-field on the rotor, then

power input to the rotor $= T_f\omega + T_b\omega$

mechanical power output from the rotor $= T_f\omega S + T_b\omega(-S)$

power absorbed in the rotor $= T_f\omega(1-S) + T_b\omega(1+S)$

... expressed as copper-loss $= \frac{1}{2}|I_{2d}^f|^2 R_{2f} + \frac{1}{2}|I_{2d}^b|^2 R_{2b}$

Whence $\omega T_f = \frac{1}{2}|I_{2d}^f|^2 \frac{R_{2f}}{1-S}$ and $\omega T_b = \frac{1}{2}|I_{2d}^b|^2 \frac{R_{2b}}{1+S}$ (3.9)

and the mechanical power output $= \frac{1}{2}|I_{2d}^f|^2 \frac{SR_{2f}}{1-S} - \frac{1}{2}|I_{2d}^b|^2 \frac{SR_{2b}}{1+S}$ (3.10)

The power output in equation (3.10) exactly equals the copper-loss in the variable elements of the equivalent circuit, and for this reason these are referred to as the equivalent mechanical loads. The variable load in the backward circuit is a negative element and it represents a negative mechanical load. Expressed differently, the rotor copper-loss in the backward circuit is greater than the power input from the reverse air-gap field ($S \neq 0$) and, as there is no direct interaction between the two rotor circuits, the difference has to be supplied mechanically. Consequently the

practical machine can never operate as a motor at synchronous speed as then there would be no power available to supply the backward circuit copper-loss.

It follows from equations (3.9), (3.10) that the developed torque is

$$\omega T_E = \left(\tfrac{1}{2}\left|I_{2d}^f\right|^2 \frac{R_{2f}}{1-S}\right) - \left(\tfrac{1}{2}\left|I_{2d}^b\right|^2 \frac{R_{2b}}{1+S}\right) \qquad (3.11)$$

This is numerically equal to the difference between the copper losses in the two 'rotor meshes' of the equivalent circuit, but there is no logical connection between these quantities.

3.7 The evaluation of the electrical performance equations

In the explanations of the previous sections, two forms of the electrical performance equation are used and the dependent variables are interpreted both as winding currents in an actual machine and as mesh currents in an equivalent circuit. Either equation may be used for the evaluation of these variables, e.g., taking the inverse of equation (2.16a)

$$\begin{bmatrix} I_{1d} \\ I_{2d}^f \\ I_{2d}^b \end{bmatrix} = \frac{1}{\Delta} \begin{bmatrix} \left(\frac{R_{2f}}{1-S} + j X_{2f}\right)\left(\frac{R_{2b}}{1+S} + j X_{2b}\right) \\ -j X_d \left(\frac{R_{2b}}{1+S} + j X_{2b}\right) \\ -j X_d \left(\frac{R_{2f}}{1-S} + j X_{2f}\right) \end{bmatrix} \begin{bmatrix} V_{1d} \end{bmatrix} \qquad (3.12)$$

where $\Delta = \left(R_{1d} + j X_{1d}\right)\left(\frac{R_{2f}}{1-S} + j X_{2f}\right)\left(\frac{R_{2b}}{1+S} + j X_{2b}\right) + \frac{1}{2} X_d^2 \left(\frac{R_{2f}}{1-S} + j X_{2f}\right) + \frac{1}{2} X_d^2 \left(\frac{R_{2b}}{1+S} + j X_{2b}\right)$

It is difficult to interpret equation (3.12) because of the complicated nature of the terms and the presence of speed dependent factors, and it is informative to use graphical displays for typical ranges of the parameters. Interest centres on I_{1d} as a terminal current which can be measured quite simply, as distinct from the currents I^f_{2d}, I^b_{2d} which have no physical existence. The corresponding variable frequency rotor currents I_{2af}, I_{2ab} are simply related to I^f_{2d}, I^b_{2d} (equation (2.17)), but it is almost impossible to measure these in a cage rotor with any degree of accuracy.

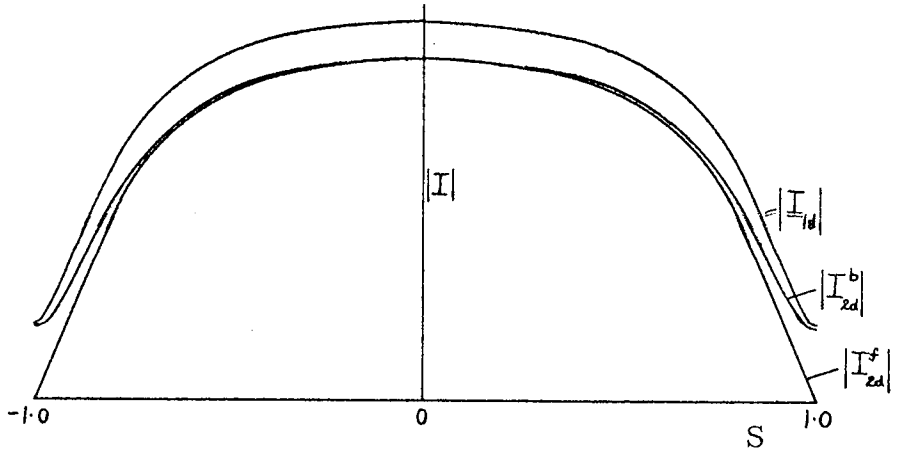

Fig. 3.7

The forms of the current/speed curves for the 3 currents are shown in Fig. 3.7; the curve of $|I^b_{2d}|$ is similar to that of $|I_{1d}|$ and the values are practically equal at $S = 1$; the curve of $|I^f_{2d}|$ is also similar to $|I_{1d}|$ at low speeds but it falls rapidly over the working range becoming zero at $S = 1$.

3.7.1 The ξ functions

Advantage is taken of the fact that there is no mutual coupling between the $2d^f$ and $2d^b$ rotor axes (equation (2.16a)), to define the rotor currents in terms of the stator current and the winding reactances: i.e.,

$$\frac{I^f_{2d}}{I_{1d}} = -\frac{X_d}{X_{2f}}\,\xi_{2f} \quad , \quad \frac{I^b_{2d}}{I_{1d}} = -\frac{X_d}{X_{2b}}\,\xi_{2b} \quad , \quad \frac{I^f_{2d}}{I^b_{2d}} = \frac{X_{2b}}{X_{2f}}\,\frac{\xi_{2f}}{\xi_{2b}} \qquad (3.13)$$

.. where $\xi_{2f} = 1\Big/\left\{1 - j\,\frac{1}{1-S}\,\frac{R_{2f}}{X_{2f}}\right\}$, and $\xi_{2b} = 1\Big/\left\{1 - j\,\frac{1}{1+S}\,\frac{R_{2b}}{X_{2b}}\right\}$

ξ_{2f} and ξ_{2b} are dimensionless factors referred to as 'Xi functions'. The variations of the moduli and arguments of these functions for various values of the ratio X_2/R_2 over the speed range $0 \leqslant S \leqslant 1$ are shown in Fig. 3.8, and a simple graphical technique for the construction of these diagrams for any value of X_2/R_2 is given in Appendix II.

Referring to the curves of ξ_{2f}, it is seen that for normal values of X_2/R_2 ($\simeq 20$) the modulus is almost unity over the range $0 \leqslant S \leqslant 0.8$ and over the working range it decreases rapidly ($|\xi_{2f}| \simeq (1-S)(X_2/R_2)$) becoming zero at $S = 1$; the argument is nearly constant over the range $0 \leqslant S \leqslant 0.8$ and then increases rapidly to $\pi/2$ at $S = 1$. The corresponding curves for ξ_{2b} show that little error is incurred by replacing the modulus by unity, particularly over the normal working range; for the same

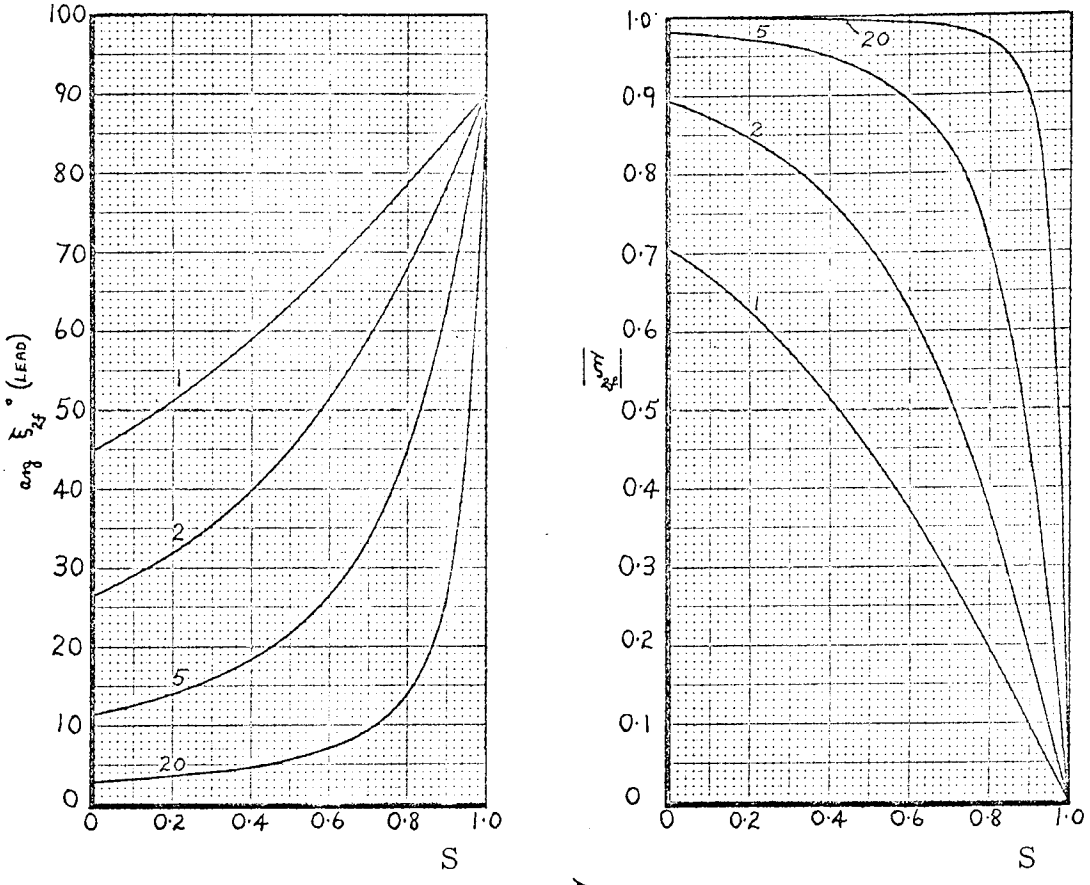

(a) ξ_{2f}

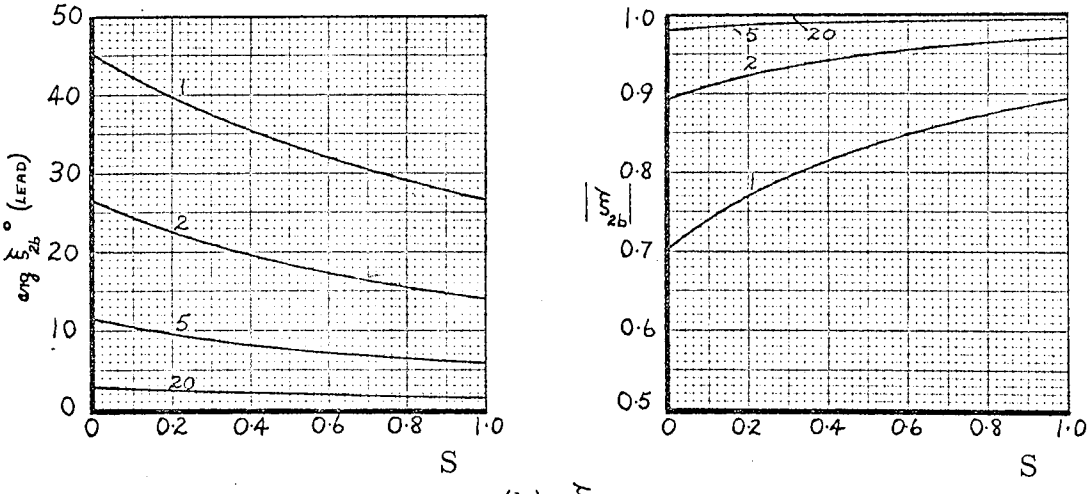

(b) ξ_{2b}

Fig. 3.8 Graphs showing the variation of the ξ functions with speed for 4 values of X_2/R_2.

conditions, the argument decreases slightly.

Any allowance that is made for skin effect modifies $\tilde{\xi}_{2b}$: e.g., suppose that over the normal working range the backward resistance is effectively twice the d.c. value and the ratio X_2/R_2 is halved, then the effect on the modulus is negligible and although the argument is doubled, this is still quite small.

3.7.2 The winding currents

3.7.2.1 The stator current

The use of $\tilde{\xi}$ functions reduces the equivalent circuit to a simple series network in which two of the elements are speed dependent. This is shown in Fig. 3.9.

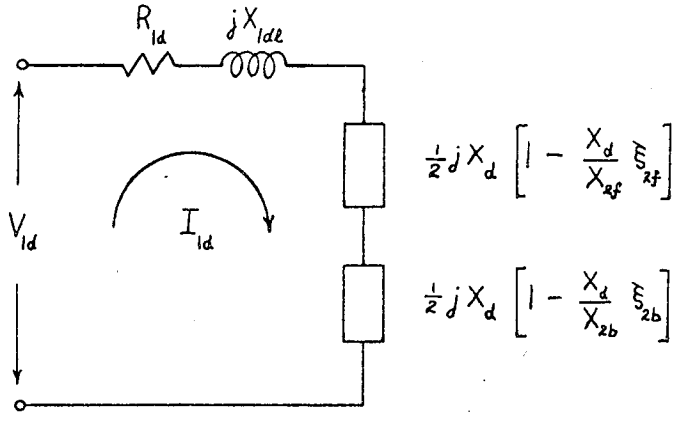

Fig. 3.9

The mesh current is given by

$$I_{1d} = V_{1d} \Big/ \left\{ R_{1d} + jX_{1d}\left[1 - \tfrac{1}{2}\frac{X_d^2}{X_{1d}X_{2f}}\tilde{\xi}_{2f} - \tfrac{1}{2}\frac{X_d^2}{X_{1d}X_{2b}}\tilde{\xi}_{2b}\right]\right\} \qquad (3.14)$$

The form of the stator current/speed characteristic is determined

by substituting typical values into equation (3.14) and neglecting the stator resistance.

E.g., let $X_{2f} = X_{2b} = X_2$, $R_{2f} = R_{2b} = R_2$, $R_{1d} = 0$,

$X_{1d} X_2/X_d^2 = 1.1$, $X_2/R_2 = 20$.

Then $\xi_{2b} \simeq 1\angle 0°$ and $I_{1d} \simeq 2.2\, V_{1d} \Big/ \{jX_{1d}(1.2 - \xi_{2f})\}$.

Substituting numerical values for ξ_{2f} gives the characteristic shown in Fig. 3.3:

at $S = 0$, $\xi_{2f} = 0.9975 + j0.0499$, and $|I_{1d}| \simeq 9.65\, V_{1d}/X_{1d}$

at $S = 1$, $\xi_{2f} = 0 + j\ 0$, and $|I_{1d}| \simeq 1.83\, V_{1d}/X_{1d}$.

The variation of I_{1d} for 4 values of X_2/R_2 over the speed range $0.9 \leqslant S \leqslant 1.0$ is shown in Fig. 3.10 (overleaf); the values assumed in the calculations are

$$X_{1d} X_{2f}/X_d^2 = X_{1d} X_{2b}/X_d^2 = 1.1, \quad R_{1d} = 0,$$

and the current scale factor V_{1d}/X_{1d} is replaced by unity. It is seen that for typical values of X_2/R_2, the real part of I_{1d} is small for speeds near to the synchronous value but it rises almost linearly over the normal operating range. The imaginary part is more nearly constant for the same conditions and is much larger than the real part for speeds near to the synchronous value, with the result that the total current increases slowly over the working range and then rises rapidly in the region of pull-out; for small

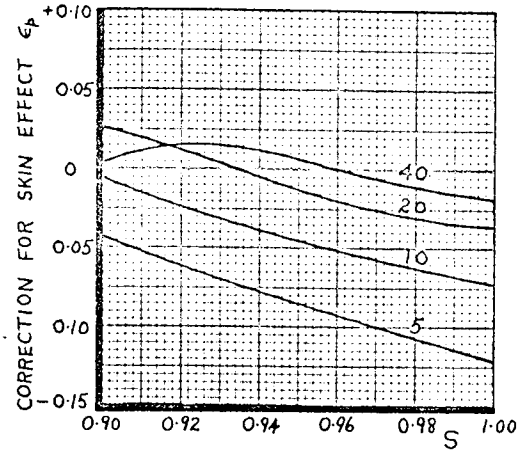

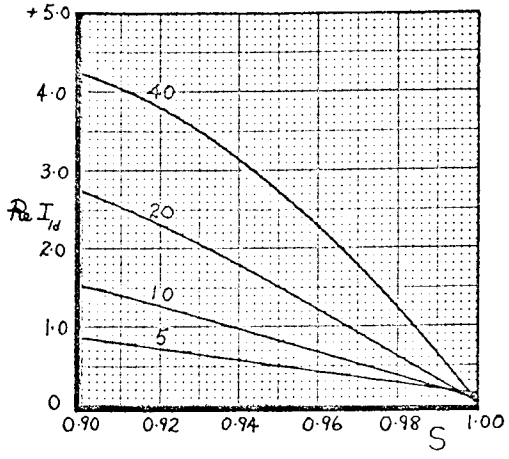

(a) In-phase values

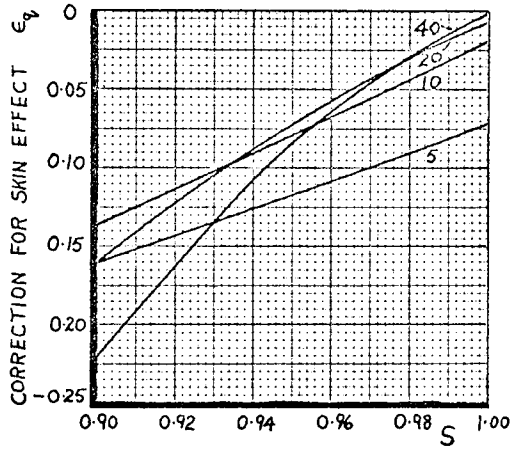

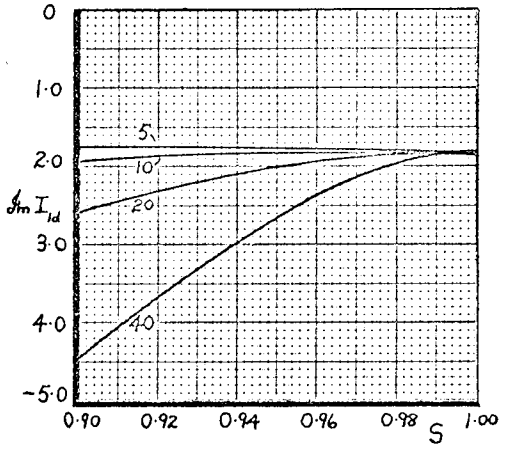

(b) Quadrature values

Fig. 3.10 The stator current

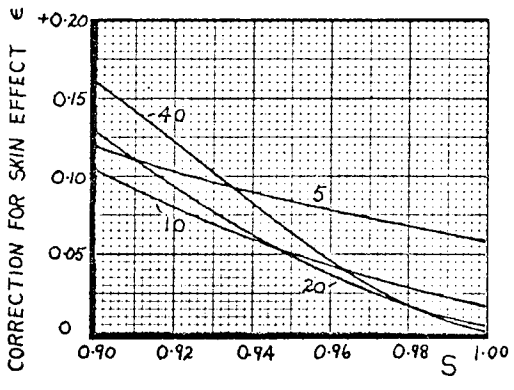

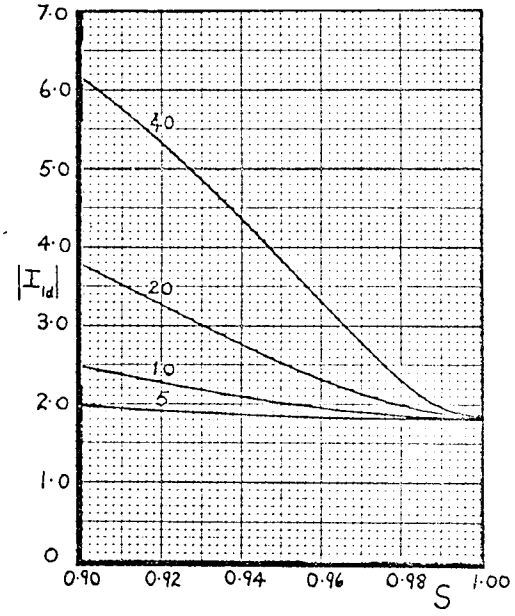

(c) Total values

values of X_2/R_2 the imaginary part actually decreases slightly.

Also shown in Fig. 3.10 is the modification of the stator current by skin effect in the rotor bars, based on an assumed condition $R_{2b} = 2R_{2f}$. Although this represents a 100% increase in the value of the backward resistance, the overall change in the current is small because of the relatively large apparent value of the forward resistance near to the synchronous speed: e.g., at $S = 0.96$ for $X_2/R_2 = 20$, $|I_{1d}|$ is only decreased by 1.57%. To improve the graphical presentation, differences between the currents for the two conditions are plotted - these are defined by

$$\text{Re } I_{1d}^{(2)} = \text{Re } I_{1d} - \epsilon_{\text{Re}}, \quad \text{Im } I_{1d}^{(2)} = \text{Im } I_{1d} - \epsilon_{\text{Im}}, \text{ and } \left|I_{1d}^{(2)}\right| = |I_{1d}| - \epsilon$$

.. where $I_{1d}^{(2)}$ represents the value of the stator current when skin effect is allowed for.

The real part of I_{1d} is increased slightly by skin effect, the change being more noticeable at no-load; while the imaginary part is affected in the opposite sense, with a slight decrease at no-load becoming more marked as the speed is decreased. Although the improvement in the operating power factor is a function of X_2/R_2 (v. Fig. 4.11), the net change in the modulus is practically independent of this ratio so that the percentage change is larger for lower values of X_2/R_2.

3.7.2.2 No-load conditions

For typical values of X_2/R_2 the no-load speed is close to the synchronous value and as the modulus of the current changes only slightly in this region, the no-load current can be taken as the value at synchronous speed. This approximation is used with the values of the no-load current given in table 3.1.

TABLE 3.1

X_2/R_2	40.00	26.67	20.00	13.33	10.00
I_{1d}	1.833	1.832	1.832	1.829	1.826

It is seen that the value of $|I_{1d}|$ is practically independent of X_2/R_2 and can be expressed with little error as

$$|I_{1d}| = \frac{V_{1d}}{X_{1d}}\left\{\frac{X_{1d}X_{2b}}{X_{1d}X_{2b} - \frac{1}{2}X_d^2}\right\} \qquad (3.15)$$

With typical values of the winding reactances, the no-load current is almost twice the corresponding phase value for a two-phase machine; it is reduced slightly by skin effect.

The no-load conditions are discussed further in section 4.7.2.3 of the cross-field theory.

****

The discussion of the stator current is continued in sections 4.7.2 and 5.4.1 .

3.7.2.3 The rotor currents

The values of the rotor currents I_{2d}^{f}, I_{2d}^{b} are derived from the stator current by the use of the ξ functions (equation (3.13)). The variations are shown in Fig. 3.11 (p. 78) and Fig. 3.12 (p. 79) for 4 values of X_2/R_2 over the speed range $0.9 \leq S \leq 1.0$; the additional reactance ratios assumed in the calculations are

$$X_{2f}/X_d = X_{2b}/X_d = 1.05 \quad .$$

The forward current $|I_{2d}^{f}|$ is zero at synchronous speed and rises almost linearly over the working range with a slope approximately proportional to the X_2/R_2 ratio. Skin effect decreases both the real and imaginary parts, and the net change follows a similar variation to the current modulus. For the example previously given: with $X_2/R_2 = 20$ and $S = 0.96$, the reduction in $|I_{2d}^{f}|$ is 1.54% .

The variation of the backward current $|I_{2d}^{b}|$ is very similar to that of the stator current because $|\xi_{2b}|$ is practically unity and arg. ξ_{2b} is small. The changes due to skin effect are also similar to the corresponding changes in I_{1d} for the same reasons, although the reduction in the quadrature component of I_{2d}^{b} is larger. Using the above example, the reduction in $|I_{2d}^{b}|$ is 1.65% .

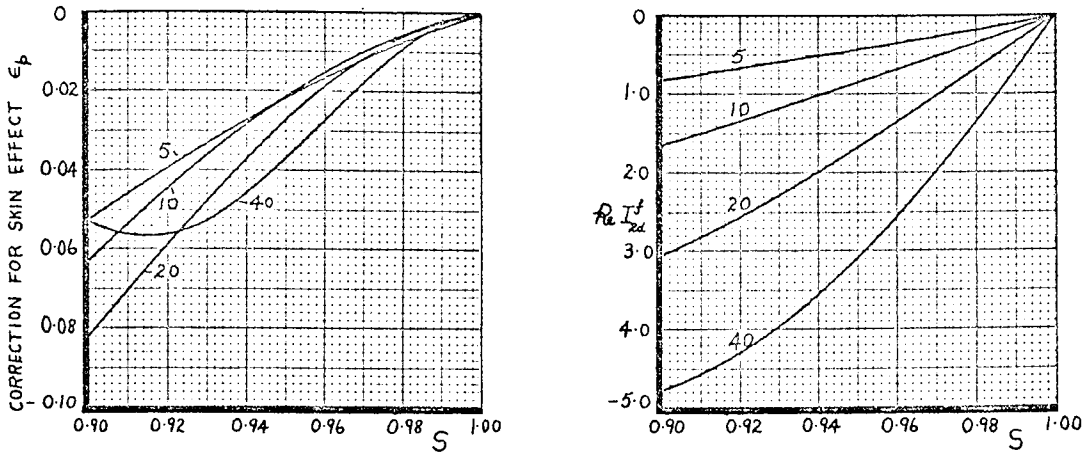

(a) In-phase values

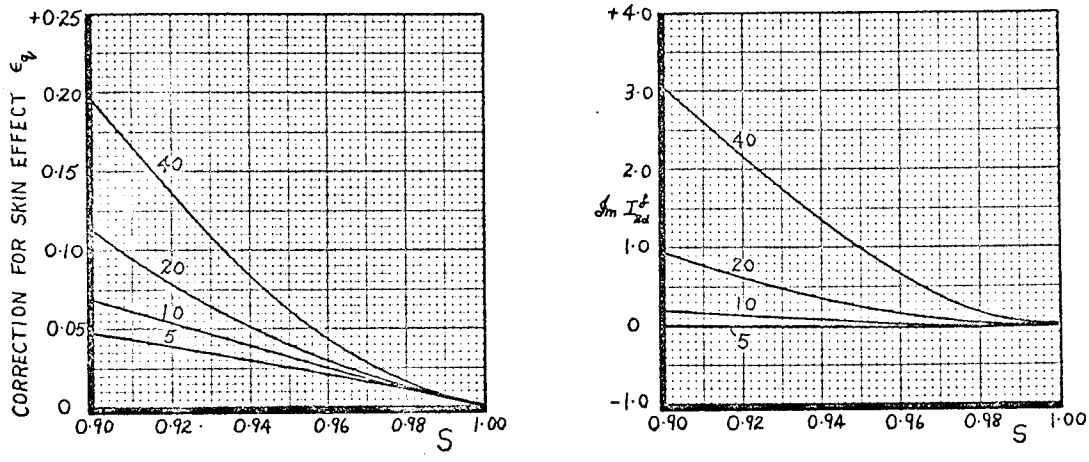

(b) Quadrature values

Fig. 3.11 The rotor current I^f_{2d}

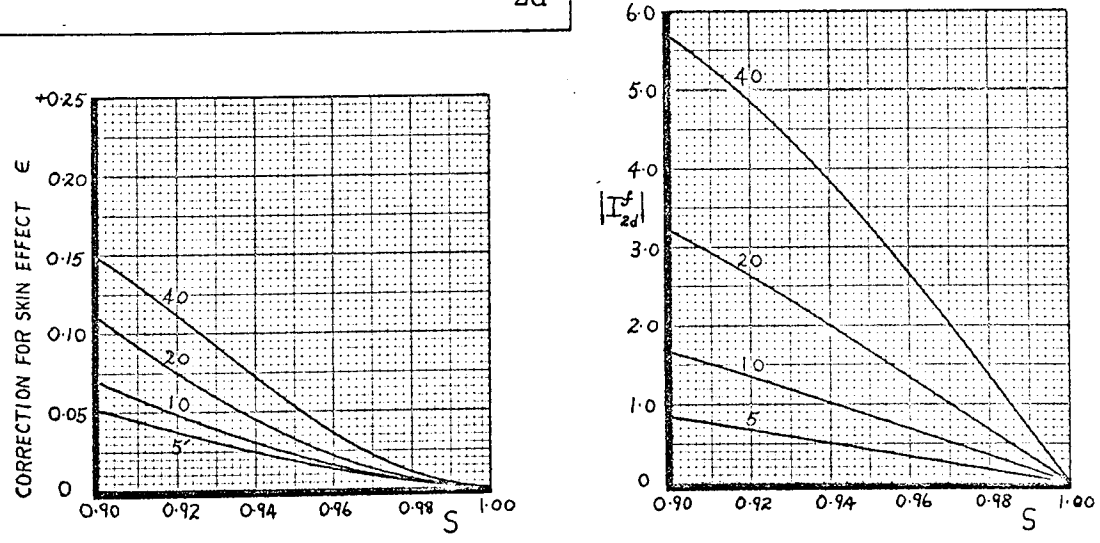

(c) Total values

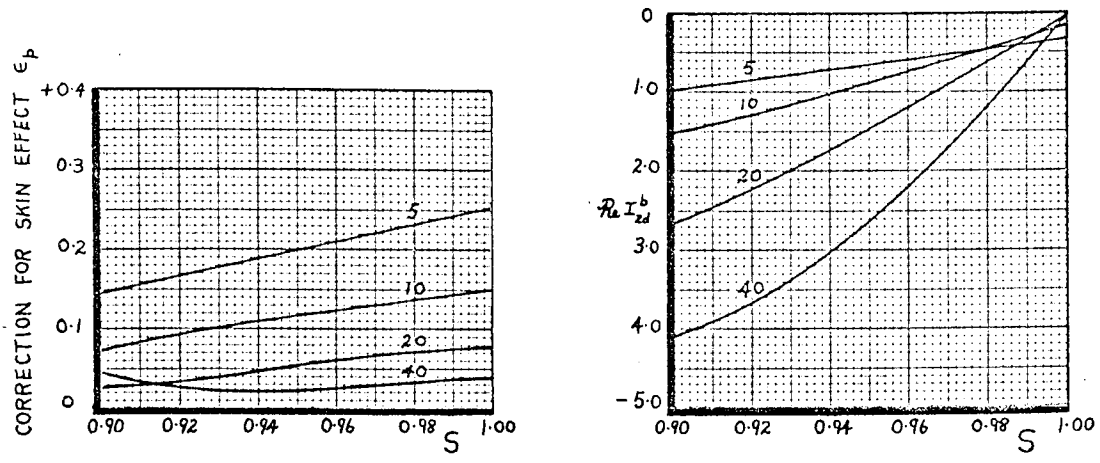

(a) In-phase values

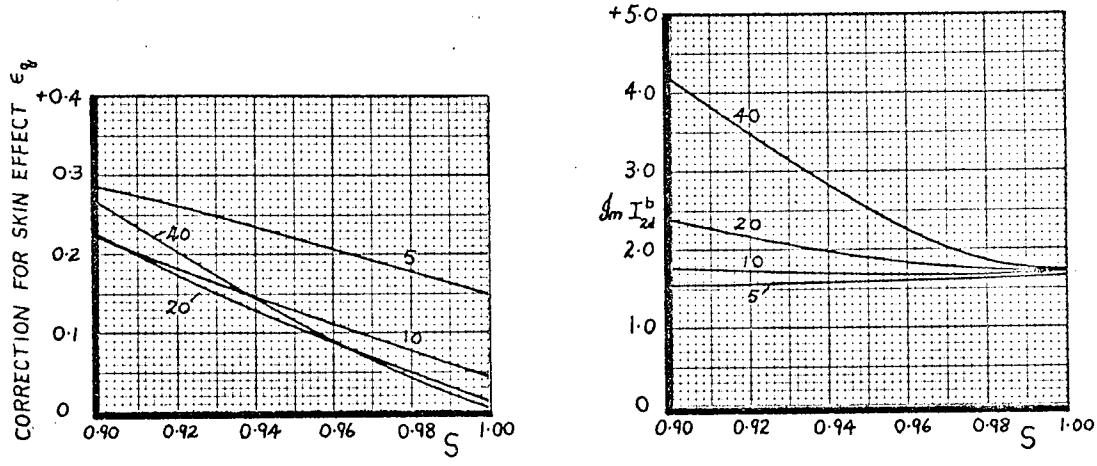

(b) Quadrature values

Fig. 3.12 The rotor current I^b_{2d}

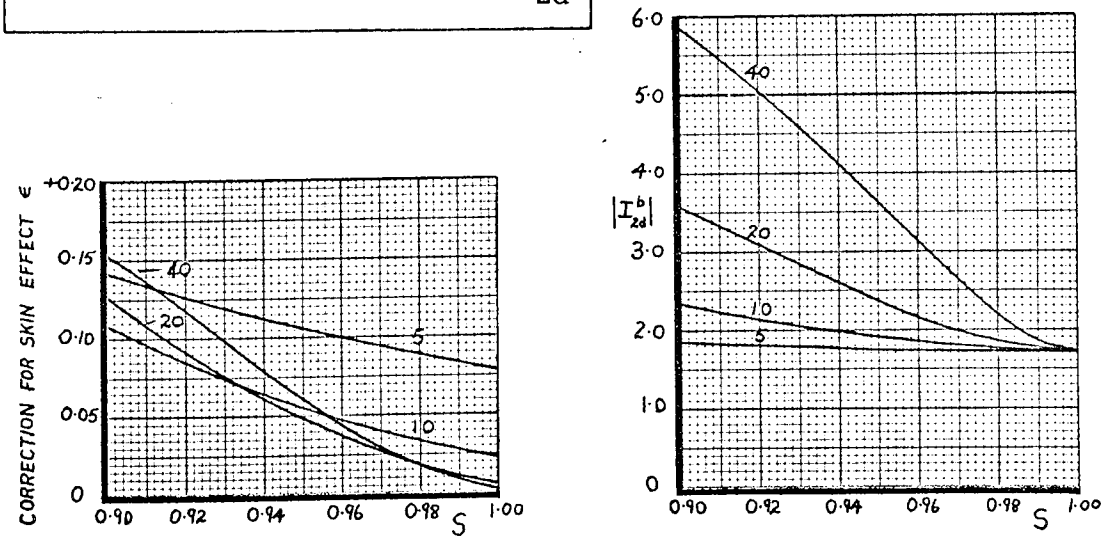

(c) Total values

3.8 Comment

The rotating-field theory, as presented in this chapter, is the qualitative explanation of the mode of operation of the single-phase induction motor in terms of oppositely rotating m.m.f. waves. The use of this concept makes it unnecessary to make continual reference to skin effect phenomena as special effects, because the essence of the theory is that the two frequency components of the rotor current are treated separately.

CHAPTER IV

THE CROSS-FIELD THEORY

CHAPTER IV

THE CROSS-FIELD THEORY

4.1 Chapter outline

In Chapter II the f, b rotor currents of the general theory (equation (2.12a)) are identified with the sequence currents, and symmetrical-component theory is used to define a set of hypothetical d, q rotor currents which lead to an alternative set of performance equations (equation (2.20a)). These are simplified by neglecting those parts of the rotor coupling terms introduced through the inclusion of skin effect, to give the equations of the cross-field theory (equation (2.22)). The physical description of the mode of operation of the single-phase induction motor in terms of this equation is the subject of the present chapter.

No new physical principles are introduced in the cross-field theory and it is advantageous to 'parallel' the discussion with that based on the rotating-field theory in Chapter III. The nature of the cross-field is examined; explanations are given for the form of the e.m.f. induced in the rotor and the production of torque; and a phasor diagram is developed as part of the discussion of the normal operation. In addition, a second set of ξ functions is

defined to simplify the evaluation of the winding currents.

It is shown that the physical descriptions of the cross-field theory apply equally to either a cage or a wound rotor machine, although the performance equations necessarily relate to a machine in which skin effect is absent.

4.2 The induced e.m.f.'s in the rotor

The instantaneous values of the induced e.m.f.'s in the open-circuited rotor windings (2a, 2b) are expressed

$$e_{2a} = -p i_{1d} M_d \cos\theta \quad , \qquad e_{2b} = p i_{1d} M_d \sin\theta \qquad \text{(equation (3.1))} \qquad (4.1)$$

Substituting for the stator current $i_{1d} = \hat{I}_{1d} \cos(\omega t + \phi_1)$, and noting that the angular position of the rotor (θ) is a function of time, the e.m.f.'s are evaluated as

$$e_{2a} = -j \hat{I}_{1d} X_d \cos(\omega t + \phi_1) \cos\theta + S \hat{I}_{1d} X_d \cos(\omega t + \phi_1) \sin\theta \qquad (4.2)$$

$$e_{2b} = j \hat{I}_{1d} X_d \cos(\omega t + \phi_1) \sin\theta + S \hat{I}_{1d} X_d \cos(\omega t + \phi_1) \cos\theta \qquad (4.3)$$

Let $$e_{2a} = e_{2d} \cos\theta + e_{2q} \sin\theta \quad , \qquad e_{2b} = -e_{2d} \sin\theta + e_{2q} \cos\theta \qquad (4.4)$$

then $$e_{2d} = -j I_{1d} X_d \cos(\omega t + \phi_1) = e^f_{2d} + e^b_{2d} \qquad (4.5)$$

$$e_{2q} = S I_{1d} X_d \cos(\omega t + \phi_1) = e^f_{2q} + e^b_{2q} \qquad (4.6)$$

The induced e.m.f.'s (e_{2a}, e_{2b}) vary sinusoidally in space and are comprised of two terms which originate from the pulsation of the stator winding m.m.f. (the transformer e.m.f. e_{2d}), and the

rotation of the rotor windings (the rotational e.m.f. e_{2q}). Equation (4.4) describes the resolution of e_{2a}, e_{2b} on to two stationary axes in line with, and at right-angles to, the stator winding axis respectively, and is used in the derivation of the performance equations (2.20a, b). The relationships of the e.m.f.'s e_{2d}, e_{2q} with the e.m.f.'s of the rotating field theory are deduced from equation (3.3) and expressed in equations (4.5), (4.6).

The physical interpretation of these equations is that in the cross-field theory, corresponding phase windings in the two layers of the pseudo-stationary model rotor are connected in parallel. It is tacitly assumed in equation (4.4) that the pairs of parallel connected windings are replaced by single windings having the same flux-linkage with the stator winding. In the trivial case where the circuit parameters of the two layers are the same this replacement would actually be possible, but in general the parallel connection must be treated as a mathematical 'operation' devoid of further physical interpretation. Although the induced e.m.f.'s and currents in the d and q axis windings of the separate layers are simply related, this is masked by the parallel connection and the voltage-balance equations for both the d and q axis windings must be included in the performance equations of the cross-field theory.

4.3 The cross-field

The currents in the q axis windings of the pseudo-stationary rotor set up a magnetic field cosinusoidally distributed about an axis at right-angles to that of the stator. This is the 'cross-field' and a physical interpretation of equation (2.22) is referred to as the cross-field theory of the single-phase induction motor.

While there can be no satisfactory proof in linear theory that a cross-field either does or does not exist, the following development [1] shows that it is nevertheless a reasonable assumption. Consider a machine with a hypothetical cage rotor having an infinite number of bars, and let the stator winding be excited. At standstill, e.m.f.'s are induced in the rotor bars through the pulsation of the stator field. These circulate currents in the closed winding and a magnetic field is set up opposing the stator field as shown in Fig. 4.1a.

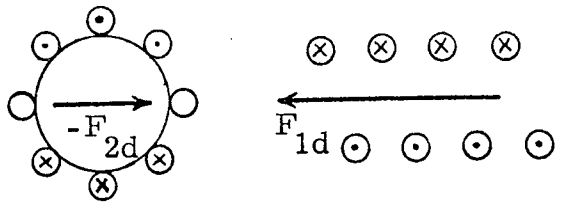

Fig. 4.1a

The machine behaves as a single-phase transformer (with an air-gap) and the rotor windings could be replaced by a short-circuited coil having an axis in line with that of the stator winding. Now suppose that the rotor is driven at constant speed; e.m.f.'s are induced in the rotor bars by transformer action and the rotor may be replaced by the stationary coil previously mentioned, because the assumption of a large number of rotor bars means that to a stationary observer there always appears to be a bar in a given position regardless of rotation. The rotation of the bars also gives rise to a rotational induced e.m.f., in accordance with equation (4.6), which causes currents to flow and, in turn, sets up a second magnetic field as shown in Fig. 4.1b.

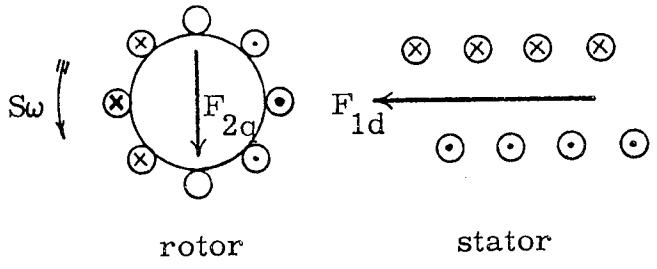

Fig. 4.1b

This field is also stationary in space for the same reason as the transformer field and could be produced, equally well, by a stationary short-circuited coil having an axis at right-angles to the stator winding axis. Hence the action of the stator m.m.f. on the

closed rotor windings may be described in terms of two stationary hypothetical coils (EMT, 33), the second coil being associated with the cross-field. The axis of this cross-field is at right-angles to that of the main field and there can be no interaction between the two in a smooth air-gap machine. Since the cross-field originates in the rotor the power associated with it, which is mainly reactive, must be supplied from reconverted mechanical energy imposed as a load on the shaft. The complete development of the induced e.m.f.'s and the currents in the rotor coils is considered in section 4.5.1 .

The idea of a cross-field is also suggested by the rotating-field theory. Two contra-rotating m.m.f. waves exist in the rotor which can be resolved on to two stationary axes at right-angles. Except at standstill, the m.m.f.'s are unequal and therefore the resolutes are, in general, non-zero. The stator m.m.f. is produced along one axis only and the equivalent contra-rotating vectors must always be equal. Hence the quadrature axis m.m.f. vector originated in the rotor is not modified by the action of the stator m.m.f., and the cross-field conveniently explains the existence of a flux-linkage with a winding located in the stator q axis.

In the model rotor each winding layer can be replaced by

two stationary coils and a cross-field theory developed for each layer, based on equation (2.12a). Advantage may be taken of the phase relations between the d and q axis quantities, both in the theory and in the evaluation of the winding currents (from equation (2.15a)). In this way a modified theory is developed in which skin effect is included. However the accepted form of the theory as outlined above is based on equation (2.22) and this does not apply to a cage rotor machine. Nevertheless the underlying principles are the same and there is no loss of generality if the qualitative discussion is limited to the simpler case of the single-layer rotor.

4.4 The developed torque

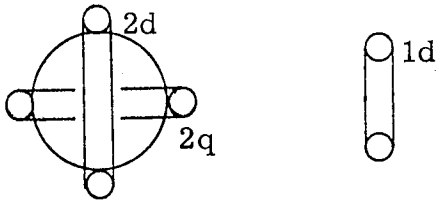

Fig. 4.2a

A schematic layout of the machine is shown in Fig. 4.2a where the stator winding is represented by a single coil, and the rotor winding by the two pseudo-stationary coils.

$F_d = F_{1d} + F_{2d}$

$F_q = F_{2q}$

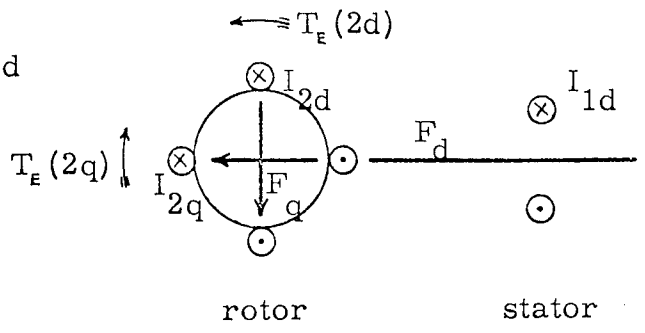

Fig. 4.2b

The positive directions of the currents and m.m.f.'s are shown in Fig. 4.2b. The m.m.f. F_d is the resultant m.m.f. in the d axis and is equal to the vector sum of the separate stator and rotor m.m.f.'s, while F_q is the m.m.f. in the q axis described in the previous section. It is assumed that both the currents and m.m.f.'s are sinusoidally distributed.

The force on the individual rotor conductors is governed by the relation F = BLI, and this must also apply to the force on the conductors which form the hypothetical stationary coils as it is impossible to distinguish between the two sets of conductors in the limiting case of a rotor with an infinite number of bars. Therefore the torque developed from the interaction of the currents flowing in the coils (Fig. 4.2b) and the flux-density is

$$T_E = Re\, K(F_q I_{2d}^* - F_d I_{2q}^*) \qquad (K \text{ is a real constant}) \qquad (4.7)$$

The standstill torque is zero because there is no coupling between the d and q axes and therefore both I_{2q} and F_q are zero. At

any other speed, rotation will continue in the positive direction if the net torque defined by equation (4.7) is positive. The first term is a 'motor' torque produced by the interaction of the q axis flux-density with the d axis rotor current, while the second term represents the equivalent 'generator' torque necessary to supply the losses in the cross-field and results from the interaction of the resultant flux-density in the d axis and the q axis rotor current.

Equation (4.7) can be rewritten as

$$T_E = Re\,\frac{1}{\omega}\left\{X_{2q}\,I_{2q}\,I_{2d}^{*} - (X_d I_{1d} + X_{2d} I_{2d})\,I_{2q}^{*}\right\}$$

$$= Re\,\frac{1}{\omega}\left\{-X_d\,I_{1d}\,I_{2q}^{*} - (X_{2d} - X_{2q})\,I_{2d}\,I_{2q}^{*}\right\} \qquad (4.8)$$

$$= Re\,\frac{1}{\omega}\left\{-X_d\,I_{1d}\,I_{2q}^{*}\right\} \qquad (X_{2d} = X_{2q}) \qquad (4.9)$$

Equation (4.9) is identical with (2.20b); the torque is expressed, correctly, in terms of the stator and rotor currents but the internal generator action explicit in equation (4.7) is completely masked. The second term in equation (4.8) is referred to as the saliency torque and is primarily a function of the geometry of the machine and the saturation of the magnetic flux paths; in the smooth air-gap machine this torque is normally quite small.

A reordering of the terms in equation (4.7) leads to a different explanation of the mechanism of torque production in the machine. The motor torque results from the interaction of the flux-density produced by the stator winding and the q axis rotor

current. A second torque is developed by the q axis flux-density and the d axis rotor current, but this is nullified by the torque due to the d axis rotor flux-density and the q axis rotor current. If the rotor reactances in the two axes are equal, only the first mentioned torque is apparent from equation (4.9). The explanation given is strictly in accordance with equation (4.8), taken term by term, and demonstrates that the net torque is consistent with motor operation. However the torque term $Re\ \frac{1}{\omega}\{-X_d I_{1d} I_{2q}^*\}$ represents neither a motor nor a generator torque but is the resultant positive torque necessary for motor action. The torques developed in the rotor are both larger than the net torque by an amount approximately equal to the cross-field rotor copper-loss.

It is shown in section 4.7 that the q axis rotor current I_{2q} may be expressed in terms of the stator current I_{1d} as

$$I_{2q} = -\frac{X_d}{X_2} \xi_{2q} I_{1d} \qquad (4.10)$$

Substituting for I_{2q}^* in equation (4.9) and taking the real part

$$T_E = \frac{1}{\omega} \frac{X_d^2}{X_2} |I_{1d}|^2 Re\ \xi_{2q} \qquad (Re\ \xi_{2q} = Re\ \xi_{2q}^*) \qquad (4.11)$$

Equation (4.11) is identical with equation (3.5) stated in the rotating-field theory and the discussion of the function $Re\ \xi_{2q}$ on pps. 56 - 58 also applies here.

4.4.1 The instantaneous value of the developed torque

The mean value of the torque is used in the explanations given above, and the adjectives 'motor', 'generator', 'positive', 'negative' are applied in this context: e.g., the instantaneous value of the motor torque is alternately positive and negative, but the mean value is positive. The concept of an oscillatory torque is introduced in the rotating-field theory and is also an essential part of the cross-field theory. The rotor q axis winding behaves as a single-phase inductive circuit and there is a continuous interchange of energy between the magnetic field (the cross-field) and the 'supply'. As the input electrical energy to this winding is derived from converted mechanical energy, the variations in the stored electrical energy cause similar variations in the kinetic energy which are observed as a small oscillation superimposed on the steady speed. The amplitude is governed by the inertia of the moving parts and is normally too small to account completely for the variations in the kinetic energy, hence the developed torque must also be oscillatory. This applies to the operation of the machine at all speeds except standstill: e.g., on no-load the resultant shaft torque is oscillatory but the mean value is zero.

4.5 Normal operation

The discussion of the normal operation and the explanation of the various terms in the performance equation (2.22) is facilitated by the use of phasor diagrams, so that these are related to the operation of the actual machine instead of the equivalent circuit for the machine, as is the case in the rotating-field theory.

The phasor diagram for the standstill condition is shown in Fig. 4.3 (overleaf). The machine behaves as a single-phase transformer on short-circuit; the d axis stator and rotor currents are large, but the developed torque is zero. The magnetizing current and mutual flux-linkage are reduced because of the voltage drop in the stator leakage impedance.

Suppose now that the shaft is flicked by hand to cause rotation. The d axis currents remain almost constant in both magnitude and phase, and a small rotational e.m.f. is induced in the q axis circuit approximately proportional to the speed. This circulates a current I_{2q} having a magnitude proportional to speed, and a phase angle which is almost constant because the rotor leakage parameters are small and independent of speed. The developed torque (equation (4. 9)) is proportional to the vector product of the d axis stator and q axis rotor currents and therefore is proportional to speed. Hence the operation is unstable

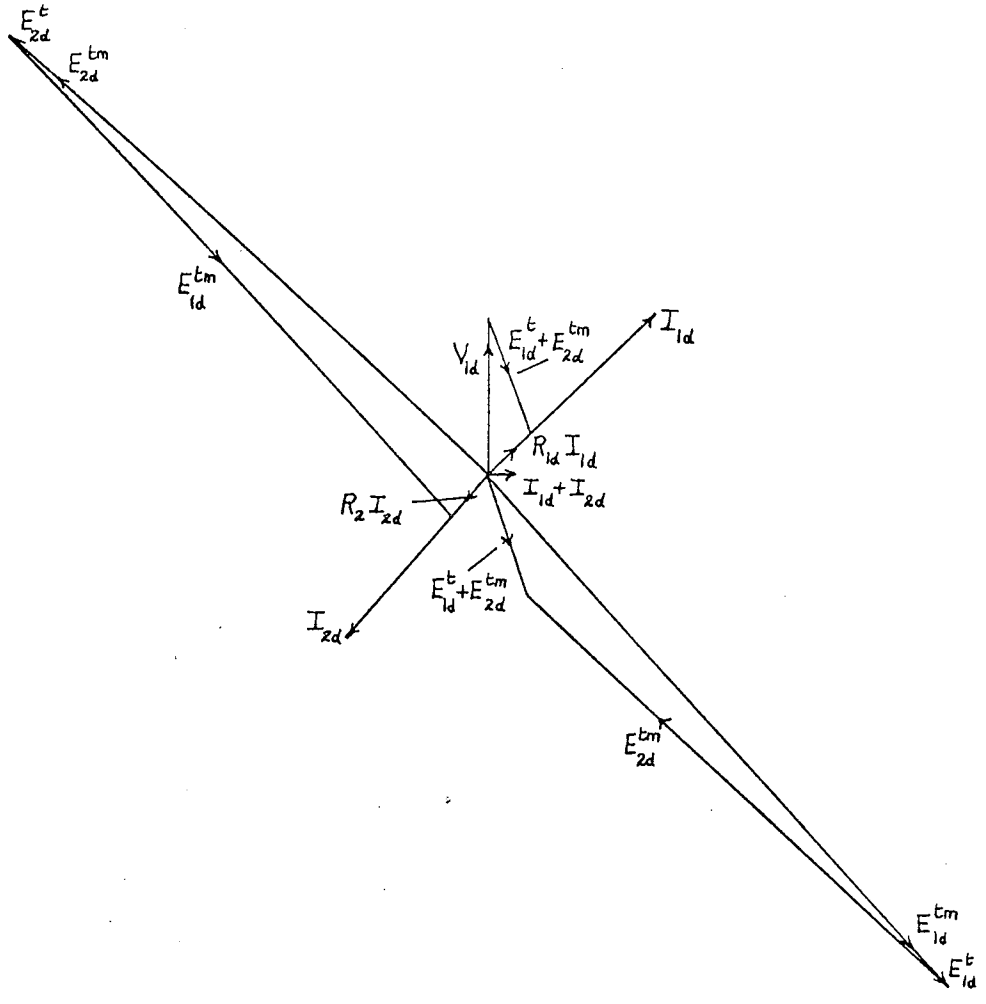

Fig. 4.3 The phasor diagram at standstill for the single-phase induction motor

(The notation is explained in section 4.5.1.)

and the speed increases. The stable operating speed is slightly below the synchronous value.

On no-load the value of the stator current is approximately a minimum and is non-zero, while the q axis rotor current is close to the maximum value. Therefore the phase angle between these currents must be $\pi/2$ for the net torque to be zero. When a load is applied to the shaft the speed decreases, $|I_{2q}|$ decreases, $|I_{1d}|$ increases, and the phase angle between the two currents is reduced until the developed torque equals the load torque. A phasor diagram is shown in Fig. 4.4 (overleaf) for the full-load conditions in the machine; separate diagrams are used to illustrate the current and induced e.m.f.'s in each winding.

4.5.1 The induced e.m.f.'s on load

The conditions existing in the machine for a typical value of load are examined in more detail, using the simplified representation of the machine windings by stationary lumped coils depicted in Fig. 4.2a [2].

Let the single-phase induction motor be replaced by an equivalent commutator machine (for the purpose of this explanation), driven at constant speed, with the d axis brush pair short-circuited and the q axis brush pair temporarily

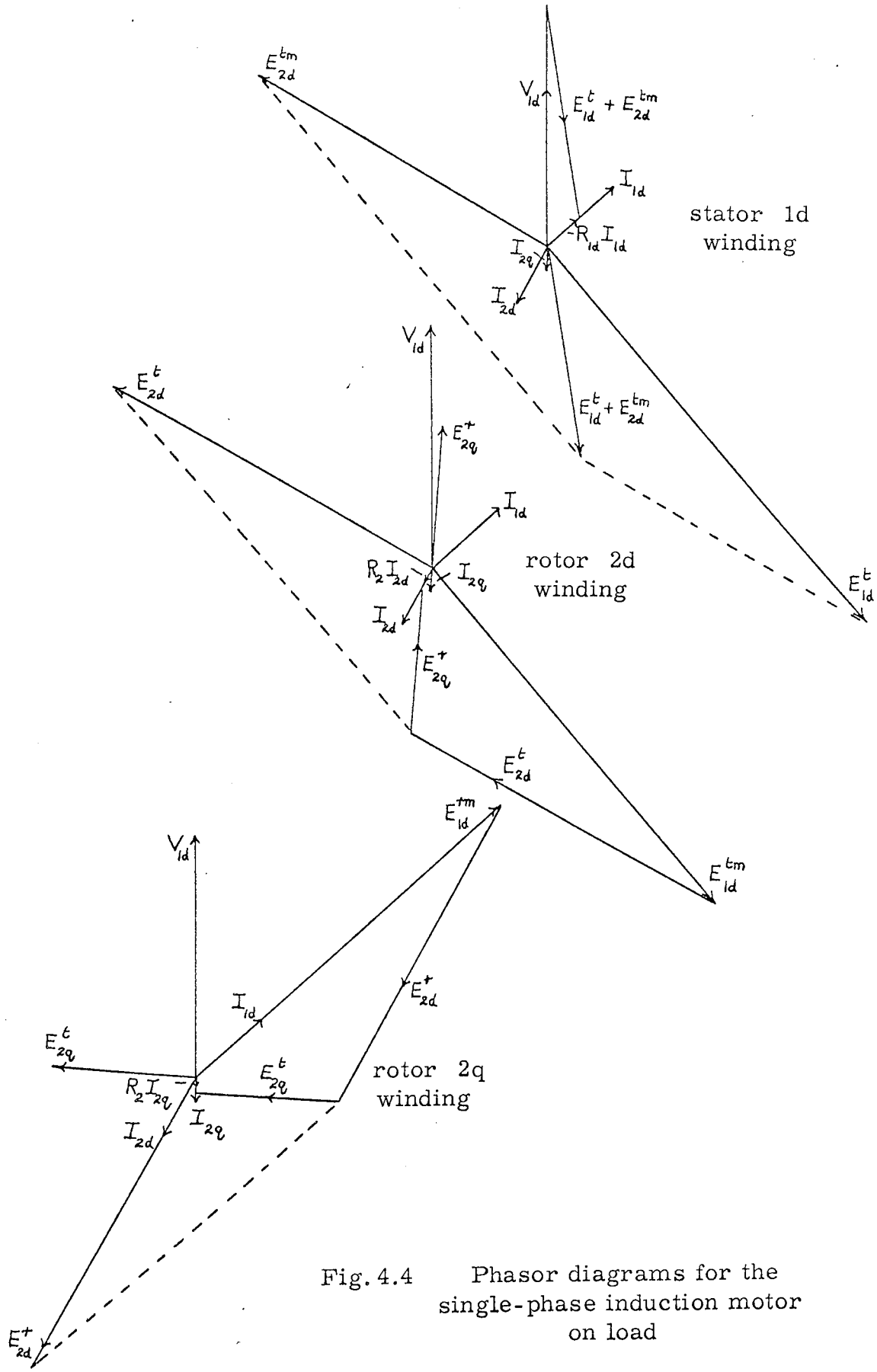

Fig. 4.4 Phasor diagrams for the single-phase induction motor on load

open-circuited. Then the 1d and 2q coils behave as a single-phase transformer regardless of rotation; the pulsation of the stator field induces a transformer e.m.f. E_{1d}^{tm} * in the rotor coil and the pulsation of the resulting rotor field induces an e.m.f. E_{2d}^{tm} in the stator coil. The m.m.f.'s of the two coils act in opposite directions to maintain the air-gap flux-density almost constant over the normal operating range. In fact the explanation could be simplified further, without any loss of general principles, by neglecting the leakage impedance of the stator winding which amounts to an assumption of constant air-gap flux in the d axis.

The e.m.f. induced by the rotation of the actual rotor conductors in the d axis field is represented by the vector sum $(E_{1d}^{rm} + E_{2d}^{r})$ in the q axis rotor coil. The values of these induced e.m.f.'s are shown on the phasor diagram overleaf (Fig. 4.5), where the following relations exist

$$E_{1d}^{rm} = j S E_{1d}^{tm} \qquad E_{2d}^{r} = j S E_{2d}^{t}$$

If the q axis rotor coil is now closed a current circulates through the winding and establishes a stationary field in line with the q axis brushes. The current is mainly magnetizing

---

* Additional superscripts t, r, m are used to indicate the causes of the induced e.m.f.'s: e.g., tm - transformer action of the mutual flux; rm - rotation in the mutual flux. The subscript indicates the source of the flux-linkage.

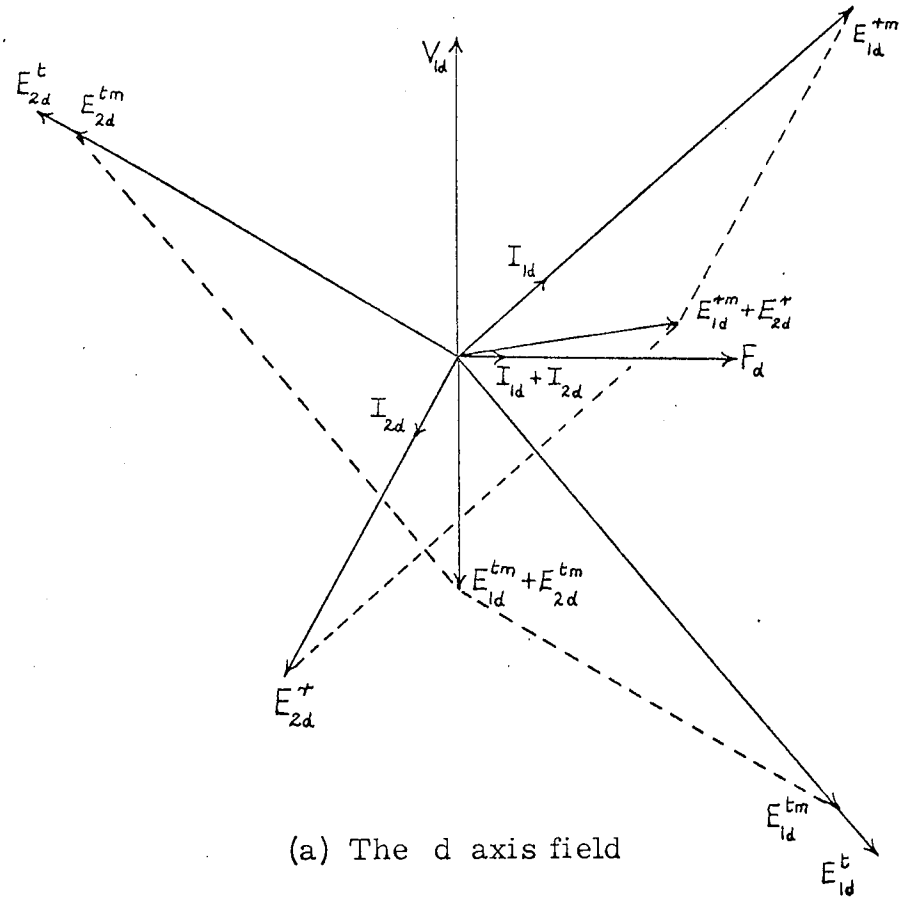

(a) The d axis field

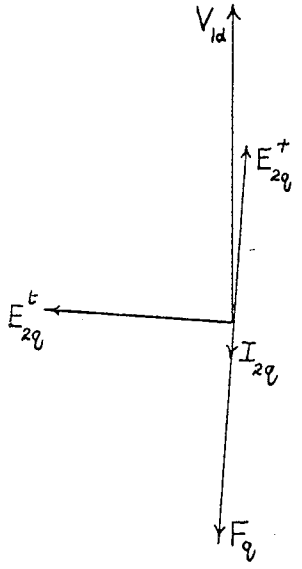

(b) The q axis field

Fig. 4.5 Phasor diagrams for the single-phase induction motor

and is limited by the e.m.f. induced from the pulsation of the q axis field and, to a lesser extent, by the voltage drop in the rotor winding resistance. A second rotational e.m.f. is induced in the rotor by the rotation of the actual conductors in the q axis field and this is represented by the vector E^{r}_{2q} in the d axis rotor coil, where

$$E^{r}_{2q} = -jSE^{t}_{2q}$$

The negative sign is introduced because of the sign convention. The action of the induced e.m.f. E^{r}_{2q} may be likened to that of a voltage applied to the secondary terminals of the single-phase transformer representing the conditions in the d axis, to reduce the primary and secondary currents and the phase angle between them, by effectively increasing the secondary impedance.

The use of the commutator machine enables the various induced e.m.f.'s to be studied separately, but in practice these e.m.f.'s coexist, and the apparent self-excitation process in the q axis following the short-circuiting of the q axis brush pair is a fiction. Hence three induced e.m.f.'s are shown on the phasor diagram (p. 96) for each rotor winding and the resultant e.m.f.'s circulate the currents I_{2d}, I_{2q}. The pulsation of the mutual flux produced by the stator winding and the total flux of the 2d rotor winding induce transformer e.m.f.'s (E^{tm}_{1d}, E^{t}_{2d}) in the 2d

rotor winding, and rotation in the mutual flux induces an e.m.f. E_{1d}^{rm} in the 2q rotor winding. The third e.m.f. induced in the 2d rotor winding (E_{2q}^{r}) is the result of rotation in the 2q rotor field. The remaining e.m.f.'s induced in the 2q rotor coil (E_{2q}^{t}, E_{2d}^{r}) result from the pulsation of the total q axis flux and rotation in the 2d rotor field, respectively.

4.6 The equivalent circuit

The symmetrical form of the electrical performance equation appropriate to the cross-field theory is derived from the corresponding equation for the rotating-field theory by means of the power-invariant transformation equation (2.21). It is significant that the essential operating features of the machine are retained in equation (2.23), with the exception of the rotational voltage terms. Thus the d axis stator and rotor coils are coupled by transformer action, while the two rotor coils are coupled by internal generator action represented in the impedance matrix by negative resistance. Also there is no coupling between the stator d axis and rotor q axis coils.

An equivalent circuit having the same impedance matrix is shown in Fig. 4.6a.

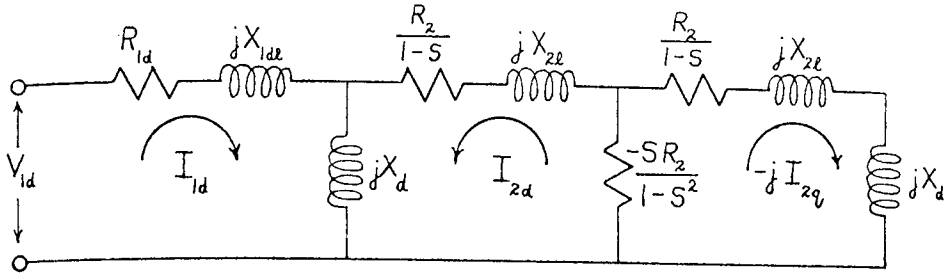

Fig.4.6a

The mesh currents are identified with the hypothetical winding currents and there is a 1:1 correspondence between the elements of the network and the winding parameters. An alternative circuit (Fig. 4.6b) is obtained by reversing the direction of the q axis rotor current.

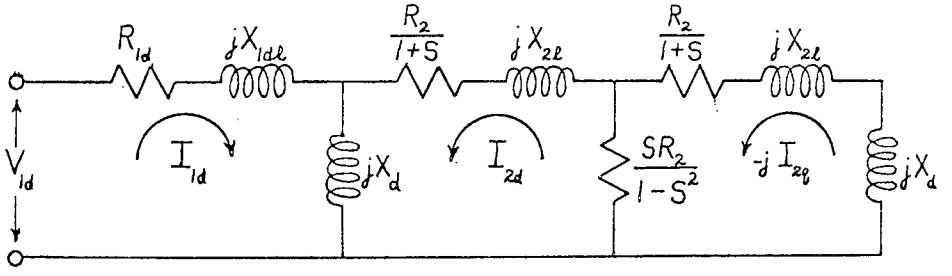

Fig. 4.6b

This avoids the complication of a negative resistance in a practical circuit. Otherwise the parameters are the same as in the previous case, with the exception of the apparent rotor resistance $R_2/(1-S)$, which is replaced by $R_2/(1+S)$. A second advantage, therefore, is that this circuit can be used in a study of

the conditions which exist at synchronous speed.

Similar circuits result from the inclusion of skin effect in the performance equation, but the network elements are not simply related to the winding parameters and it is more convenient to use the equivalent circuit of the rotating-field theory. A network representation may be deduced for the symmetrical form of equation (2.12a) but this is not an equivalent circuit for the machine because it does not include the constraint defined by equation (2.13b).

4.7 The evaluation of the electrical performance equations (3)

The winding currents I_{1d}, I_{2d}, I_{2q} are evaluated from the inverse of equation (2.22) as

$$\begin{bmatrix} I_{1d} \\ I_{2d} \\ I_{2q} \end{bmatrix} = \frac{1}{\Delta} \begin{bmatrix} R_2^2 - (1-s^2)X_2^2 + 2j R_2 X_2 \\ -jX_d\left[R_2 + j(1-s^2)X_2\right] \\ SX_d R_2 \end{bmatrix} \begin{bmatrix} V_{1d} \end{bmatrix} \qquad (4.12)$$

where $\Delta = \left[(R_{1d} + jX_{1d})(R_2 + jX_2)^2 + X_d^2(R_2 + jX_2)\right] + \left[(R_{1d} + jX_{1d})X_2^2 - jX_d^2 X_2\right] S^2$

The denominator Δ is $(1-S^2)$ times the corresponding denominator in equation (3.12) (neglecting skin effect), because rows 2, 3 of equation (2.16a) are divided by (1-S), (1+S) respectively.

The present denominator may be separated into real and imaginary parts as

$$\Delta = U + jW \tag{4.13}$$

..where $U = R_{1d}R_2^2 - 2R_2X_{1d}X_2 + R_2X_d^2 - R_{1d}X_2^2(1-S^2)$

$$W = 2R_{1d}R_2X_2 + R_2^2X_{1d} - X_2(X_{1d}X_2 - X_d^2)(1-S^2)$$

Over the normal operating range, W is small compared with U, and is zero at a speed slightly below the synchronous value.

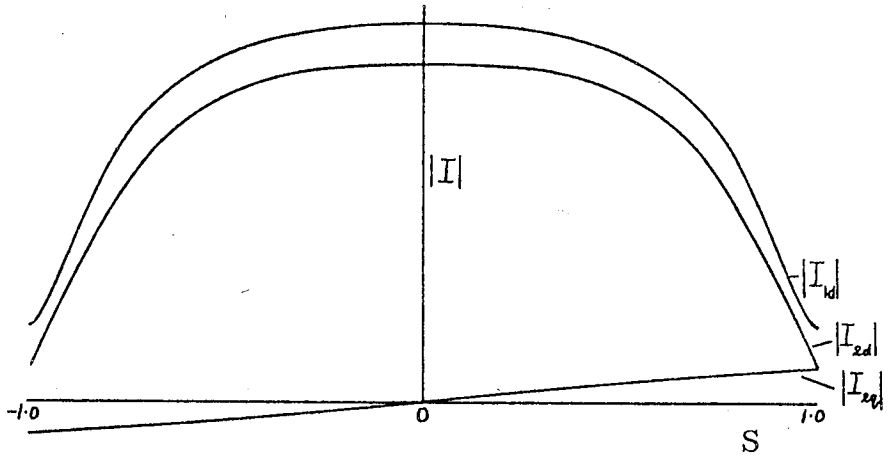

Fig. 4.7

The forms of the current/speed curves for the 3 currents are shown in Fig. 4.7; $|I_{1d}|$, and $|I_{2d}|$ are even functions as would be expected from equation (4.12), but $|I_{2q}|$ is an odd function because of the odd power of speed in the numerator of the current expression.

4.7.1 The $\underset{\sim}{\xi}$ functions

As with the rotating-field theory, the rotor currents are expressed in terms of the stator current by the introduction of suitable $\underset{\sim}{\xi}$ functions. These are defined by

$$\frac{I_{2d}}{I_{1d}} = -\frac{X_d}{X_2}\,\underset{\sim}{\xi}_{2d}\,, \qquad \frac{I_{2q}}{I_{1d}} = -\frac{X_d}{X_2}\,\underset{\sim}{\xi}_{2q}\,, \qquad \frac{I_{2q}}{I_{2d}} = \frac{\underset{\sim}{\xi}_{2q}}{\underset{\sim}{\xi}_{2d}}\,. \tag{4.14a}$$

The alternative definitions in terms of the winding parameters and speed can be deduced from equation (4.12) (these are given in Appendix II), but it is simpler to use the corresponding definitions of the functions $\underset{\sim}{\xi}_{2f}$, $\underset{\sim}{\xi}_{2b}$ from the rotating-field theory (equation (3.13)), when

$$\underset{\sim}{\xi}_{2d} = \tfrac{1}{2}\left(\underset{\sim}{\xi}_{2f} + \underset{\sim}{\xi}_{2b}\right), \qquad \underset{\sim}{\xi}_{2q} = -\tfrac{1}{2}j\left(\underset{\sim}{\xi}_{2f} - \underset{\sim}{\xi}_{2b}\right) \quad \text{(neglecting skin effect)} \tag{4.14b}$$

The functions $\underset{\sim}{\xi}_{2d}$, $\underset{\sim}{\xi}_{2q}$ are shown in Fig. 4.8 (overleaf) for various values of the ratio X_2/R_2 over the speed range $0 \leqslant S \leqslant 1$. The $\underset{\sim}{\xi}$ functions are examined in Appendix II and a construction is given for use with any value of X_2/R_2. The variation of the modulus of $\underset{\sim}{\xi}_{2d}$ is similar to that for $\underset{\sim}{\xi}_{2f}$, but at synchronous speed $|\underset{\sim}{\xi}_{2d}| \simeq 0.5$ (for $X_2/R_2 > 5$) so that the rotor current $|I_{2d}|$ is approximately one-half of the stator current and the two are almost in antiphase. The phase shift in $\underset{\sim}{\xi}_{2d}$ has a maximum value of about $20°$(e) and this normally occurs for speeds in the range $0.9 \leqslant S \leqslant 1.0$. The behaviour of $\underset{\sim}{\xi}_{2q}$ is quite different

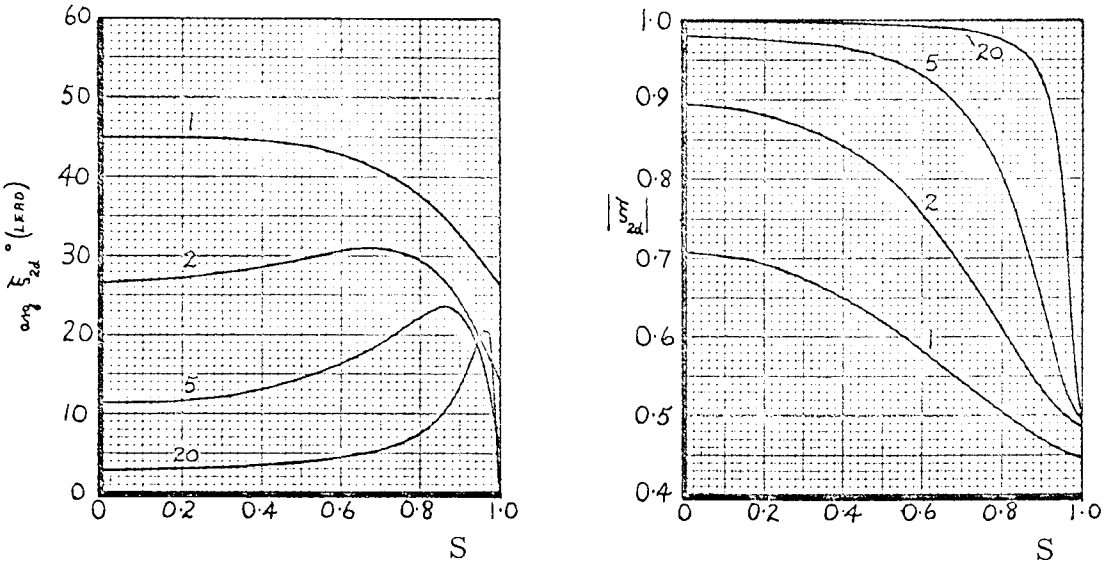

(a) ξ_{2d}

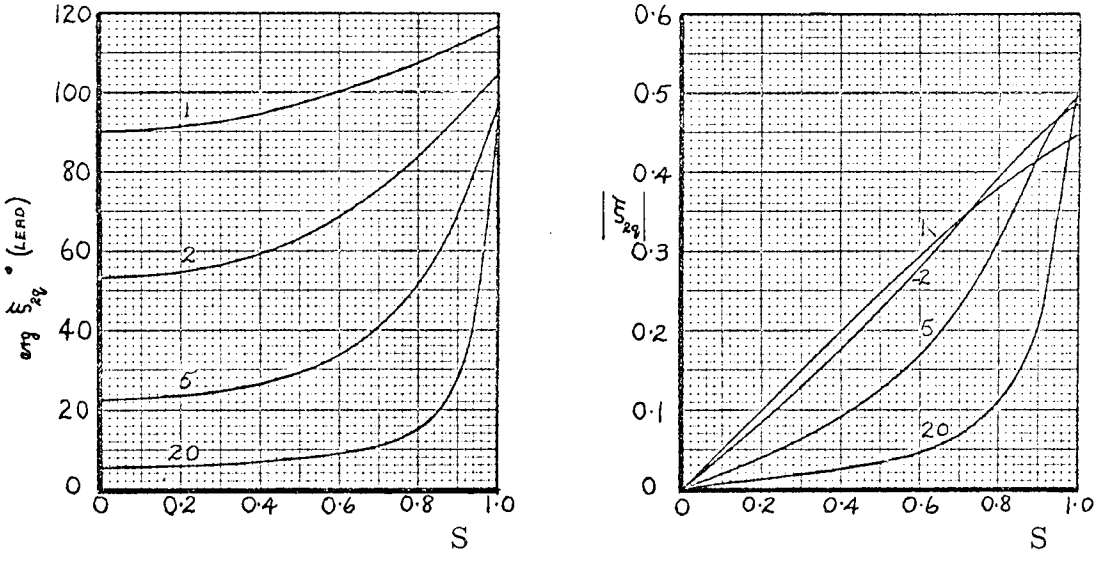

(b) ξ_{2q}

Fig. 4.8 Graphs showing the variation of the ξ functions with speed for 4 values of X_2/R_2.

from the other functions; for values of speed in the range $0 \leqslant S \leqslant 0.5$, the modulus is proportional to speed but thereafter, for typical values of X_2/R_2, it increases rapidly and at synchronous speed is equal to $|\underset{\sim}{\xi}_{2d}|$. The curves for arg $\underset{\sim}{\xi}_{2q}$ show similar variations, with a phase change of almost $\pi/2$ over the range $0 \leqslant S \leqslant 1$. A horizontal line on the graph through the 90° ordinate is a zero torque line, since the scalar product $I_{1d} . I^*_{2q}$ in the torque equation is then zero and hence the developed torque is zero.

4.7.2 The winding currents

4.7.2.1 The stator current

The stator current is evaluated from row 1 of equation (4.12) in terms of $\underset{\sim}{\xi}$ functions as

$$I_{1d} = V_{1d} \Big/ \left\{ R_{1d} + j X_{1d} \left[1 - \frac{X_d^2}{X_{1d} X_2} \underset{\sim}{\xi}_{2d} \right] \right\} \qquad (4.15)$$

When skin effect is neglected, it follows from equations (4.14b) and (3.14) that the expressions for the stator current deduced from either theory are the same and the remarks of section 3.7.2.1 also apply here. In the present section, these remarks are extended from the further insight afforded by the cross-field theory.

The denominator of equation (4.15) can be expressed

$$R + jX = \left\{ R_{1d} + X_d \left[\frac{X_d}{X_2} \mathcal{I}m\, \underset{\sim}{\xi}_{2d} \right] \right\} + j \left\{ X_{1d\ell} + X_d \left[1 - \frac{X_d}{X_2} \mathcal{R}e\, \underset{\sim}{\xi}_{2d} \right] \right\} \qquad (4.16)$$

This impedance may also be deduced from a voltage-balance equation for the input mesh of the equivalent circuit or, of course, from row 1 of the performance equation (2.22).

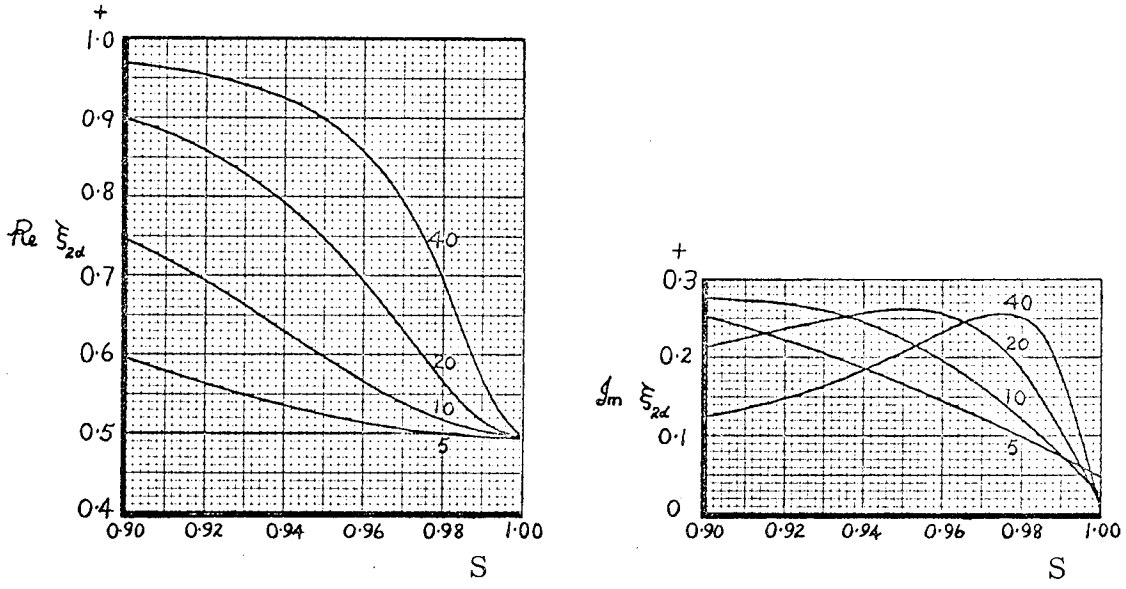

Fig. 4.9

The real and imaginary parts of the function ξ_{2d} are shown in Fig. 4.9, and are used in the evaluation of equation (4.16). The real part (R) of the motor impedance is sensibly constant over the range $0 \leq S \leq 0.5$, but at higher speeds it increases to a maximum value and then falls, being quite small at synchronous speed. A similar maximum is not observed with the imaginary part (X) of the motor impedance which is compounded from the total reactance of the stator winding and a proportion X_d/X_2 of the function Re ξ_{2d}. Since the latter is a monotonic decreasing

function, the reactance increases steadily over the range $0 \leq S \leq 1$.

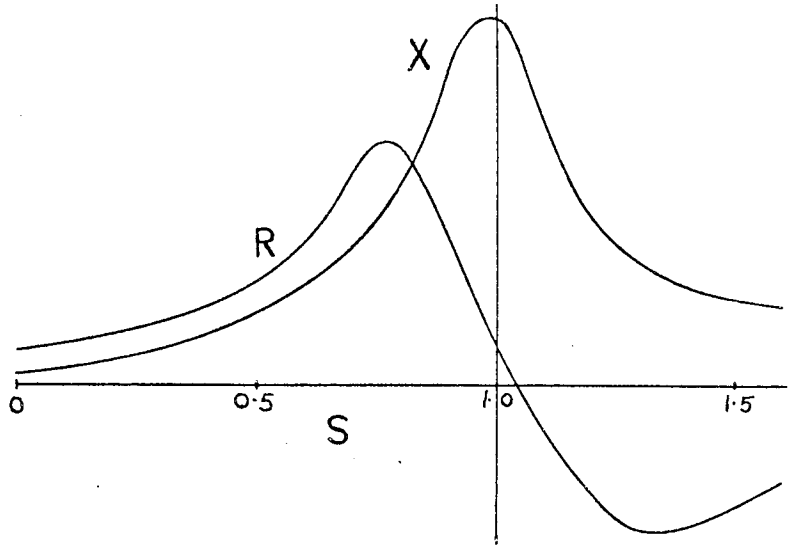

Fig. 4.10

These variations are shown in Fig. 4.10; the net effect causes the stator current to be almost constant at low speeds, and then to fall over the normal operating range. The power-factor follows a similar variation to that of the current; it is quite low on no-load (typically 0.2), rises sharply over the normal operating range and then levels out to the standstill value (typically 0.7).

The variations of the modulus and argument of the current over the speed range $0.9 \leq S \leq 1.0$ for 4 values of the ratio X_2/R_2 are shown in Fig. 4.11 (overleaf) - these correspond to the curves of Fig. 3.10, being calculated for the conditions specified in section 3.7.2.1 .

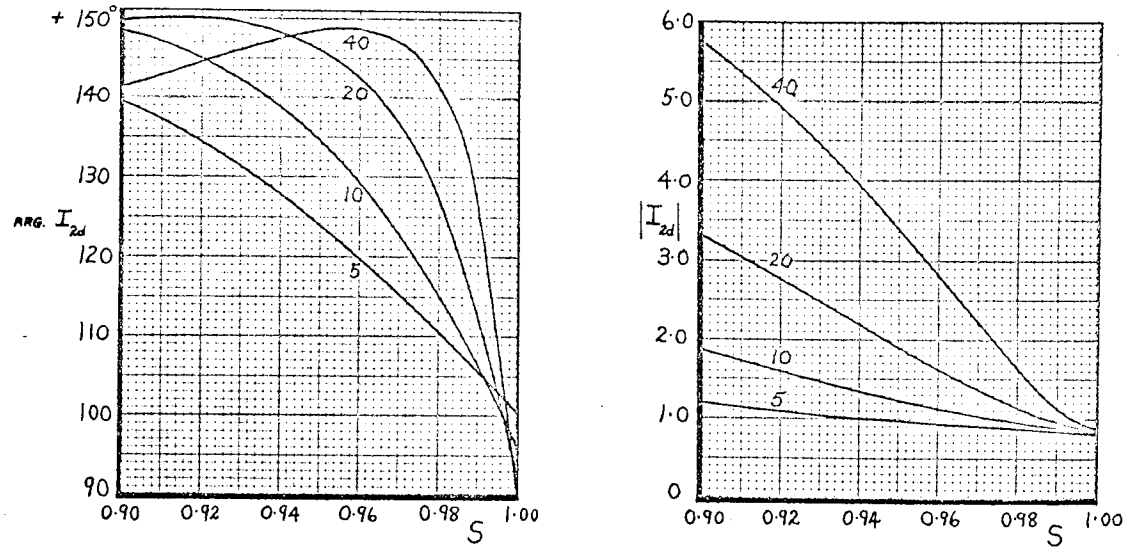

(a) The rotor current I_{2d}

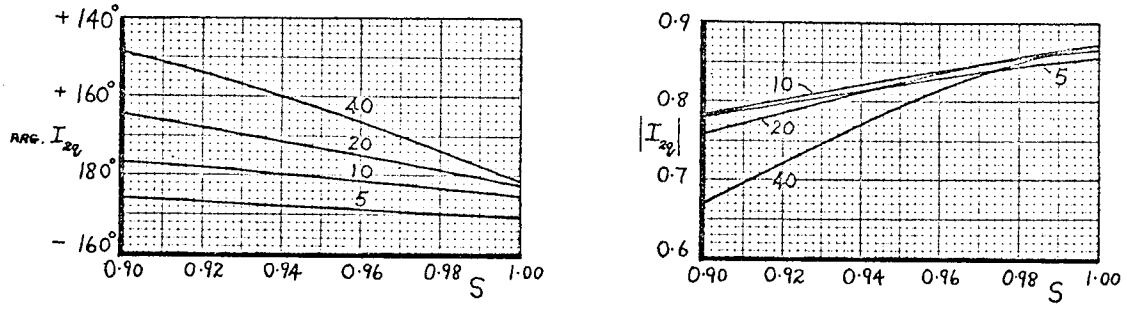

(b) The rotor current I_{2q}

Fig. 4.11 The rotor and stator currents

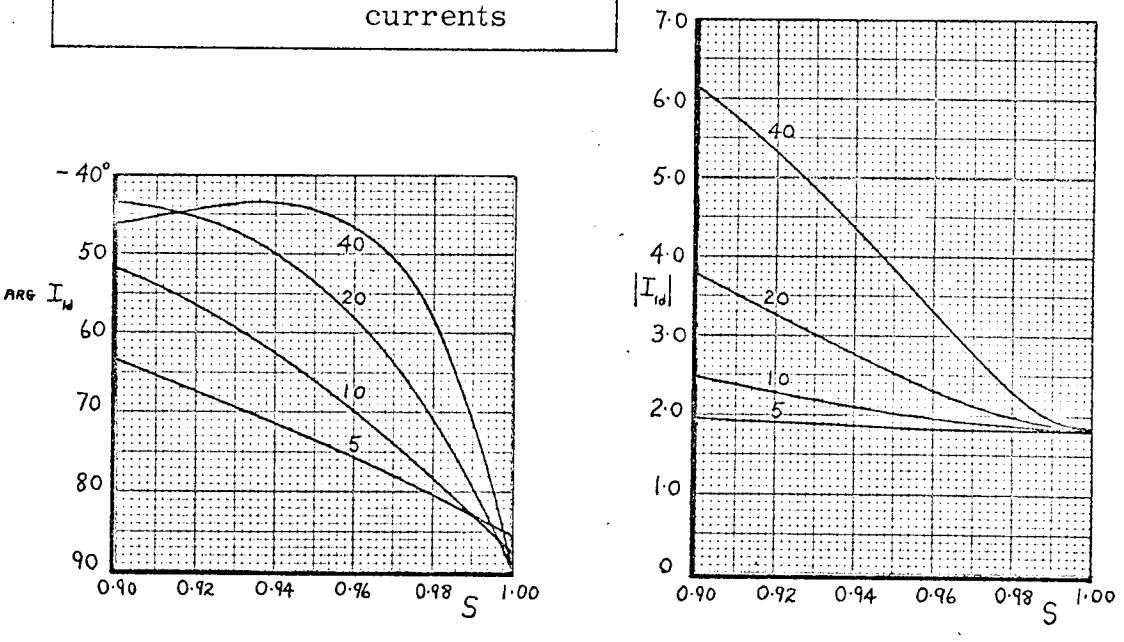

(c) The stator current I_{1d}

4.7.2.2 The rotor currents

The values of the rotor currents I_{2d}, I_{2q} are derived from the stator current by use of the ξ functions defined in equation (4.14a). These variations are shown in Fig. 4.11 (p. 109), and specimen calculations are given in Appendix III.

The curves of the argument and modulus of the d axis rotor current are of a similar form to the corresponding curves for the stator current, with a somewhat greater change in the phase angle over the speed range and a reduction in the modulus. At synchronous speed $|I_{2d}|$ is slightly less than a half of $|I_{1d}|$, and is equal to $|I_{2q}|$.

Fig. 4.8 shows that arg ξ_{2q} changes considerably over the range $0.9 \leqslant S \leqslant 1.0$ and this has the effect of keeping I_{2q} almost in antiphase with V_{1d}. For speeds greater than 0.96, the X_2/R_2 ratio has little effect on $|I_{2q}|$ and this lies between 0.82 and 0.87 (approximately).

4.7.2.3 No-load conditions

The no-load speed is the value of speed for which the currents I_{1d}, I_{2q} are in phase quadrature. Referring to equation (4.12), this is given by

$$S^{nl} = \left\{1 - \left(\frac{R_2}{X_2}\right)^2\right\}^{1/2} \qquad (4.17)$$

The no-load current is determined from equations (4.12) and (4.17) as

$$I_{1d}^{nL} = V_{1d} \Big/ \left\{ R_{1d} + j X_{1d} \left[1 - \tfrac{1}{2} \frac{X_d^2}{X_{1d} X_2} \left(1 + j \frac{R_2}{X_2} \right) \right] \right\} \tag{4.18}$$

Let the magnetizing component of the current be approximated as

$$I_{1d}^{nL}(mag) = V_{1d} \Big/ \left\{ j X_{1d} \left[1 - \tfrac{1}{2} \frac{X_d^2}{X_{1d} X_2} \right] \right\} \tag{4.19}$$

$$= \frac{V_{1d}}{j X_{1d}} + \frac{V_{1d}}{j X_{1d}} \frac{1}{\left\{ 2 \frac{X_{1d} X_2}{X_d^2} - 1 \right\}} \tag{4.20}$$

Equation (4.20) consists of two parts; the first is the approximate phase value of the magnetizing current of a similar two-phase machine; the second is the additional current required for single-phase operation. The latter term is usually about 0.8 of the former (for $X_2/X_d \simeq 1.05$). A further insight into the equation is gained with the aid of the equivalent circuit (Fig. 4.6b, p. 101) adapted for the purpose by omitting the resistors and the coupling between the d, q rotor circuits.

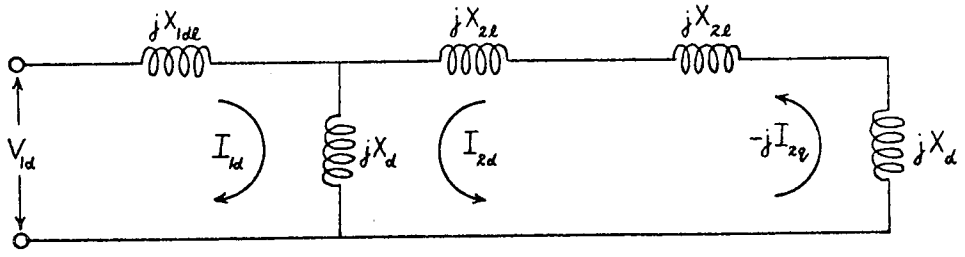

For this condition

$$I_{1d} = I_{1d}^{nL}(mag), \qquad I_{2d} = -\tfrac{1}{2} \frac{X_d}{X_2} I_{1d}, \qquad I_{2q} = j I_{2d}. \tag{4.21}$$

Evaluating I_{2q} as the q axis magnetizing current from equations (4.19) and (4.21)

$$I_{2q} = -V_{1d} \Big/ \left\{ X_d \left[2 \frac{X_{1d} X_2}{X_d^2} - 1 \right] \right\} \tag{4.22}$$

Thus the magnitude of the second term in equation (4.20) is X_d/X_{1d} times the q axis magnetizing current. The phase difference between the two quantities is consistent with the idea that the q axis current is the result of converted mechanical energy and is not supplied directly from the d axis current.

The d axis magnetizing current $(I_{1d} + I_{2d})$ is lower than the two-phase value because of the shunt effect of the q axis circuit. Thus

$$I_{1d} + I_{2d} = \frac{V_{1d}}{j X_{1d}} \frac{\left(1 - \frac{1}{2} \frac{X_d}{X_2}\right)}{\left(1 - \frac{1}{2} \frac{X_d^2}{X_{1d} X_2}\right)} \simeq \frac{V_{1d}}{j X_{1d}} \left(\frac{X_d}{X_2}\right) \tag{4.23}$$

where the approximate value is lower than the more accurate value. The ratio of the q and d axis magnetizing currents is

$$\frac{|I_{2q}|}{|I_{1d}| + |I_{2d}|} = \frac{1}{2 \frac{X_2}{X_d} - 1} \tag{4.24}$$

Equation (4.24) is important in the empirical allocation of the core losses between the two axes. It is usual to assume a ratio of 45/55 which corresponds to a value of X_2/X_d of approximately 1.05 .

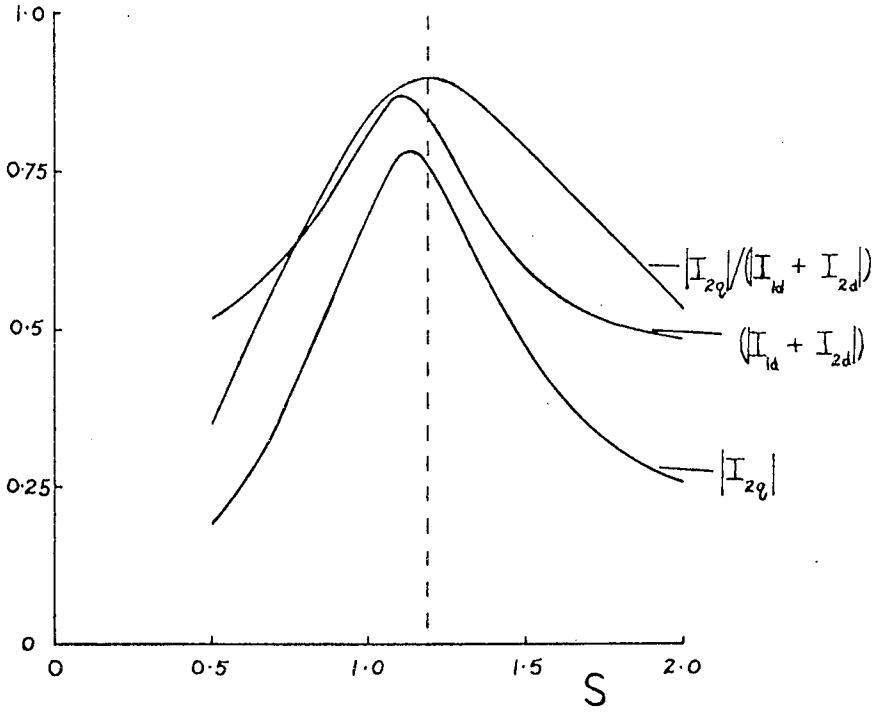

Fig. 4.12

Typical curves of the magnetizing currents in the two axes and of the ratio between them, are shown in Fig. 4.12 for speeds near to the synchronous value.

4.8 Comment

In the cross-field theory the mode of operation of the machine is discussed in terms of pseudo-stationary coils; a general form of the theory may be developed for a double-layer model rotor in which skin effect is included, but the accepted form as presented in this chapter is restricted to the single-layer rotor. Hence the cross-field theory is not applicable to machines

which exhibit skin effect. With this proviso, the theory provides an alternative viewpoint which is equally as valid, and as simple, as the rotating-field theory. Skin effect phenomena can be included in the performance equations for the single-layer rotor using 2d, 2q variables (equation (2.20a)), but a physical interpretation of the additional terms is meaningless.

CHAPTER V

THE HARMONY OF THE TWO THEORIES

CHAPTER V

THE HARMONY OF THE TWO THEORIES

5.1 Chapter outline

The conditions for the equivalence of the rotating-field and cross-field theories are established in Chapter II, and 'term by term' explanations are given in succeeding chapters for the alternative performance equations. The purpose of the present chapter is to examine the extent to which these explanations are complementary, in a study of the overall performance of the machine.

It is shown in section 3.3 that a single magnetic field exists in the machine and that this is related to the resultant m.m.f. waveform. In the linear theory, which follows that section, the importance of the premiss is lost because the physical descriptions are developed more conveniently by reference to the resolutes of the m.m.f. waveform. However, in a complete theory a knowledge of how the single magnetic field varies is necessary for the explanation of the oscillatory component of the developed torque, the assessment of the effect of saturation, and for the apportionment of losses. The nature of this field is examined for the air-gap region and it is shown that in the

single-phase induction motor, unlike the two-phase machine, the apparent variation of the field depends upon the choice of reference axis.

The study of the air-gap field is extended by a discussion of the hysteresis loss which would occur in an ideal smooth rotor. Apart from this simple example, core losses are not discussed in detail. However, an examination is made of the usual modifications to the equivalent circuits which permit simple approximations for the losses to be included in the performance calculations; these modifications are necessarily empirical, and any subsequent agreement between predicted and test characteristics is not an argument in favour of one theory or another.

A study is made of the performance characteristics over the normal operating range, including the extent to which these are modified by skin effect and changes in the X_2/R_2 ratio. It is shown that if the operating speed is near to the synchronous value then the stator current, developed torque, and speed are only slightly affected by skin effect, but that a noticeable reduction in efficiency occurs for all speeds. The use of the cross-field theory for a cage rotor machine is examined and it is concluded that in the determination of the stator current and developed torque, less error is incurred by neglecting skin effect

than by using modified values of the rotor parameters. The numerical values used to illustrate the various points are taken from the performance calculations given in Appendix III.

5.2 The air-gap magnetic field

5.2.1 Stationary reference axes

In the rotating-field theory, the stator m.m.f. is resolved into oppositely rotating waves and it is assumed that similar waves are set up by the rotor. The two forward rotating waves combine to form a resultant forward rotating m.m.f. wave, while the two backward rotating waves form the resultant backward rotating m.m.f. wave. The equivalent m.m.f. vectors are designated $\frac{1}{2}\hat{F}_f$, $\frac{1}{2}\hat{F}_b$ in the notation of equation (3.4), and are shown in Fig. 5.1 (overleaf) as two contra-rotating vectors in space. The length of each vector is constant for a given value of speed, and the velocity is constant. Hence the locus of the resultant m.m.f. is an ellipse.

In the cross-field theory *, the d axis stator and

---

* The differences in the two forms of the cross-field performance equations are limited to the rotor self-impedance and mutual coupling terms, and the mutual flux-linkage between the stator and rotor is the same in each case. Hence a qualitative discussion of the air-gap field is not modified by skin effect. This point is returned to in section 5.3.1 .

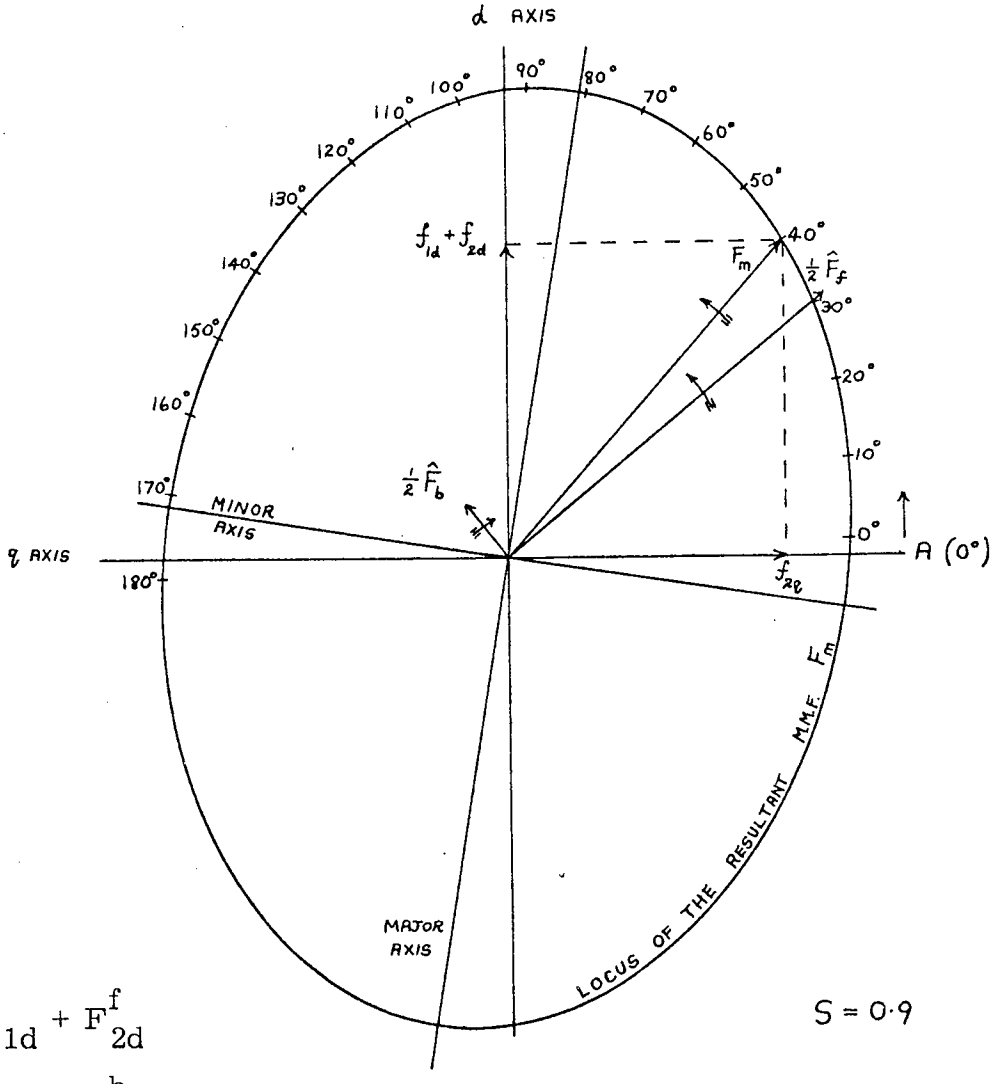

$$F_f = F_{1d} + F^{f}_{2d}$$

$$F_b = F_{1d} + F^{b}_{2d}$$

Fig. 5.1 The locus of the resultant m.m.f. vector viewed from the stator.

rotor m.m.f.'s form a resultant m.m.f. which is stationary in space and pulsating in time. In the q axis, only the rotor m.m.f. is present and this is also stationary in space and pulsating in time. The equivalent instantaneous values of the m.m.f. waves are designated $(f_{1d} + f_{2d})$, (f_{2q}), respectively, and are shown on Fig. 5.1 (p. 119) as two stationary vectors having a variable amplitude and displaced in phase, in line with the d, q axes. The two vectors pulsate at line frequency and the locus of the resultant is the same ellipse as described above for the rotating-field theory.

The relations between the m.m.f.'s in the two theories are defined from equation (2.21) as

$$(F_{1d} + F_{2d}^{f}) = (F_{1d} + F_{2d}) + j\,(F_{2q}) \quad , \quad (F_{1d} + F_{2d}^{b}) = (F_{1d} + F_{2d}) - j\,(F_{2q}) \qquad (5.1)$$

Given the d, q axis quantities, the f, b quantities may be deduced from a phasor diagram using the relations defined in equation (5.1). Both sets of phasors are modified and transferred to a space vector diagram: the d, q currents are represented as instantaneous values of m.m.f. along the d, q axes and the f, b currents as one-half of the maximum values of the rotating m.m.f.'s. In the latter case the angles on the time diagram between the stator voltage reference phasor and the f, b current phasors (measured anticlockwise), are marked out to the left and right of the d axis on the space diagram to be consistent with the opposite

directions of rotation of the f and b vectors. The positions of the vectors on the space diagram which correspond to the positions on the time diagram define the datum (0°) on the locus of the resultant m.m.f.. This is marked in equal time intervals (defined by the position of a vector rotating at synchronous speed) and the resultant vector traces the elliptic locus once per cycle of the supply frequency.

The resultant m.m.f. vector F_m rotates in the same direction as the forward rotating component and in the same direction as the rotor. The instantaneous value of the angular velocity exhibits a periodic variation about a mean value which is the same as the velocity of the forward rotating component.

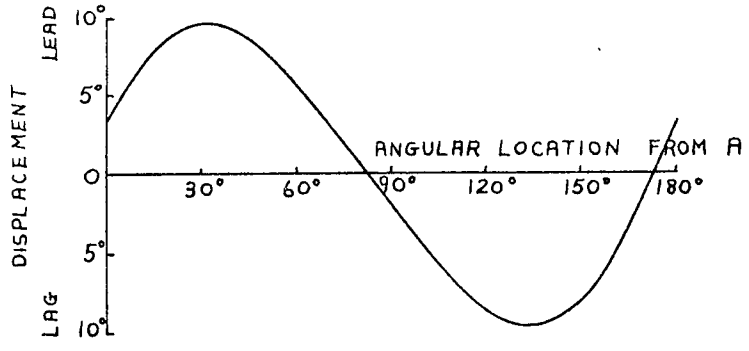

(A is defined in Fig. 5.1, p. 119)

Fig. 5.2

The cyclic variation is shown in Fig. 5.2, where the zeros correspond to the locations of the principal axes of the ellipse (measured from the datum A). The fundamental period is twice

that of the supply, but the variation is not a simple sine wave because the oscillation is the result of a change of relative angular position between the resultant m.m.f. vector and a hypothetical vector rotating at a constant angular velocity. To achieve a given displacement in advance of the resultant requires a larger angular velocity than the same position behind the resultant, and hence the principal slopes of the displacement curve, through the zeros, are different. The variable amplitude and angular velocity of the resultant m.m.f. vector are linked directly with the oscillatory variation superimposed on the mean speed of the rotor and the oscillatory developed torque. These oscillations are not observed when the locus of the resultant m.m.f. is a circle.

The condition for a pure positive rotating m.m.f. vector is that

$$f_{1d} + f_{2d} = j f_{2q} \tag{5.2}$$

or, using the rotating-field theory, from equation (5.1)

$$F_{1d} + F^{b}_{2d} = 0$$

Assuming that an equivalent equation can be written in terms of the winding currents, the substitution of these from equation (4.12) results in the twin conditions that

$$S = 2\frac{X_2}{X_d} - 1, \quad \text{and} \quad S = \left\{1 - \frac{R_2^2}{X_2 X_{2\ell}}\right\}^{\frac{1}{2}} \tag{5.3}$$

These equations are not compatible except in the hypothetical case of a rotor with zero leakage impedance. The physical requirements for a pure rotating-field are that the amplitudes of the resultant d and q axis m.m.f. vectors are the same and that there is a phase displacement of $\pi/2$ between the vectors.

(i) The diagram given on p. 113 (Fig. 4.12) is typical of the conditions found in many machines, and it shows that the magnitudes of $(I_{1d} + I_{2d})$ and (I_{2q}), (and hence the corresponding m.m.f.'s) cannot be equal even at a speed above the synchronous value.

(ii) The condition that the vectors be in time phase quadrature is realised at a speed defined by the second relation in equation (5.3): i.e., slightly below no-load.

Hence a pure rotating m.m.f. waveform cannot exist in a practical machine, although the rotor m.m.f. can be represented by a pure rotating vector for the synchronous speed condition (this vector rotates in the opposite direction to the rotor).

At the value of speed for which the d, q m.m.f.'s are in time phase quadrature the major and minor axes of the ellipse are coincident with the d and q axes respectively. Below this speed, and hence over the normal operating range, the principal axes are

rotated slightly backward, while above the given value of speed the axes are rotated slightly forward.

5.2.2 Rotating reference axes

The preceding explanations relate to the variation of the resultant m.m.f. with respect to stationary reference axes (stator axes). Consider now the variation of the same m.m.f. waveform when viewed from the rotor [1].

5.2.2.1 Synchronous speed

First, let the explanation be simplified by assuming the rotor leakage impedance to be negligibly small and the rotor speed to equal the synchronous value. Then the backward rotating m.m.f. $\frac{1}{2}\hat{F}_b$ is zero and the forward rotating m.m.f. $\frac{1}{2}\hat{F}_f$ is stationary with respect to the rotor.

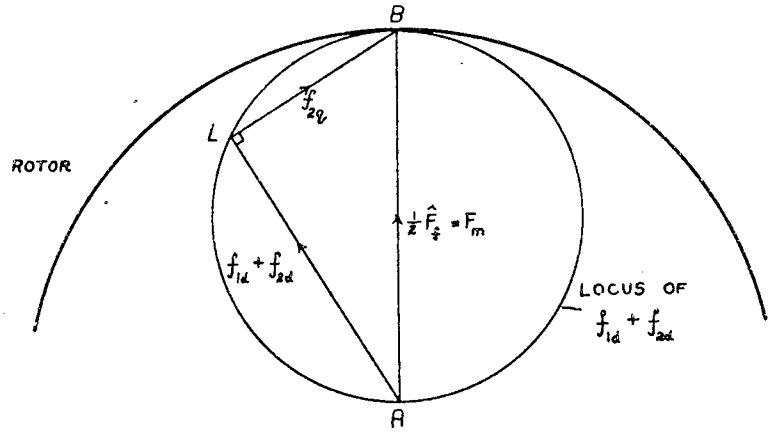

Fig. 5.3

The m.m.f. may be represented (Fig. 5.3) as the diameter (AB) of a circle, with the circumference as the locus of the d axis m.m.f. vector. As the rotor moves through 2π the extremity of $(f_{1d} + f_{2d})$ traces out the circumference of the circle twice. The other end of the d axis m.m.f. vector is located on the diameter at the intersection with the circumference (A); while a line (LB) drawn from the locus point to the other end of the diameter (B) represents the q axis m.m.f. vector, since it is at right-angles to the d axis m.m.f. vector and the sum of the two is equal, at all times, to the forward m.m.f. .

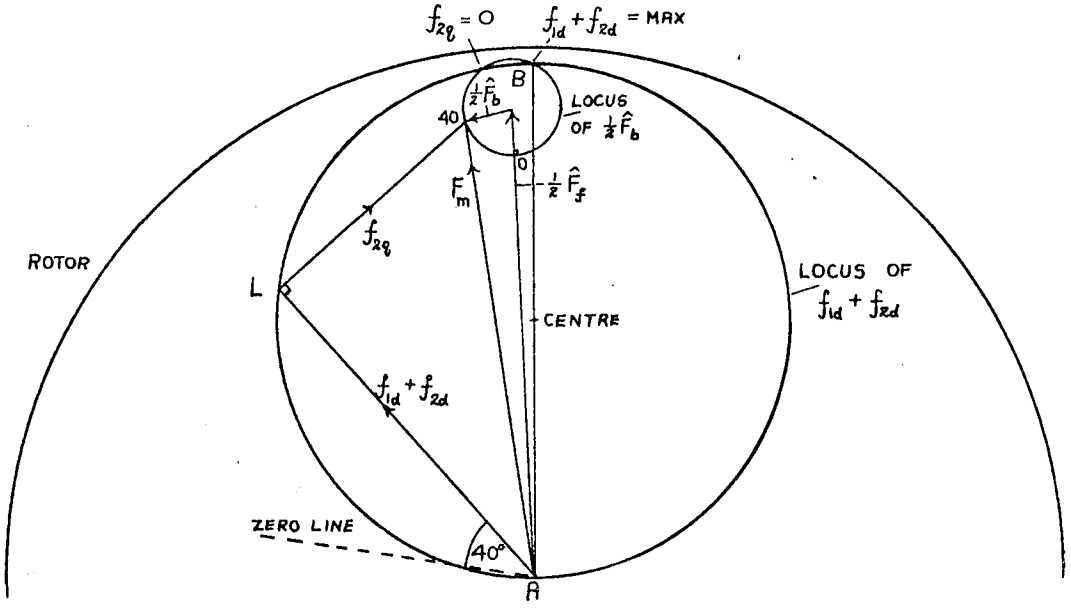

Fig. 5.4a

Now suppose that the rotor impedance is not negligible. The resultant m.m.f is no longer equal to the forward m.m.f., but is

compounded from this and the small backward m.m.f. as shown in Fig. 5.4a. The forward m.m.f. vector is stationary with respect to the rotor but the backward m.m.f. rotates at twice synchronous speed. On the diagram the locus of the extremity of the backward m.m.f. vector is represented by a small circle. The resultant m.m.f. is also equal to the vector sum of the d, q axis m.m.f.'s, as in the simplified case, and the locus of the extremity of the d axis m.m.f. vector (L) is a circle. The diameter (AB) of the larger circle is equal to the maximum value of $(f_{1d} + f_{2d})$, and the space angle between this and the zero line (defined above) is equal to the time phase angle between the d axis m.m.f. phasor and the stator voltage reference phasor. This phase angle is not the same as the phase angle of the resultant m.m.f. phasor and therefore on the space diagram the forward m.m.f. vector and the diameter (AB) are displaced by a small angle. A line (LB) represents the direction of the q axis m.m.f. and the intercept between the two circular loci is equal to the instantaneous value in time of this vector. The two circular loci intersect in two points; the first (B), previously mentioned, represents the maximum value of $(f_{1d} + f_{2d})$; the second represents the position at which (f_{2q}) is zero. Thus at synchronous speed the resultant m.m.f. vector appears to oscillate about a fixed position at twice

the supply frequency, and at the same time to vary in amplitude.

5.2.2.2 Asynchronous speeds

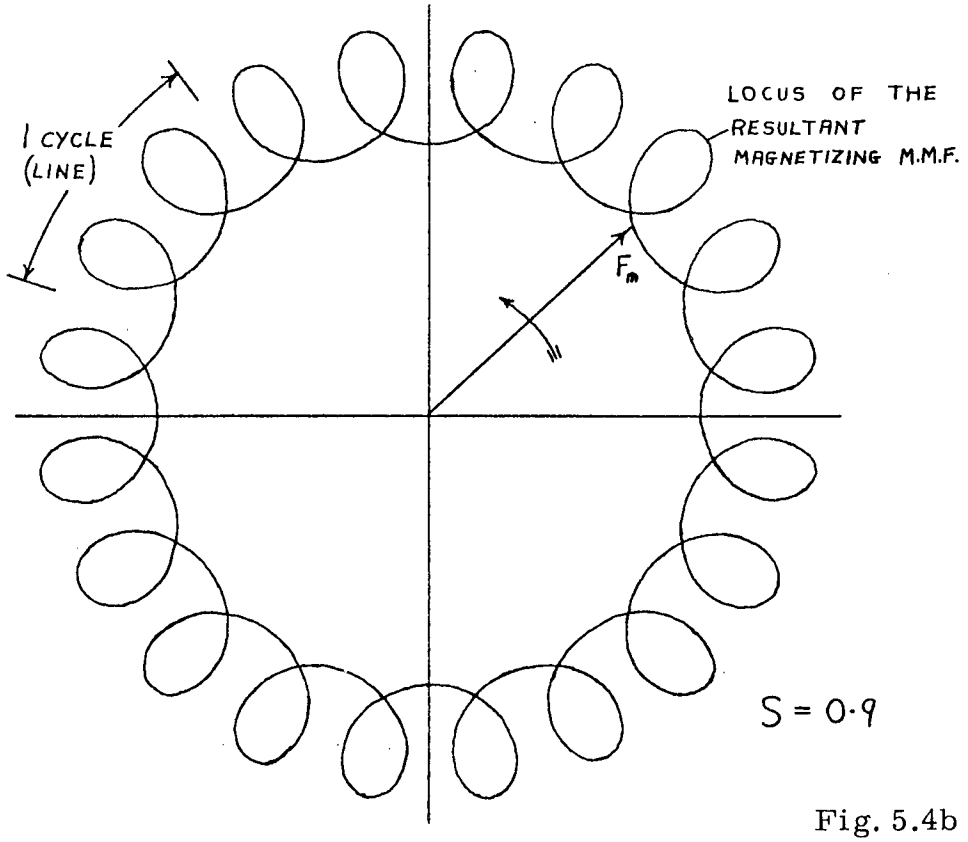

Fig. 5.4b

At any speed other than synchronous the forward m.m.f. vector appears to rotate with an angular velocity $(1-S)\omega$ with respect to the rotor. The backward m.m.f. vector rotates at angular velocities $-(1+S)\omega$ and -2ω with respect to the rotor and the forward m.m.f. vector respectively. The same basic construction for the space diagram which is used for synchronous

speed is applicable for any given angular position in the general case, but as the forward m.m.f. vector rotates the resultant m.m.f. vector not only varies in amplitude but also rotates. Below synchronous speed this rotation is anticlockwise and the locus of the extremity of the vector is a retrograde epicycle (Fig. 5.4b) being formed from two component vectors rotating in opposite directions [2]. Above synchronous speed the rotation of the resultant m.m.f. vector is clockwise and the locus is a direct epicycle since the component vectors now rotate in the same direction when viewed from the rotor. In the time taken to complete one cycle at supply frequency, the backward m.m.f. vector traces out the circular locus twice and the forward m.m.f. vector moves through an angle $2\pi(1-S)$. Hence the number of rotations of the backward vector in a complete cycle of the forward vector is $2/(1-S)$ and if this is an integer then the locus closes in 2π.

5.2.2.3 Hysteresis losses in a smooth rotor

The resultant m.m.f. vector rotates in a forward direction (for normal motor operation) at a speed which is alternately faster then slower than the rotor speed, and the behaviour of the m.m.f. in an element near to the periphery of a smooth rotor is shown in Fig. 5.5 (overleaf) for one complete

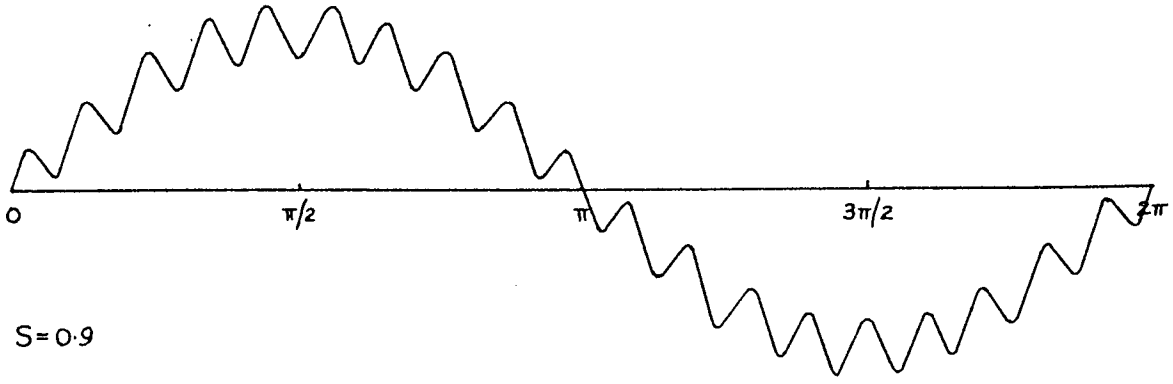

Graph showing the variation of the resultant m.m.f. at a point on the rotor, as the resultant m.m.f. vector moves through 2π.

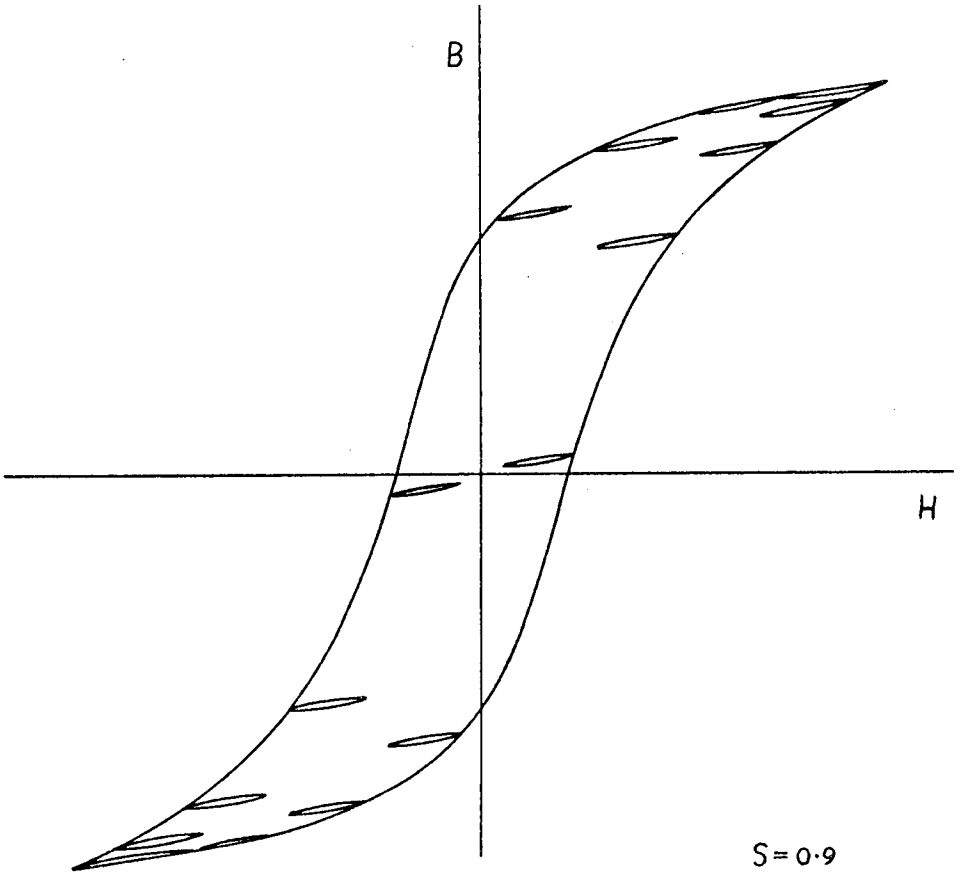

The hysteresis loop for a point on the rotor showing the presence of recoil loops.

Fig. 5.5

revolution of the m.m.f. vector. Also shown is the probable form of the hysteresis loop for the same element. The superimposed ripple on the m.m.f. waveform, which results from the cyclic change in the angular velocity of the m.m.f. vector relative to the rotor, introduces recoil loops onto the main hysteresis loop. While these loops are being traversed the hysteresis torque on the rotor reverses in sign to oppose the rotation, and although the torque is proportional to the area of the loop, the exact relationship is difficult to determine as it is a function of the average level of magnetization set by the resultant m.m.f.. At synchronous speed the area of the main loop shrinks to zero to leave the recoil loops superimposed on one another to form a symmetrical loop. Two points should be noted about the diagrams; firstly, at the particular speed chosen the m.m.f. pattern closes in 2π and the complete hysteresis loop is symmetrical, whereas for many values of speed a single loop is not symmetrical and is not repeated in the next cycle; secondly, in all of the diagrams in which the m.m.f. is referred to the rotor, the speed is assumed to be constant (for simplicity), although in practice there is a superimposed double-frequency oscillation which modifies the m.m.f. patterns.

5.3 The approximate representation of core loss on the equivalent circuit.

Core losses account for a significant part of the input power to single-phase f.h.p. machines and some allowance for these losses in the performance calculations is essential, even though a rigorous analysis is not possible. This is usually done by adding resistors of a suitable value to the equivalent circuit to give a power loss equal to the core loss at a given value of load. Either the cross-field or the rotating-field circuit may be used because of the approximate nature of the modifications, although the latter circuit is more representative of the physical conditions in the rotor.

The simplest method is to connect a single resistor in parallel with the input terminals, to give a constant loss for all values of load, and to increase (empirically) the resistances of the stator and rotor windings to allow for part of the stray loss. No distinction is made between the hysteresis and eddy-current losses as it is not possible to conduct a satisfactory loss-separation test [3] on a practical machine, and all losses are assumed to be supplied at line frequency since a stationary circuit is used. The tooth pulsation loss is not included on the equivalent circuit but is subtracted directly from the output.

A refinement is to associate the loss resistor with the magnetizing reactances in the two forms of equivalent circuit as shown in Fig. 5.6 (overleaf), so that as the load is increased and the voltage drop across the magnetizing branch decreases, the core loss is reduced. For example:-

(i) Cross-field theory - Identical resistors are connected in parallel with the separate magnetizing reactances in the d, q axis magnetizing circuits. The core loss in the q axis varies approximately as S^2, because the q axis magnetizing current is almost a linear function of speed.

(ii) Rotating-field theory - The loss resistors (nominally half the cross-field value) are connected in parallel with the separate magnetizing reactances of the f, b circuits. Different values of resistance are sometimes used to obtain a closer correlation between theory and practice.

The methods of allowing for the losses are the same as those used in the theory of the two-phase machine, but larger errors arise in the predicted losses for any given value of load. In the two-phase machine a pure rotating-field exists in the air-gap and, with a smooth rotor, the errors are mainly associated with the 'non-linearity' of the iron which makes it

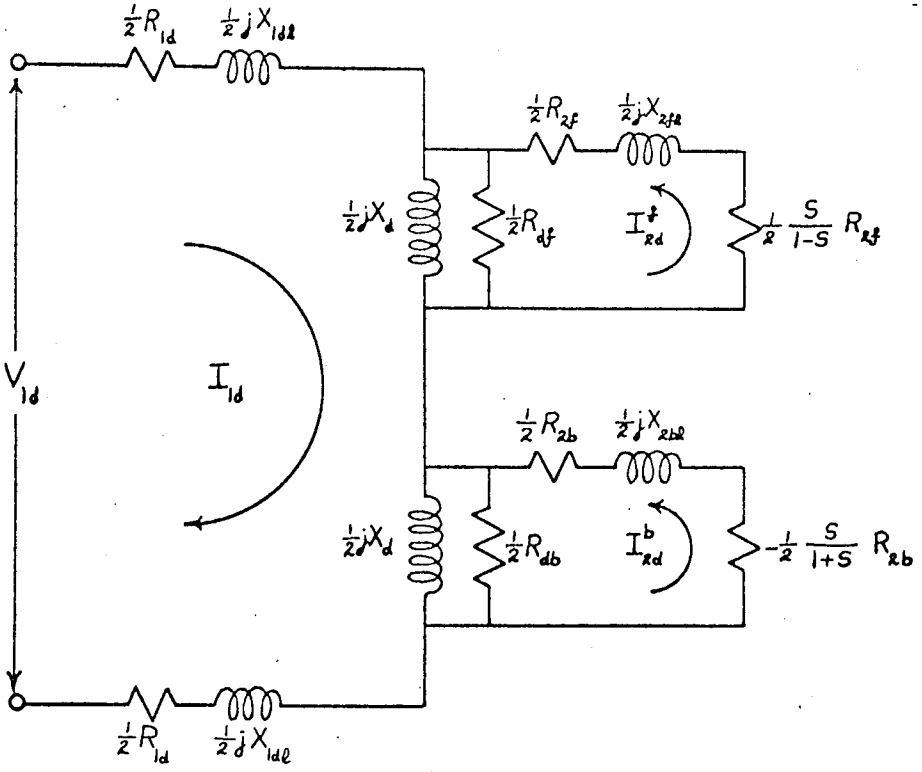

rotating-field theory

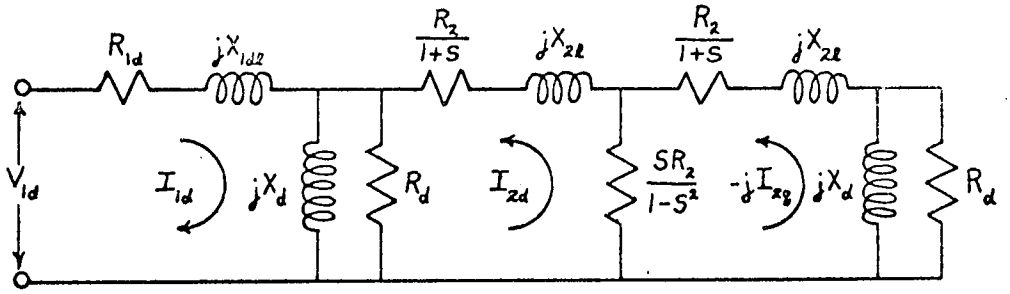

cross-field theory

Fig. 5.6 The modification of the equivalent circuits to allow for iron loss.

impossible to accurately represent the losses by a resistor of fixed value in the equivalent circuit. In the single-phase machine, an additional source of error is the separation (indicated by the equivalent circuit) of the losses into components associated with either the f, b or d, q components of the magnetic field.

5.3.1 Skin effect

Skin effect phenomenon in the iron, similar to that in the rotor bars, is of negligible importance because of the high resistance to current flow in the iron and the laminated construction; in a practical machine, any change in the losses would be completely masked by saturation effects.

However, the iron losses are changed as an indirect result of the skin effect in the rotor bars; this affects the forward and backward components of the magnetizing current and, in turn, the form of the magnetic field.

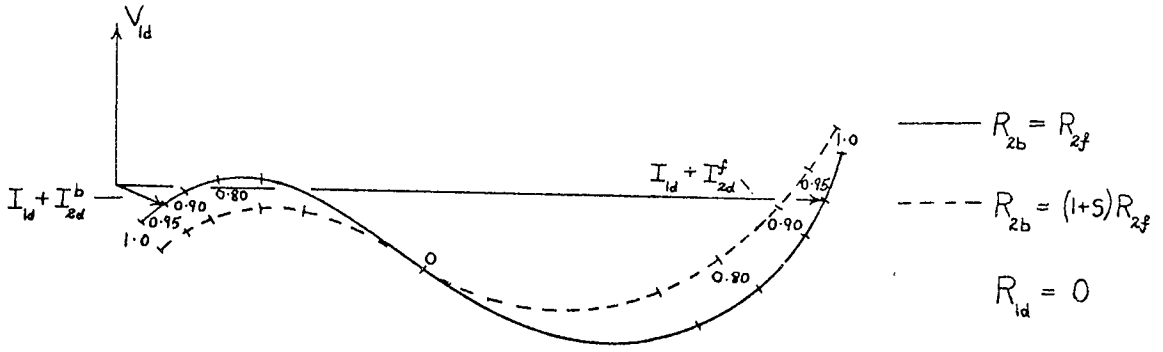

Fig. 5.7

The extent of the changes in the components of the current is shown in Fig. 5.7. Skin effect reduces the forward component, increases the backward component, and increases the phase-displacement between the components. These changes have little effect on the maximum amplitude of the magnetic field in the air-gap, but the minimum amplitude is noticeably reduced. The increased phase-displacement causes the principal axes of the elliptic locus (stationary reference axes) to be shifted in the direction of rotation. The increased amplitude of the oscillation superimposed on the otherwise pure rotating-field has a greater effect on the losses than the slight reduction in the mean value, with the result that the losses are increased by skin effect. Referring to the equivalent circuit (p. 62), changing the value of the backward resistor R_{2b} has the effect of increasing the backward voltage, but it is probable that the value of the backward loss-resistor would have to be reduced to allow completely for the additional loss.

5.4 Operating characteristics

The operating characteristics are graphical representations of the performance of the machine for given values of either the power output or the speed. The data for the curves

are derived from the performance equations and specimen calculations together with tabulated results are given in Appendix III. In this section attention is given to the terminal values of stator current, power input and output, shaft torque and speed, and efficiency; only passing reference is made to the rotor currents as these are considered fully in the two previous chapters.

The modification of the characteristics by skin effect is considered in detail and, in this connection, it is useful to refer to the equivalent circuit of the rotating-field theory, where the performance of the machine is likened to that of two coupled two-phase machines having speed dependent terminal voltages.

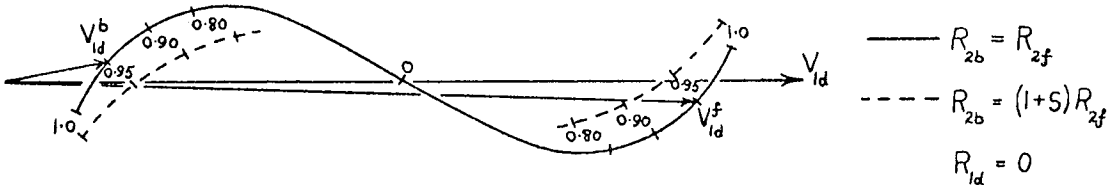

Fig. 5.8

Skin effect is allowed for by changing the rotor parameters of one of the machines, and the corresponding changes in the terminal voltages are illustrated by Fig. 5.8; for a given value of speed, skin effect causes a reduction in the forward voltage, an increase in the backward voltage, and an increase in the phase-displacement between these voltages.

5.4.1 Stator current

Expressions for the stator current are derived in sections 3.7 and 4.7, and typical values of the winding parameters are assumed in order to deduce current/speed characteristics for the rotating-field and cross-field theories respectively. Either theory may be used in the analysis of a wound rotor machine as the two sets of characteristics are identical but with a cage rotor machine, when skin effect must be taken into account, it has been shown that only the rotating-field theory is applicable. In the present section this restriction is disregarded, and the extent of the error incurred through the use of the cross-field theory for the analysis of a cage rotor machine, is examined by comparison of the characteristics with those obtained from the rotating-field theory.

5.4.1.1 The locus of the current

Let the stator resistance be neglected, and let V_{1d}/X_{1d} be treated as a current scale factor. Then the stator current is evaluated for the rotating-field theory (equation (3.14)) as

$$I_{1d} = \frac{V_{1d}}{jX_{1d}} \Big/ \left\{ 1 - \tfrac{1}{2} \frac{X_d^2}{X_{1d} X_{2f}} \xi_{2f} - \tfrac{1}{2} \frac{X_d^2}{X_{1d} X_{2b}} \xi_{2b} \right\} \qquad (5.4)$$

this equation may be written in the form

$$I_{1d} = \frac{V_{1d}}{jX_{1d}} \frac{a_0 + a_1 S + a_2 S^2}{b_0 + b_1 S + b_2 S^2} \qquad (5.5)$$

where $a_0 \ldots b_2$ are functions of the winding parameters and are complex constants; in particular both a_1 and b_1 are functions of $(R_{2f} - R_{2b})$ and $(X_{2f} - X_{2b})$. Generally, (a_2/a_1) is not equal to (b_2/b_1) and the locus of I_{1d} is a quartic curve which does not have a simple construction.

(i) wound rotor machine

The values of the forward and backward parameters of a wound rotor are independent of the component frequencies in the rotor current and are therefore equal. Hence a_1 and b_1 are zero, and the locus of I_{1d} is a circle having a parameter S^2. This is shown as curve (a) in Fig. 5.9 (overleaf), where the following numerical values have been assumed:

$$X_{1d} X_2/X_d^2 = 1.1,\ X_2/R = 10,\ X_{2f} = X_{2b} = X_2,\ R_{2f} = R_{2b} = R\ .$$

(ii) cage rotor machine

In this case the values of the rotor leakage parameters are modified by skin effect. The exact variation of the parameters is impossible to determine analytically, but some idea of the order of the changes is afforded by the example in section 1.3.

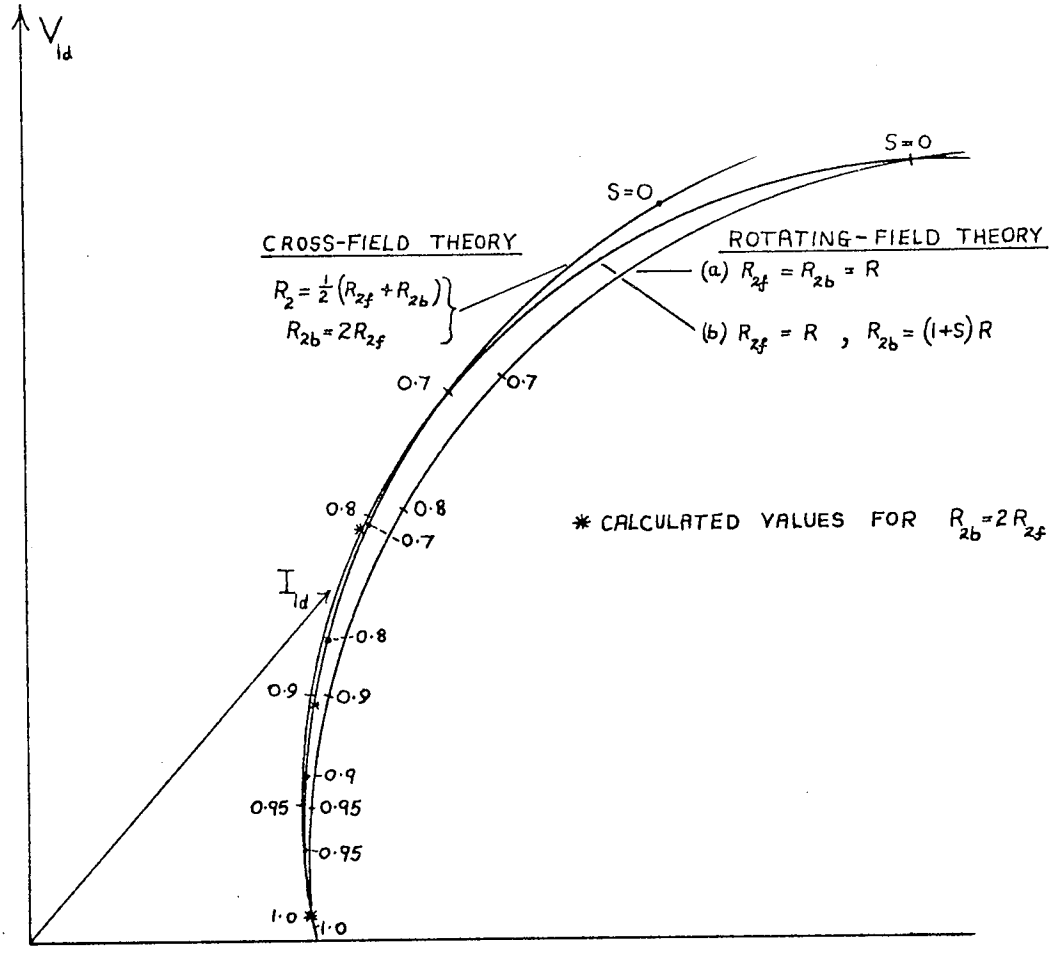

Fig. 5.9 Stator current loci

This is the basis for the values assumed in the discussion of skin effect in Chapter III, namely

$X_{2f} = X_{2b} = X_2$, $R_{2f} = R$, and either $R_{2b} = 2R$ or $R_{2b} = (1+S)R$.

It is reasonable to assume that R is the d.c. value of the rotor resistance and to neglect changes in R_{2f} since the working range ($0.9 \leq S \leq 1.0$) is of principal interest.

Equation (5.4) can then be simplified and written

$$I_{1d} = \frac{V_{1d}}{jX_{1d}} \Big/ \left\{ 1 - \frac{1}{2} \frac{X_d^2}{X_{1d} X_2} \left(\xi_{2f} + \xi_{2b} \right) \right\} \qquad (5.6)$$

Typical points on the alternative loci (for $R_{2b} = 2R$, and $R_{2b} = (1+S)R$) are shown in Fig. 5.9 for the numerical values assumed in (i) above.

It is seen from Fig. 5.9 that for a given value of speed the stator current is slightly reduced by skin effect and the operating power factor is improved. The current loci which include skin effect are closely approximated by the locus curve drawn from the cross-field equation (2.22), in which skin effect is allowed for by increasing the rotor resistance (v. section A3.6.3). However, serious discrepancies exist between corresponding parameter points on the two loci, and the use of the cross-field approximation results in a much smaller value of current at a lower power factor (v. Table A3.3, Appendix III).

In fact over the normal operating range, there is far less error in the current locus predicted by the cross-field equations if skin effect is neglected altogether, because an approximation in which only the rotor resistance is modified, gives a predicted performance exactly the same as that obtained from the use of the rotating-field theory with a smaller value of X_2/R_2 .

Alternative expressions are used for the modified value of the backward resistance which lead to almost identical results over the normal operating range. However the assumption that the variation of R_{2b} is of the form $(1+S)R$ has the advantage that the locus of the stator current (equation (5.6)) is a circle having a parameter S (instead of S^2). The equivalent circuit reduces to that for one phase of a balanced two-phase induction motor having an additional leakage impedance in series with that of the stator winding. Hence the performance of the single-phase induction motor with a cage rotor can be predicted from the standard circle diagram for the two-phase machine, provided that allowance is made for the effect of the backward torque. Although this procedure is to be found in elementary theories of the operation of the machine, where it is assumed that the variation of the factor $R_{2b}/(1+S)$ can be neglected over the normal working range, the present reasoning is quite different and is believed to

be original; here, the factor $R_{2b}/(1+S)$ is actually replaced by a constant (R) as a result of the assumed modification of R_{2b} by skin effect.

5.4.1.2 Current/speed characteristics

The existence of circular loci enables the current/speed characteristics of the wound rotor machine to be obtained quite simply for different values of the parameter ratios, and 4 examples are given in Fig. 5.10.

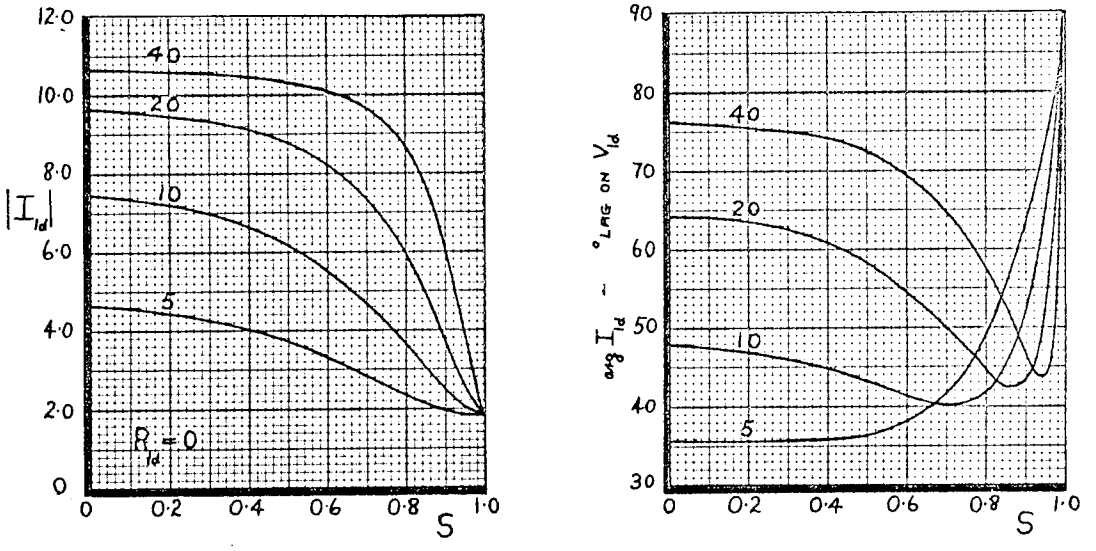

Fig. 5.10

Allowances for skin effect are not included on the diagrams as detailed characteristics for the operating range ($0.9 \leq S \leq 1.0$) are given in Chapter III (Fig. 3.10, p. 74).

The circle diagram can also be used to show the effect of including the stator resistance in the performance calculations, and a typical illustration is given in Fig. 5.11.

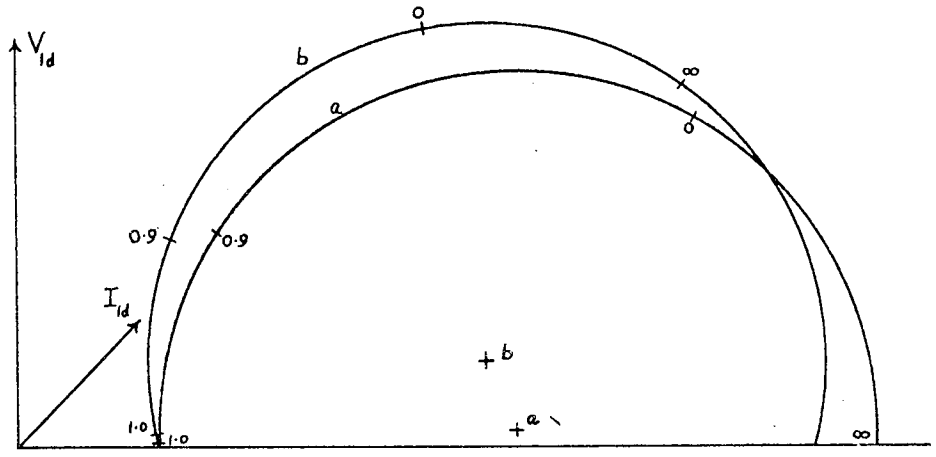

locus diagrams for the current

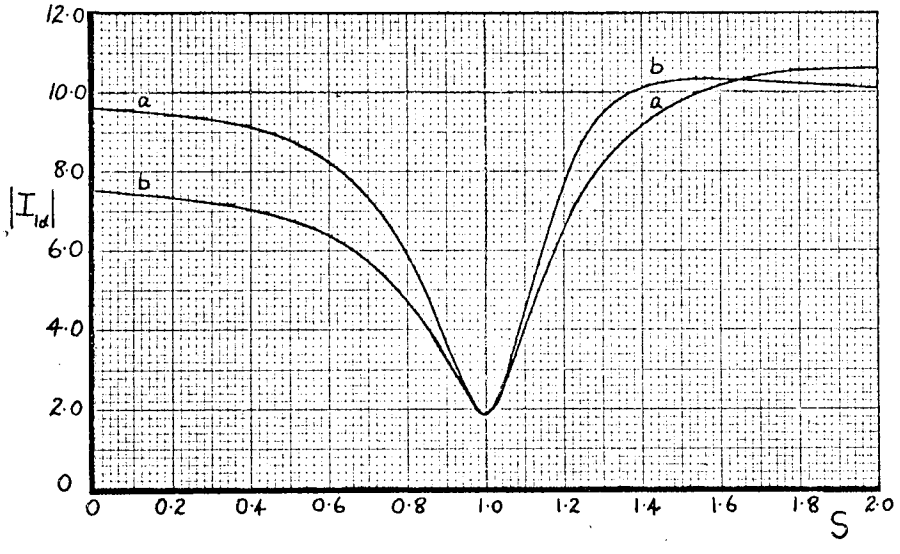

current/speed characteristics

(the stator resistance is included
in curve b of each diagram.)

Fig. 5.11

The assumed numerical values for the parameter ratios are

$$X_{1d}X_2/X_d^2 = 1.1,\ X_2/X_d = 1.05,\ X_2/R_2 = X_{1d}/R_{1d} = 20,$$

and the current scale factor V_{1d}/X_{1d} is replaced by unity. Four of the parameter points are given for each circle, others are positioned by inserting the parameter lines (drawn perpendicular to a line joining the '∞ point' and the centre of the appropriate circle). The resulting current/speed characteristics for the extended speed range $0 \leqslant S \leqslant 2$ are also shown in Fig. 5.11; it is seen that for motor operation the current is reduced and the power factor improved when the stator resistance is included, although these changes are quite small over the operating range; above synchronous speed the modified characteristic exhibits a maximum value which does not occur when R_{1d} is neglected, otherwise the characteristics are similar.

5.4.2 Developed torque

The mechanism of torque production in the machine is discussed in sections 3.4 and 4.4, and it is shown that the qualitative explanations appropriate to the principal theories are complementary. The present section is the mathematical counterpart to these explanations.

Referring to the rotating-field theory, the developed torque is expressed by equations (3.9) and (3.11) as

$$\omega T_E = \omega T_f - \omega T_b = \left(\frac{1}{2}\left|I_{2d}^f\right|^2 \frac{R_{2f}}{1-S}\right) - \left(\frac{1}{2}\left|I_{2d}^b\right|^2 \frac{R_{2b}}{1+S}\right) \tag{5.7}$$

Using ξ functions (equation (3.13)) to replace the rotor currents by the stator current, equation (5.7) becomes

$$\omega T_E = \omega T_f - \omega T_b = \left(\frac{1}{2}\left|I_{1d}\right|^2 X_{1d} \frac{X_d^2}{X_{1d} X_{2f}} \mathcal{J}_m \xi_{2f}\right) - \left(\frac{1}{2}\left|I_{1d}\right|^2 X_{1d} \frac{X_d^2}{X_{1d} X_{2b}} \mathcal{J}_m \xi_{2b}\right) \tag{5.8}$$

Values of the stator current and ξ functions are substituted in equation (5.8) and the resulting forward, backward, and total torques are plotted in Fig. 5.12 (overleaf) to a base of speed ($0.9 \leq S \leq 1.0$) for 4 values of the X_2/R_2 ratio. In the first set of curves, skin effect has been neglected and the following numerical values assumed

$$X_{1d}\, X_2/X_d^2 = 1.1,\ X_2/X_d = 1.05,\ X_{2f} = X_{2b} = X_2,\ R_{1d} = 0,$$

the torque scale factor V_{1d}^2/X_{1d} is replaced by unity.

The second set of curves in Fig. 5.12 shows the modifications to the forward and backward torques caused by skin effect (assuming $R_{2b} = 2R_{2f}$); differences between corresponding values of torque are plotted, the notation being

$$\omega T_{f,b}(\text{skin effect}) = \omega T_{f,b} - \epsilon_{f,b}$$

Skin effect increases the total impedance of the machine and it is

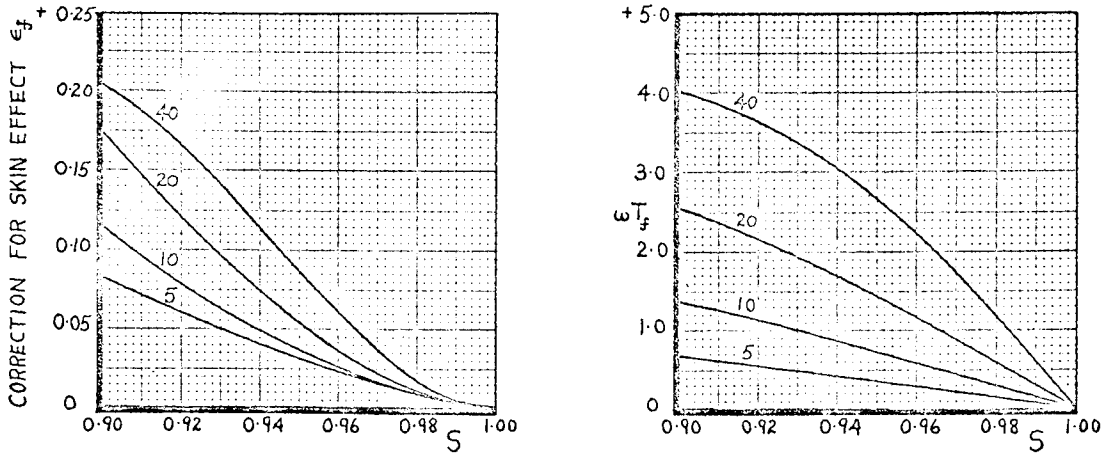

(a) The forward torque

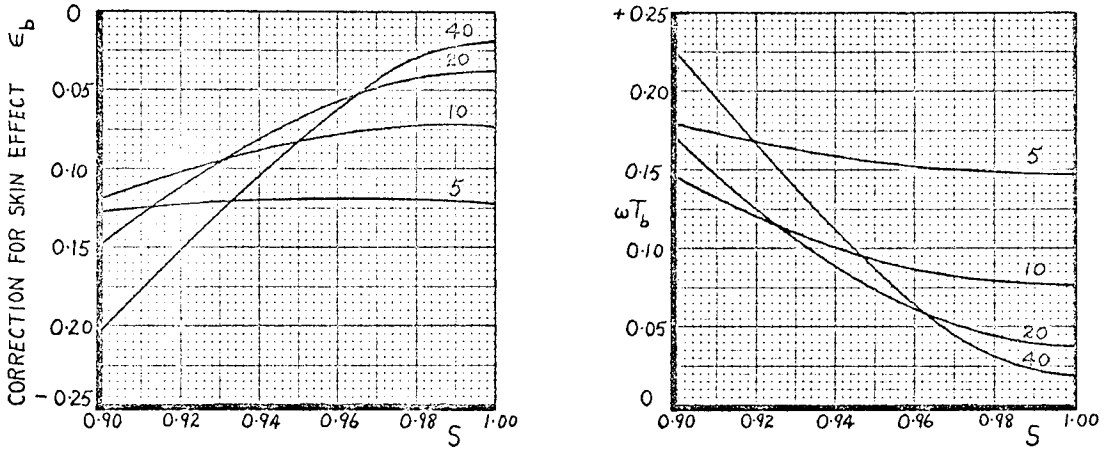

(b) The backward torque

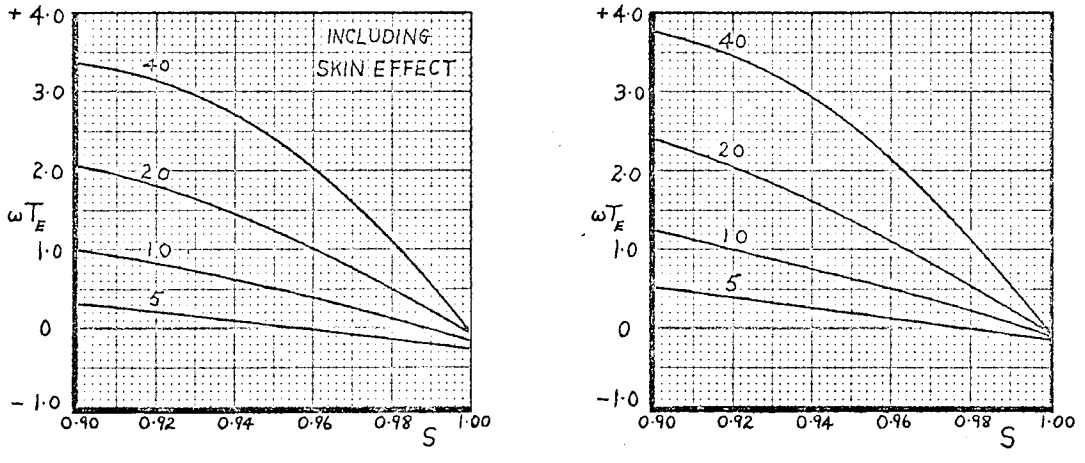

(c) The net torque

Fig. 5.12 The developed torque

seen that for a given value of speed, this reduces the forward torque and increases the backward torque by almost equal amounts. For the numerical values chosen, the backward torque is practically doubled and there is a noticeable reduction in both the value of developed torque and no-load speed (Fig. 5.12c).

5.4.2.1 Complete torque/speed characteristics

The reduction in developed torque is principally of interest over the operating range. The general shape of the torque/speed characteristic is not affected and it is convenient to omit skin effect in order to simplify the evaluation of the torque equation.

Let $R_{2f} = R_{2b} = R_2$ and $X_{2f} = X_{2b} = X_2$ in equation (5.8), then

$$\omega T_E = |I_{1d}|^2 X_{1d} \frac{X_d^2}{X_{1d} X_2} \mathrm{Re}\, \xi_{2q} \qquad \text{(equations (3.5), (4.11))} \qquad (5.9)$$

Values of $|I_{1d}|$ and $\mathrm{Re}\, \xi_{2q}$ are used to plot the torque/speed characteristics; these are shown in Fig. 5.13 (a) for 4 values of the X_2/R_2 ratio over the speed range $0 \leq S \leq 1$. It is apparent from the curves that increasing the rotor resistance decreases the slope of the characteristic over the operating range so that the change in speed resulting from a given change in load is more marked; at no-load the negative slope is approximately inversely proportional to R_2. An increase in R_2 also decreases the pull-out

speed and, unlike the two-phase machine, reduces the pull-out torque; in a similar way, skin effect adversely affects the pull-out performance.

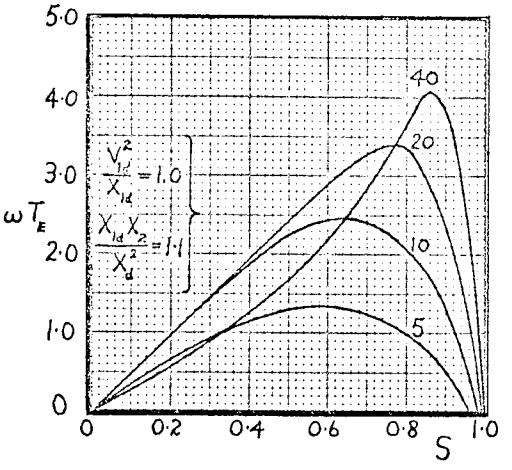

(a) The variation of T_E for different values of X_2/R_2

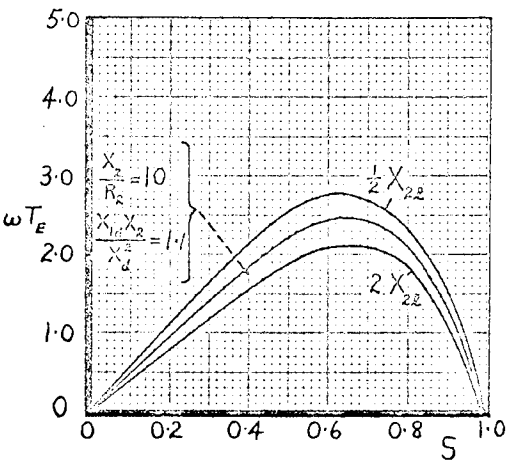

(b) The variation of T_E for different values of $X_{2\ell}$

Fig. 5.13

The second set of curves in Fig. 5.13 shows the effect of varying the rotor leakage reactance, assuming that the leakage reactances of the rotor and stator windings are equal for the condition - $X_2/R_2 = 10$, and that the stator reactance is maintained constant. Increasing $X_{2\ell}$ decreases the developed torque for a given value of speed and increases the pull-out speed.

Reference to the rotating-field theory reveals that, unlike the two-phase machine, the single-phase torque/speed

characteristic is not symmetrical about the line - S = 1: below synchronous speed, the developed torques of the forward and backward fields act in opposite directions thus reducing the net torque and giving the characteristic features of zero starting torque and a sub-synchronous no-load speed; above synchronous speed, the developed torques act in the same direction thus causing a large negative torque.

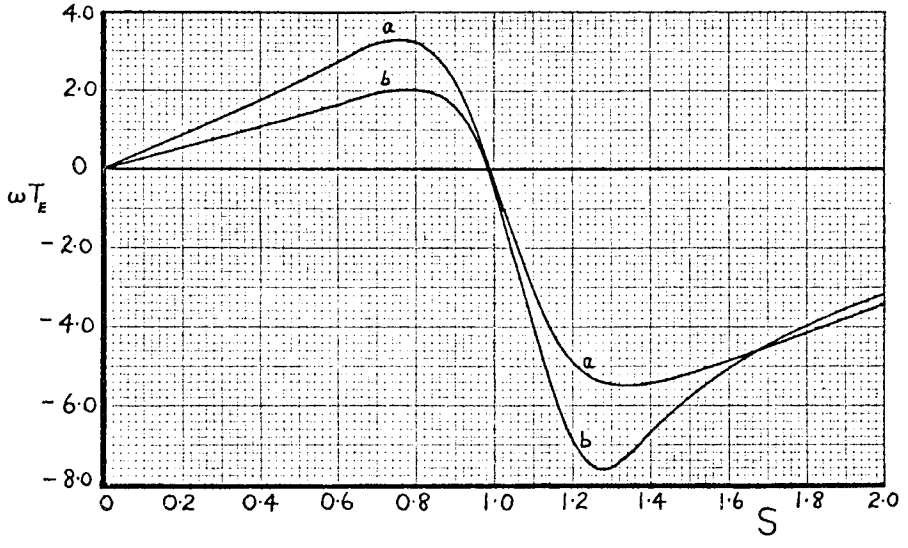

(R_{1d} is included in curve b)

Fig. 5.14

Torque/speed characteristics, which correspond to the current/speed characteristics of Fig. 5.11, are shown in Fig. 5.14 (curve 'a') for the extended speed range $0 \leq S \leq 2$; it is seen that the differences in the motor and generator regions of the curve are quite marked and that, in particular, the two 'maximum' values, and the relative speeds at which these occur above and

below the synchronous value, are not the same. Similar differences are noted in the characteristic of the two-phase machine when the stator resistance is included in the performance calculations, and it follows that in the single-phase machine the inclusion of R_{1d} will increase the existing differences still further (v. curve 'b', Fig. 5.14). Over the normal operating range, the stator resistance causes only a small reduction in the torque for a given value of speed whereas the maximum available torque is considerably reduced.

5.4.2.2 An alternative form of the torque equation

Graphical techniques provide a convenient method for obtaining the torque/speed characteristic, enabling results of tolerable accuracy to be deduced both simply and quickly. However, calculations are frequently performed in a routine manner by an automatic computer so that equations for the characteristics are also necessary, expressed in terms of the applied voltage, winding parameters, and speed.

Let the expressions for the currents I_{1d}, I_{2q} given in equation (4.12) be substituted in the torque equation (2.20b).

Then

$$\omega T_E = \frac{V_{1d}^2}{\Delta \Delta^*}\left\{ S X_d^2 R_2 \left[(1-S^2) X_2^2 - R_2^2 \right] \right\} \qquad (5.10)$$

.. where Δ is defined in equation (4.12).

In equation (5.10), the torque is zero for 3 values of S -

$$0, \quad \left\{ 1 - \left(\frac{R_2}{X_2} \right)^2 \right\}^{\frac{1}{2}}, \quad \infty ,$$

and the term - $-R_2^2$ in the [ ] brackets is associated with the losses in the q axis which act as a drag on the motor. There is no simple expression for the maximum value of equation (5.10) or for the pull-out speed. In practice, an error in the determination of this speed does not seriously affect the calculated value of the maximum torque as the characteristic is fairly flat in the region of pull-out.

5.4.3 Power and efficiency

Reference to Table A3.1 (Appendix III) shows that with typical values of X_2/R_2 and for a given value of speed in the normal operating range, the power input is almost unaffected by skin effect although the power output and efficiency are noticeably reduced. The redistribution of the power input caused by skin effect is given in Table 5.1 (overleaf) for the particular conditions - $X_2/R_2 = 40$, $S = 0.96$; in this case the power input

is the same for both a cage and a wound rotor machine.

TABLE 5.1

($R_{1d} = 0$)

	normal ($R_{2b} = R_{2f}$)		skin effect ($R_{2b} = 2R_{2f}$)		change
Rotor copper losses					
forward field (%)	3.89		3.78		- .11
backward field (%)	5.41		10.52		+5.11
total		9.3		14.3	+5.00
Rotor output					
forward field (%)	93.35		90.85		-2.5
backward field (%)	2.65		5.15		+2.5
total (efficiency)		90.7		85.7	-5.0
Rotor input (%)		100.0		100.0	

As the power input and speed are the same for the two machines the decrease in the rotor output due to the forward and backward fields are equal, resulting in a decrease in the efficiency of twice this amount. This decrease appears as an increase in the rotor copper-loss and, subsequently, as an increase in the operating temperature of the rotor.

If the stator resistance is neglected, then the efficiency can be expressed as

$$\frac{\text{output}}{\text{input}} = \frac{\text{output}}{\text{output} + \text{rotor copper-loss}} = \frac{\alpha}{\alpha + 1}$$

.. where α = output/rotor copper-loss.

The variation of $\propto$ with speed for different values of X_2/R_2 is discussed in Appendix IV, where it is shown that if skin effect is allowed for by putting $R_{2b} = 2R_{2f}$, then for otherwise identical conditions any given value of $\propto$ is reduced by approximately half: e.g., with a typical value of $\propto = 4$, the efficiency for a given value of speed is reduced by approximately 20%.

5.4.4 Terminal characteristics

This thesis has been concerned with skin effect in single-phase motors. Many of the observations and comments of the earlier chapters find expression in, and are in effect summarized by, the terminal characteristics of the machine presented in this final section.

Characteristics are normally plotted to a base of power output, instead of speed, and examples are given in Fig. 5.15 (pps. 153, 154) for 4 values of X_2/R_2. The assumed ratios and values are

$$X_{1d}X_2/X_d^2 = 1.1,\ X_2/X_d = 1.05,\ V_{1d}/X_{1d} = 1.0,\ V_{1d}^2/X_{1d} = 1.0,$$

$$R_{1d} = 0,\ R_{2f} = R_2,\ R_{2b} = R_2 \text{ (normal)},\ R_{2b} = 2R_2 \text{ (skin effect)},$$

and the tabulated data from which the curves are plotted, are given in Appendix III. Separate sets of curves enable the extent

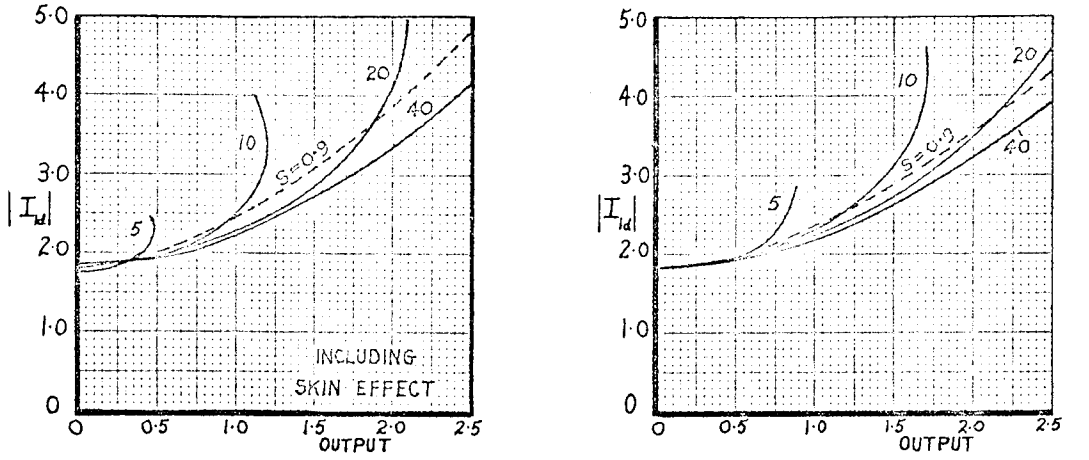

(a) stator current

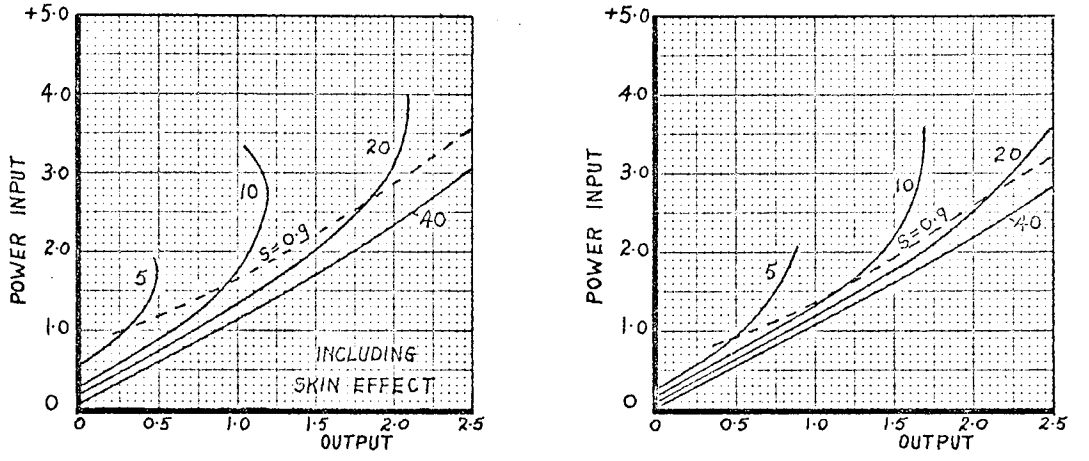

(b) power input

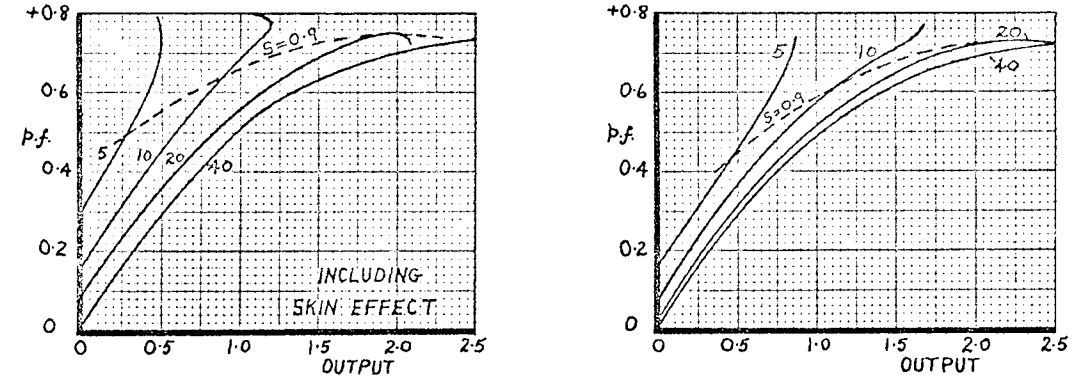

(c) power factor (lagging)

Fig. 5.15 Performance characteristics for 4 values of X_2/R_2

Graphs of the stator current, power input, and power factor plotted to a base of the power output.

(continued overleaf)

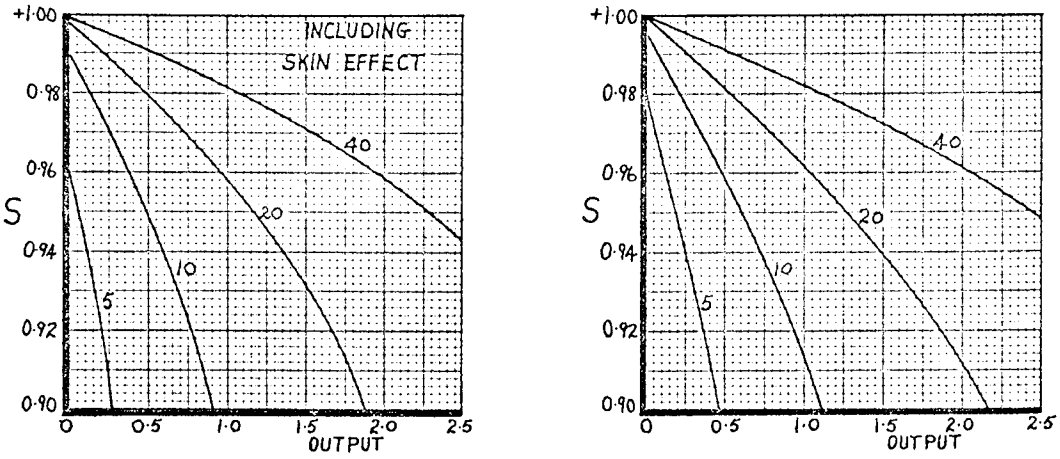

(d) speed

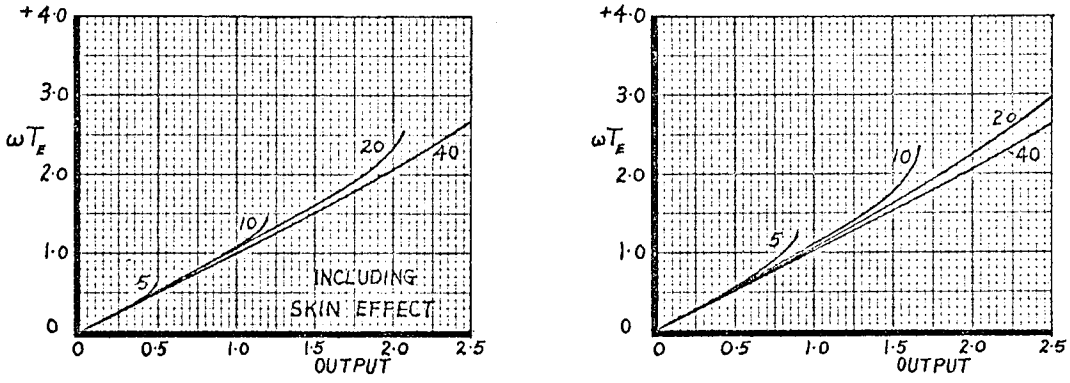

(e) developed torque

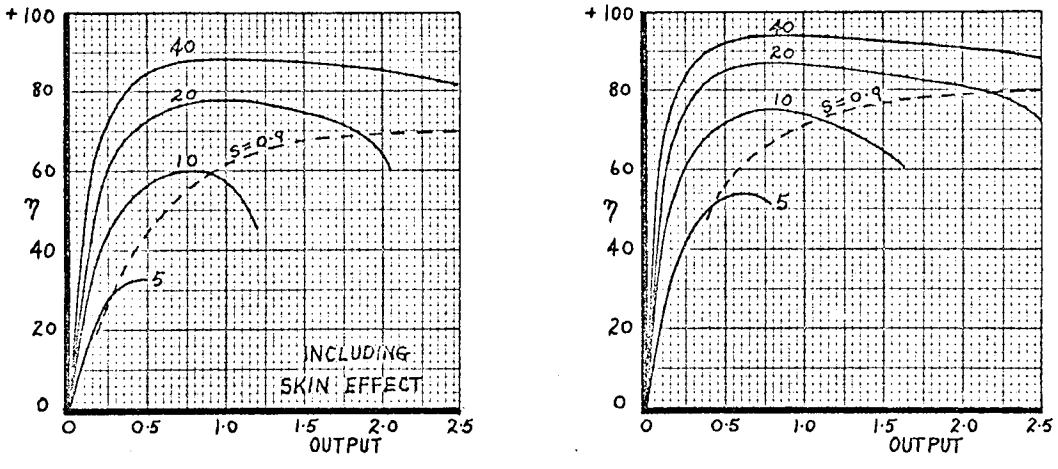

(f) efficiency %

Fig. 5.15 Performance characteristics for 4 values of X_2/R_2

Graphs of the speed, developed torque, and efficiency plotted to a base of the power output.

of the modifications due to skin effect to be simply assessed.

Complete characteristics (taken from Fig. 5.15) are shown in Fig. 5.16 (overleaf) for a hypothetical machine in which

$$R_{1d} = 0, \quad \text{and} \quad X_2/R_2 = 20.$$

Skin effect is included in a second set of characteristics, and these also show the changes in the overload performance caused by assuming

$$R_{2b} = (1+S)R_2 \quad \text{instead of} \quad R_{2b} = 2R_2 .$$

A further comparison of the extent to which the overload performance is affected by the type of allowance made for skin effect, is provided by Table A3.2 (Appendix III).

The terminal conditions of the machine for an output of 1 unit (the power scale factor being unity) are given in Table 5.2

TABLE 5.2

	normal	skin effect
stator current	2.24	2.28
power input	1.16	1.28
power factor	.516	.563
speed	.963	.959
torque	1.04	1.043
power output	1.00	1.00
efficiency %	86.6	77.85

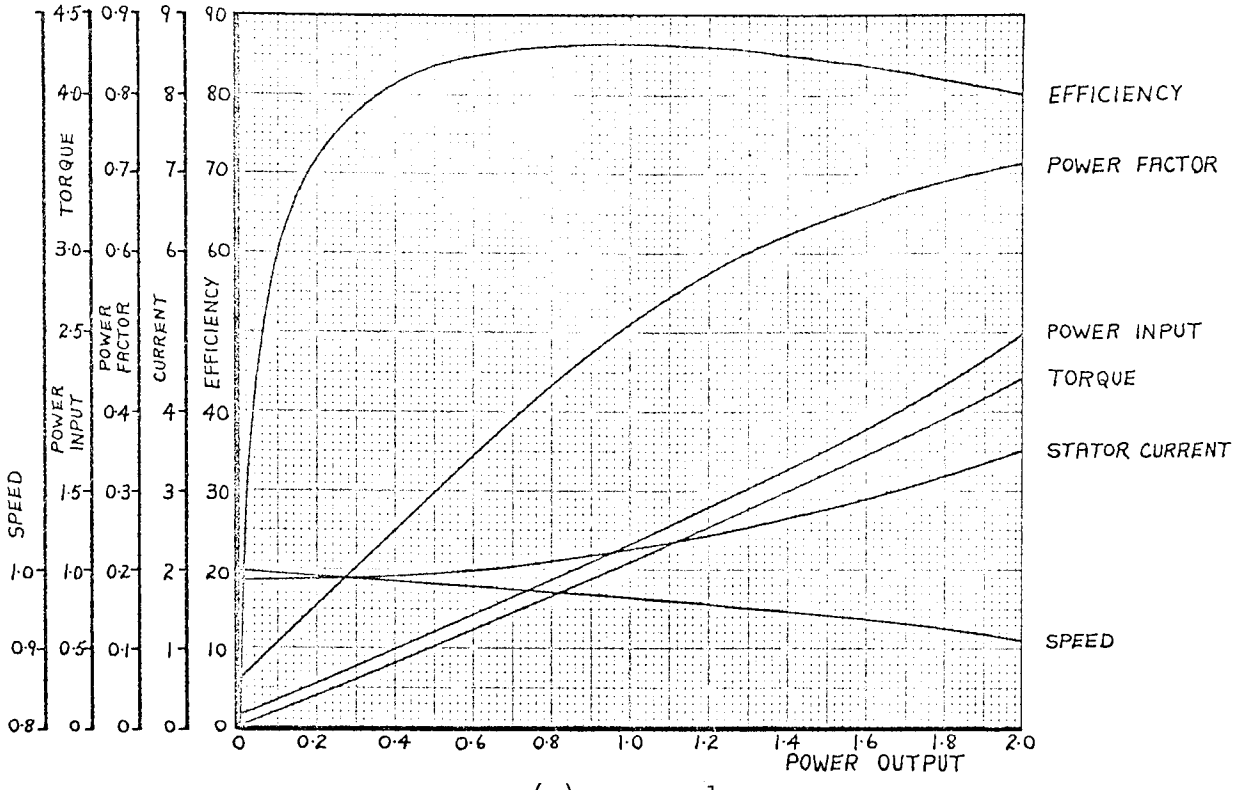

(a) normal

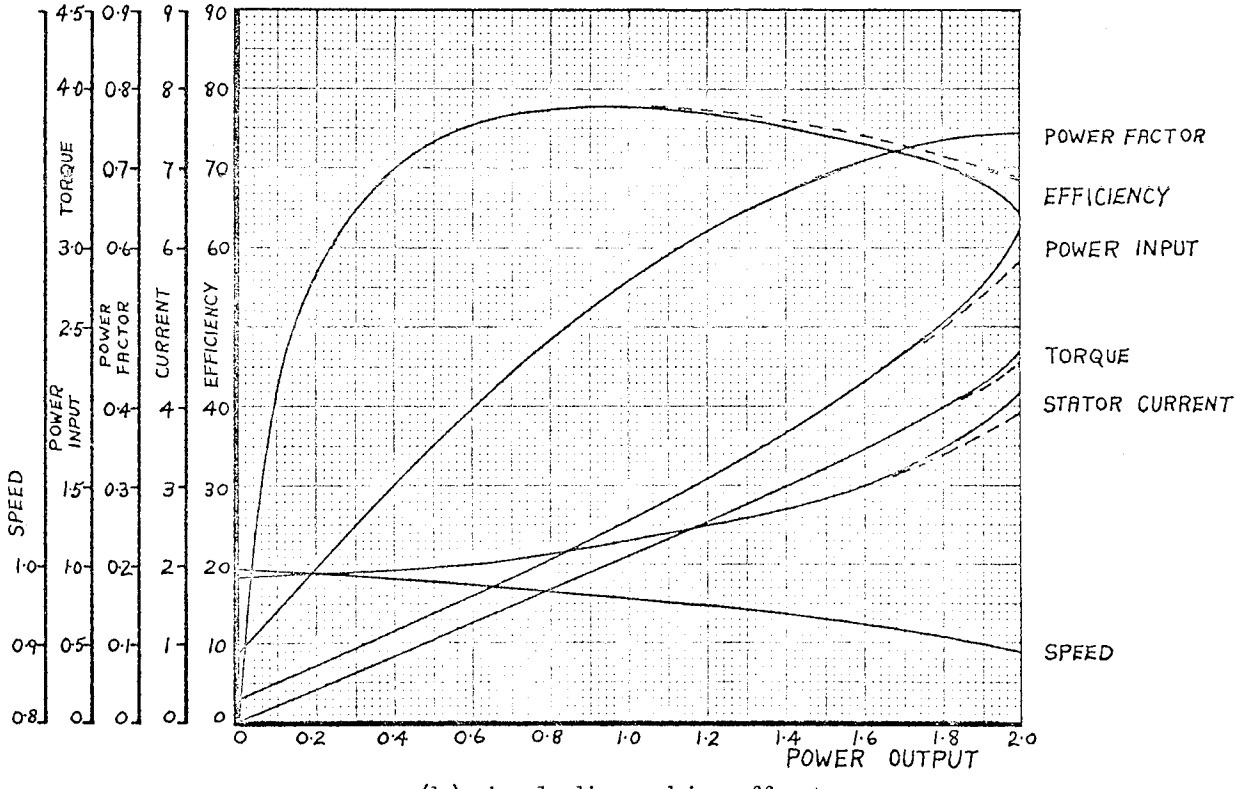

(b) including skin effect

—— $R_{2b} = 2R_{2f}$, ---- $R_{2b} = (1+S)R_{2f}$

Fig. 5.16 Complete performance characteristics

Skin effect causes a noticeable increase in the current, power input, and power factor; but the changes in the speed and torque are negligible. The fall in speed would only amount to 5 r.p.m. in a 1500 r.p.m., 4 pole, 50 c/s machine, and for the same power output the developed torque would be increased by 0.3%.

APPENDICES

APPENDIX I

THE ANALYSIS OF SKIN EFFECT IN A ROTOR CONDUCTOR OF AN IDEAL INDUCTION MOTOR

A1.1 The apparent impedance

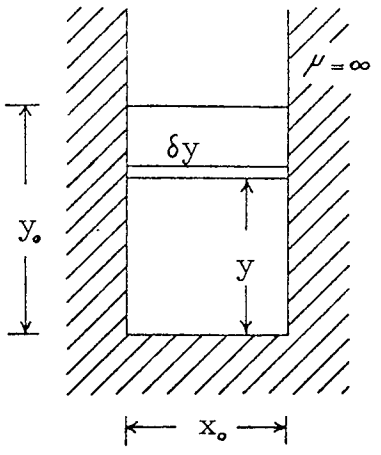

The diagram represents a rectangular conductor embedded in a theoretical slot in iron of infinite permeability. It is assumed that currents of a single frequency flow in the conductor in the axial (z) direction, and that any distortion of the otherwise uniform current density distribution is limited to the y direction.

The variation of the current density is determined from Maxwell's field equations as follows:

$\text{CURL}\ \bar{H} = \bar{J}$ (neglecting $\bar{D}$) , $\quad \text{CURL}\ \bar{E} = -j\omega\bar{B}$, $\quad \bar{J} = \sigma\bar{E}$

hence $\qquad \text{CURL CURL}\ \bar{J} = -j\omega\mu_o\sigma\bar{J}$

and $\qquad \bar{\nabla}^2\bar{J} = j h^2 \bar{J} \qquad$ where $\quad h^2 = \omega\mu_o\sigma \qquad$ (A1.1)

Expanding equation (A1.1) in rectangular coordinates

$$\frac{d^2 J_z}{dy^2} = j h^2 J_z \qquad \text{(A1.2)}$$

The boundary conditions of the problem are:

$$\text{at } y = 0,\ B_x = 0\ ; \qquad \text{at } y = y_o\ ,\ B_x = -\mu_o I/x_o$$

.. where I is the total current in the conductor.

B_x is found from the equation $\text{CURL}\,\bar{E} = -j\omega\bar{B}$ as $B_x = j\frac{1}{\omega\sigma}\frac{dJ_z}{dy}$

A solution to equation (A1.2) which satisfies the boundary conditions is

$$J_z = (1+j)\frac{mI}{x_o}\frac{\cosh(1+j)my}{\sinh(1+j)my_o} \qquad m = \frac{h}{\sqrt{2}} \qquad \text{(A1.3)}$$

Let the conductor be imagined as comprising a large number of elemental slices as shown in the diagram (p. 159), then the voltage drop across unit axial length of each slice is the same (V). In particular at $y = y_o$, there is no voltage drop due to the internal flux-linkage and - $V = \sigma J_z$ (at $y=y_o$). The impedance is therefore

$$\frac{V}{I} = \frac{(1+j)}{\sigma}\frac{m}{x_o}\frac{\cosh(1+j)my_o}{\sinh(1+j)my_o} \qquad \text{(A1.4)}$$

Separating the real and imaginary parts gives the a.c. resistance and the cross-slot component of the leakage reactance, respectively as

$$R_{ac} = \frac{m}{\sigma x_o}\frac{\sinh 2my_o + \sin 2my_o}{\cosh 2my_o - \cos 2my_o} \qquad \text{(A1.5)}$$

$$X_{ac} = \frac{m}{\sigma x_o}\frac{\sinh 2my_o - \sin 2my_o}{\cosh 2my_o - \cos 2my_o} \qquad \text{(A1.6)}$$

A1.2 The calculations for copper conductors

Take σ for copper as 4.854×10^7 $\mho/m$ AT 70°C.

Then $m = \sqrt{\pi f \mu_o \sigma} = 13.844\sqrt{f}$

If skin effect is neglected:

(i) the value of R_{ac} is given by $R = 1/\sigma x_o y_o$, hence

$$\frac{R_{ac}}{R} = m y_o \frac{\sinh 2my_o + \sin 2my_o}{\cosh 2my_o - \cos 2my_o} \qquad \text{(A1.7)}$$

(ii) the value of X_{ac} is given by $X = 2my_o/3\sigma x_o$, hence

$$\frac{X_{ac}}{X} = \frac{3}{2my_o} \frac{\sinh 2my_o - \sin 2my_o}{\cosh 2my_o - \cos 2my_o} \qquad \text{(A1.8)}$$

Values of the resistance and reactance ratios are given in Table A1.1 (p. 162) for 5 slot depths over the frequency range 0-100 c/s, and the values at 100 c/s are shown graphically in Fig. 1.1 (p. 16).

A1.3 The calculations for aluminium conductors

For aluminium, σ is 2.892×10^7 $\mho/m$ AT 70°C.

Therefore $m = 10.684\sqrt{f} = 13.844\sqrt{0.596 f}$

Hence curves for copper conductors can be rescaled so that a frequency of 59.6 c/s ($\simeq$60 c/s) for copper corresponds to a frequency of 100 c/s for aluminium.

TABLE A1.1

The variation of R_{ac}/R for different slot depths

f c/s	5mm	10mm	15mm	20mm	25mm
0	1.000	1.000	1.000	1.000	1.000
1	1.000	1.000	1.000	1.001	1.001
2	1.000	1.000	1.001	1.002	1.005
3	1.000	1.000	1.001	1.005	1.011
4	1.000	1.001	1.003	1.008	1.020
5	1.000	1.001	1.004	1.013	1.031
10	1.000	1.003	1.016	1.051	1.121
20	1.001	1.013	1.064	1.192	1.420
30	1.002	1.029	1.140	1.392	1.778
40	1.003	1.051	1.238	1.619	2.119
50	1.005	1.079	1.352	1.849	2.417
60	1.007	1.112	1.476	2.067	2.676
70	1.010	1.150	1.605	2.268	2.903
80	1.013	1.192	1.735	2.450	3.107
90	1.016	1.238	1.863	2.617	3.295
95	1.018	1.262	1.926	2.695	3.384
96	1.019	1.267	1.938	2.710	3.401
97	1.019	1.272	1.950	2.725	3.419
98	1.019	1.277	1.963	2.740	3.436
99	1.020	1.282	1.975	2.755	3.453
100	1.020	1.287	1.987	2.770	3.470

The variation of X_{ac}/X for different slot depths

f c/s	5mm	10mm	15mm	20mm	25mm
0	1.000	1.000	1.000	1.000	1.000
1	1.000	1.000	1.000	.9999	.9996
2	1.000	1.000	.9998	.9994	.9985
3	1.000	.9999	.9996	.9987	.9967
4	1.000	.9999	.9992	.9976	.9942
5	1.000	.9998	.9988	.9963	.9910
10	.9999	.9991	.9953	.9854	.9656
20	.9998	.9963	.9817	.9455	.8816
30	.9995	.9917	.9602	.8893	.7839
40	.9991	.9854	.9325	.8267	.6956
50	.9985	.9775	.9006	.7651	.6236
60	.9979	.9681	.8661	.7087	.5669
70	.9972	.9574	.8306	.6590	.5223
80	.9963	.9455	.7954	.6160	.4867
90	.9953	.9325	.7614	.5793	.4577
95	.9948	.9257	.7450	.5629	.4451
96	.9947	.9244	.7418	.5598	.4428
97	.9946	.9230	.7386	.5568	.4404
98	.9945	.9216	.7354	.5537	.4381
99	.9943	.9202	.7322	.5508	.4358
100	.9942	.9188	.7291	.5478	.4336

APPENDIX II

THE GRAPHICAL DETERMINATION OF THE ξ FUNCTIONS

The ξ functions are introduced in Chapters III, IV as a convenient method of expressing the relationship between the stator and rotor currents. Graphs are included in these chapters to illustrate the variation of the functions for several values of X_2/R_2, but it is unlikely that these exact values occur with a particular machine. In this case, the required curves are constructed either from interpolated points or from a new set of values. It is shown in this appendix that these values may be obtained from simple graphical constructions.

A2.1 ξ_{2f}, ξ_{2b}

The functions used with the rotating-field theory are

$$\xi_{2f} = 1\Big/\left\{1 - j\frac{1}{1-S}\,\frac{R_{2f}}{X_{2f}}\right\}, \qquad \xi_{2b} = 1\Big/\left\{1 - j\frac{1}{1+S}\,\frac{R_{2b}}{X_{2b}}\right\}. \tag{A2.1}$$

There is no loss of generality in omitting ξ_{2b} in the subsequent development as an examination of equation (A2.1) shows, since this may be obtained from ξ_{2f} by changing the sign of S, and the suffices from 2f to 2b.

Let equation (A2.1) be rewritten as

$$\underset{\sim}{\xi}_{2f} = \frac{j(1-S)}{\alpha + j(1-S)} = 1 - \frac{1}{1 + j\frac{1}{\alpha}(1-S)} \qquad \alpha = \frac{R_{2f}}{X_{2f}} \qquad \text{(A2.2)}$$

The locus of the $\underset{\sim}{\xi}_{2f}$ phasor for variable speed is a circle with a parameter (1-S). This is shown in Fig. A2.1 (a) (overleaf) for $X_{2f}/R_{2f} = 10$. The parameter line is extended to include $\underset{\sim}{\xi}_{2b}$ on the same diagram, although the accuracy is reduced over this part of the circle.

A2.2 $\underset{\sim}{\xi}_{2d}$

The function $\underset{\sim}{\xi}_{2d}$ used with the cross-field theory is defined in equation (4.14b) as

$$\underset{\sim}{\xi}_{2d} = \tfrac{1}{2}\left(\underset{\sim}{\xi}_{2f} + \underset{\sim}{\xi}_{2b}\right) = \frac{\alpha + j(1-S^2)}{(2\alpha - j\alpha^2) + j(1-S^2)} \qquad \alpha = \frac{R_2}{X_2}$$

$$= 1 - \frac{1}{\frac{(2+\alpha^2)+j\alpha}{1+\alpha^2} - \frac{(1-j\frac{1}{\alpha})}{1+\alpha^2}(1-S^2)} \qquad \text{(A2.3)}$$

Again, the locus of the $\underset{\sim}{\xi}_{2d}$ phasor for variable speed is a circle but the parameter is now $(1-S^2)$. This has the effect of opening out the scale on the parameter line in the region of principal interest. The locus is shown in Fig. A2.1 (b) for $X_2/R_2 = 10$.

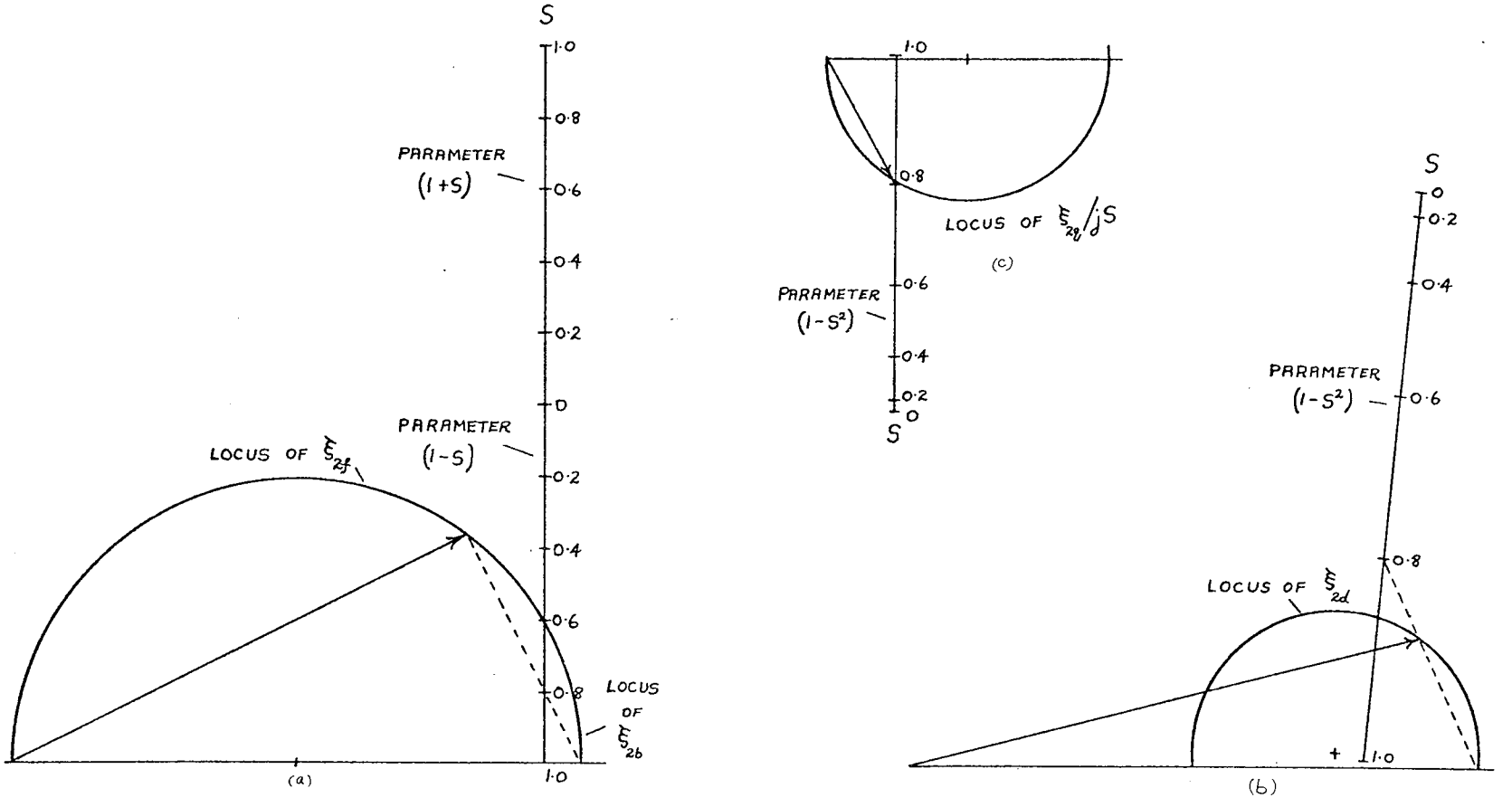

Fig. A2.1 The loci of the functions ξ_{2f}, ξ_{2b}, ξ_{2d}, ξ_{2q}/jS

A2.3 $\underset{\sim}{\xi}_{2q}$

The second function $\underset{\sim}{\xi}_{2q}$ used with the cross-field theory is defined in equation (4.14b) as

$$\underset{\sim}{\xi}_{2q} = -\tfrac{1}{2} j \left(\underset{\sim}{\xi}_{2f} - \underset{\sim}{\xi}_{2b} \right) = \frac{jS}{(2 - j\alpha) + j\frac{1}{\alpha}(1 - S^2)} \qquad \alpha = \frac{R_2}{X_2} \qquad \text{(A2.4)}$$

The locus of the $\underset{\sim}{\xi}_{2q}$ phasor is not circular even though it is a function of the $\underset{\sim}{\xi}_{2f}$ and $\underset{\sim}{\xi}_{2b}$ phasors. Let equation (A2.4) be rewritten

$$\frac{\underset{\sim}{\xi}_{2q}}{jS} = \frac{1}{(2 - j\alpha) + j\frac{1}{\alpha}(1 - S^2)} \qquad \text{(A2.5)}$$

Thus the locus of the modified phasor $\underset{\sim}{\xi}_{2q}/jS$ is circular, and is shown in Fig. A2.1 (c) for $X_2/R_2 = 10$. The radius of the circle is 0.25 and is independent of the value of X_2/R_2.

A2.4 The evaluation of the $\underset{\sim}{\xi}$ functions

In the graphical method, three values of the required function are calculated for - $S = 0,\ 1,\ \infty$, and a circle is constructed to pass through the points. The locus diagram is completed by the addition of the parameter line drawn perpendicular to a line joining the centre of the circle and the infinity point. The use of the diagrams is shown dotted in Fig. A2.1 for the value $S = 0.8$.

The equations may also be used for the direct calculation of particular values; this has been done in Table A2.1 (pps. 168-171) where values of the ξ functions are tabulated for 4 values of the X_2/R_2 ratio over the speed range $0 \leq S \leq 1$.

TABLE A2.1

sheet 1

$X_2/R_2 = 5$

S	ξ_{2f}				ξ_{2b}			
	phase	quad	mod	arg	phase	quad	mod	arg
.00	.9615	.1923	.9806	11.31	.9615	.1923	.9806	11.31
.10	.9529	.2118	.9762	12.53	.9680	.1760	.9839	10.30
.20	.9412	.2353	.9701	14.04	.9730	.1622	.9864	9.462
.30	.9245	.2642	.9615	15.95	.9769	.1503	.9884	8.746
.40	.9000	.3000	.9487	18.43	.9800	.1400	.9899	8.130
.50	.8621	.3448	.9285	21.80	.9825	.1310	.9912	7.595
.60	.8000	.4000	.8944	26.57	.9846	.1231	.9923	7.125
.70	.6923	.4615	.8321	33.69	.9863	.1160	.9932	6.710
.80	.5000	.5000	.7071	45.00	.9878	.1098	.9939	6.340
.85	.3600	.4800	.6000	53.13	.9884	.1069	.9942	6.170
.90	.2000	.4000	.4472	63.43	.9890	.1041	.9945	6.009
.91	.1684	.3742	.4104	65.77	.9892	.1036	.9946	5.978
.92	.1379	.3448	.3714	68.20	.9893	.1030	.9946	5.947
.93	.1091	.3118	.3304	70.71	.9894	.1025	.9947	5.916
.94	.0826	.2752	.2873	73.30	.9895	.1020	.9947	5.886
.95	.0588	.2353	.2425	75.96	.9896	.1015	.9948	5.856
.96	.0385	.1923	.1961	78.69	.9897	.1010	.9948	5.826
.97	.0220	.1467	.1483	81.47	.9898	.1005	.9949	5.797
.98	.0099	.0990	.0995	84.29	.9899	.1000	.9949	5.768
.99	.0025	.0499	.0499	87.14	.9900	.0995	.9950	5.739
1.00	.0000	.0000	.0000	90.00	.9901	.0990	.9950	5.711

S	ξ_{2d}				ξ_{2q}			
	phase	quad	mod	arg	phase	quad	mod	arg
.00	.9615	.1923	.9806	11.31	.0000	.0000	.0000	22.62
.10	.9605	.1939	.9798	11.41	.0179	.0075	.0194	22.83
.20	.9571	.1987	.9775	11.73	.0366	.0159	.0399	23.50
.30	.9507	.2072	.9730	12.30	.0569	.0262	.0627	24.69
.40	.9400	.2200	.9654	13.17	.0800	.0400	.0894	26.57
.50	.9223	.2379	.9525	14.46	.1069	.0602	.1227	29.40
.60	.8923	.2615	.9298	16.34	.1385	.0923	.1664	33.69
.70	.8393	.2888	.8876	18.99	.1727	.1470	.2268	40.40
.80	.7439	.3049	.8040	22.29	.1951	.2439	.3123	51.34
.85	.6742	.2934	.7353	23.52	.1866	.3142	.3654	59.30
.90	.5945	.2521	.6457	22.98	.1479	.3945	.4213	69.44
.91	.5788	.2389	.6261	22.43	.1353	.4104	.4321	71.75
.92	.5636	.2239	.6065	21.67	.1209	.4257	.4425	74.15
.93	.5493	.2072	.5870	20.67	.1046	.4401	.4524	76.63
.94	.5360	.1886	.5682	19.39	.0866	.4535	.4617	79.19
.95	.5242	.1684	.5506	17.81	.0669	.4654	.4702	81.82
.96	.5141	.1466	.5346	15.92	.0457	.4756	.4778	84.52
.97	.5059	.1236	.5208	13.73	.0231	.4839	.4844	87.27
.98	.4999	.0995	.5097	11.26	-.0005	.4900	.4900	90.06
.99	.4962	.0747	.5018	8.559	-.0248	.4938	.4944	92.88
1.00	.4950	.0495	.4975	5.711	-.0495	.4950	.4975	95.71

TABLE A2.1

sheet 2

$X_2/R_2 = 10$

S	ξ_{2f}				ξ_{2b}			
	phase	quad	mod	arg	phase	quad	mod	arg
.00	.9901	.0990	.9950	5.711	.9901	.0990	.9950	5.711
.10	.9878	.1098	.9939	6.340	.9918	.0902	.9959	5.194
.20	.9846	.1231	.9923	7.125	.9931	.0828	.9965	4.764
.30	.9800	.1400	.9899	8.130	.9941	.0765	.9971	4.399
.40	.9730	.1622	.9864	9.462	.9949	.0711	.9975	4.086
.50	.9615	.1923	.9806	11.31	.9956	.0664	.9978	3.814
.60	.9412	.2353	.9701	14.04	.9961	.0623	.9981	3.576
.70	.9000	.3000	.9487	18.43	.9966	.0586	.9983	3.366
.80	.8000	.4000	.8944	26.57	.9969	.0554	.9985	3.180
.85	.6923	.4615	.8321	33.69	.9971	.0539	.9985	3.094
.90	.5000	.5000	.7071	45.00	.9972	.0525	.9986	3.013
.91	.4475	.4972	.6690	48.01	.9973	.0522	.9986	2.997
.92	.3902	.4878	.6247	51.34	.9973	.0519	.9986	2.981
.93	.3289	.4698	.5735	55.01	.9973	.0517	.9987	2.966
.94	.2647	.4412	.5145	59.04	.9974	.0514	.9987	2.951
.95	.2000	.4000	.4472	63.43	.9974	.0511	.9987	2.936
.96	.1379	.3448	.3714	68.20	.9974	.0509	.9987	2.921
.97	.0826	.2752	.2873	73.30	.9974	.0506	.9987	2.906
.98	.0385	.1923	.1961	78.69	.9975	.0504	.9987	2.891
.99	.0099	.0990	.0995	84.29	.9975	.0501	.9987	2.877
1.00	.0000	.0000	.0000	90.00	.9975	.0499	.9988	2.862

S	ξ_{2d}				ξ_{2q}			
	phase	quad	mod	arg	phase	quad	mod	arg
.00	.9901	.0990	.9950	5.711	.0000	.0000	.0000	11.42
.10	.9898	.1000	.9948	5.767	.0098	.0020	.0100	11.53
.20	.9889	.1029	.9942	5.942	.0202	.0042	.0206	11.89
.30	.9871	.1082	.9930	6.258	.0318	.0071	.0325	12.53
.40	.9839	.1166	.9908	6.759	.0455	.0110	.0469	13.55
.50	.9786	.1293	.9871	7.529	.0630	.0170	.0652	15.12
.60	.9686	.1488	.9800	8.732	.0865	.0275	.0908	17.61
.70	.9483	.1793	.9651	10.71	.1207	.0483	.1300	21.80
.80	.8985	.2277	.9269	14.22	.1723	.0985	.1985	29.74
.85	.8447	.2577	.8831	16.97	.2038	.1524	.2545	36.78
.90	.7486	.2762	.7980	20.25	.2238	.2486	.3345	48.01
.91	.7224	.2747	.7729	20.82	.2225	.2749	.3537	51.01
.92	.6938	.2699	.7444	21.26	.2179	.3035	.3737	54.32
.93	.6631	.2607	.7125	21.47	.2091	.3342	.3942	57.97
.94	.6310	.2463	.6774	21.32	.1949	.3663	.4149	61.99
.95	.5987	.2256	.6398	20.65	.1744	.3987	.4352	66.37
.96	.5677	.1979	.6012	19.22	.1470	.4297	.4542	71.12
.97	.5400	.1629	.5640	16.79	.1123	.4574	.4710	76.21
.98	.5180	.1213	.5320	13.18	.0710	.4795	.4847	81.58
.99	.5037	.0746	.5092	8.421	.0244	.4938	.4944	87.17
1.00	.4988	.0249	.4994	2.862	-.0249	.4988	.4994	92.86

TABLE A2.1

sheet 3 $X_2/R_2 = 20$

S	ξ_{2f}				ξ_{2b}			
	phase	quad	mod	arg	phase	quad	mod	arg
.00	.9975	.0499	.9988	2.862	.9975	.0499	.9988	2.862
.10	.9969	.0554	.9985	3.180	.9979	.0454	.9990	2.603
.20	.9961	.0623	.9981	3.576	.9983	.0416	.9991	2.386
.30	.9949	.0711	.9975	4.086	.9985	.0384	.9993	2.203
.40	.9931	.0828	.9965	4.764	.9987	.0357	.9994	2.045
.50	.9901	.0990	.9950	5.711	.9989	.0333	.9994	1.909
.60	.9846	.1231	.9923	7.125	.9990	.0312	.9995	1.790
.70	.9730	.1622	.9864	9.462	.9991	.0294	.9996	1.685
.80	.9412	.2353	.9701	14.04	.9992	.0278	.9996	1.591
.85	.9000	.3000	.9487	18.43	.9993	.0270	.9996	1.548
.90	.8000	.4000	.8944	26.57	.9993	.0263	.9997	1.507
.91	.7642	.4245	.8742	29.05	.9993	.0262	.9997	1.500
.92	.7191	.4494	.8480	32.01	.9993	.0260	.9997	1.492
.93	.6622	.4730	.8137	35.54	.9993	.0259	.9997	1.484
.94	.5902	.4918	.7682	39.81	.9993	.0258	.9997	1.476
.95	.5000	.5000	.7071	45.00	.9993	.0256	.9997	1.469
.96	.3902	.4878	.6247	51.34	.9993	.0255	.9997	1.461
.97	.2647	.4412	.5145	59.04	.9994	.0254	.9997	1.454
.98	.1379	.3448	.3714	68.20	.9994	.0252	.9997	1.447
.99	.0385	.1923	.1961	78.69	.9994	.0251	.9997	1.439
1.00	.0000	.0000	.0000	90.00	.9994	.0250	.9997	1.432

S	ξ_{2d}				ξ_{2q}			
	phase	quad	mod	arg	phase	quad	mod	arg
.00	.9975	.0499	.9988	2.862	.0000	.0000	.0000	5.725
.10	.9974	.0504	.9987	2.891	.0050	.0005	.0050	5.782
.20	.9972	.0519	.9985	2.981	.0103	.0011	.0104	5.962
.30	.9967	.0547	.9982	3.143	.0163	.0018	.0164	6.288
.40	.9959	.0592	.9977	3.403	.0235	.0028	.0237	6.809
.50	.9945	.0662	.9967	3.806	.0329	.0044	.0331	7.620
.60	.9918	.0771	.9948	4.448	.0459	.0072	.0465	8.915
.70	.9861	.0958	.9907	5.548	.0664	.0131	.0677	11.15
.80	.9702	.1315	.9791	7.720	.1038	.0290	.1078	15.63
.85	.9496	.1635	.9636	9.769	.1365	.0496	.1452	19.98
.90	.8997	.2131	.9246	13.33	.1869	.0997	.2118	28.07
.91	.8817	.2253	.9101	14.34	.1992	.1176	.2313	30.55
.92	.8592	.2377	.8915	15.47	.2117	.1401	.2539	33.50
.93	.8307	.2494	.8674	16.71	.2235	.1686	.2800	37.02
.94	.7948	.2588	.8358	18.04	.2330	.2046	.3101	41.28
.95	.7497	.2628	.7944	19.32	.2372	.2497	.3444	46.47
.96	.6948	.2566	.7407	20.27	.2312	.3046	.3823	52.80
.97	.6320	.2333	.6737	20.26	.2079	.3673	.4221	60.49
.98	.5686	.1850	.5980	18.02	.1598	.4307	.4594	69.65
.99	.5189	.1087	.5302	11.83	.0836	.4805	.4877	80.13
1.00	.4997	.0125	.4998	1.432	-.0125	.4997	.4998	91.43

TABLE A2.1

sheet 4 $X_2/R_2 = 40$

S	ξ_{2f}				ξ_{2b}			
	phase	quad	mod	arg	phase	quad	mod	arg
.00	.9994	.0250	.9997	1.432	.9994	.0250	.9997	1.432
.10	.9992	.0278	.9996	1.591	.9995	.0227	.9997	1.302
.20	.9990	.0312	.9995	1.790	.9996	.0208	.9998	1.193
.30	.9987	.0357	.9994	2.045	.9996	.0192	.9998	1.102
.40	.9983	.0416	.9991	2.386	.9997	.0179	.9998	1.023
.50	.9975	.0499	.9988	2.862	.9997	.0167	.9999	.9548
.60	.9961	.0623	.9981	3.576	.9998	.0156	.9999	.8952
.70	.9931	.0828	.9965	4.764	.9998	.0147	.9999	.8425
.80	.9846	.1231	.9923	7.125	.9998	.0139	.9999	.7957
.85	.9730	.1622	.9864	9.462	.9998	.0135	.9999	.7742
.90	.9412	.2353	.9701	14.04	.9998	.0132	.9999	.7538
.91	.9284	.2579	.9635	15.52	.9998	.0131	.9999	.7499
.92	.9110	.2847	.9545	17.35	.9998	.0130	.9999	.7460
.93	.8869	.3167	.9417	19.65	.9998	.0130	.9999	.7421
.94	.8521	.3550	.9231	22.62	.9998	.0129	.9999	.7383
.95	.8000	.4000	.8944	26.57	.9998	.0128	.9999	.7345
.96	.7191	.4494	.8480	32.01	.9998	.0128	.9999	.7308
.97	.5902	.4918	.7682	39.81	.9998	.0127	.9999	.7271
.98	.3902	.4878	.6247	51.34	.9998	.0126	.9999	.7234
.99	.1379	.3448	.3714	68.20	.9998	.0126	.9999	.7198
1.00	.0000	.0000	.0000	90.00	.9998	.0125	.9999	.7162

S	ξ_{2d}				ξ_{2q}			
	phase	quad	mod	arg	phase	quad	mod	arg
.00	.9994	.0250	.9997	1.432	.0000	.0000	.0000	2.867
.10	.9994	.0252	.9997	1.447	.0025	.0001	.0025	2.893
.20	.9993	.0260	.9996	1.492	.0052	.0003	.0052	2.983
.30	.9992	.0274	.9996	1.573	.0082	.0005	.0082	3.147
.40	.9990	.0297	.9994	1.704	.0119	.0007	.0119	3.409
.50	.9986	.0333	.9992	1.908	.0166	.0011	.0166	3.817
.60	.9979	.0389	.9987	2.235	.0233	.0018	.0234	4.472
.70	.9964	.0487	.9976	2.800	.0340	.0033	.0342	5.606
.80	.9922	.0685	.9946	3.948	.0546	.0076	.0551	7.921
.85	.9864	.0878	.9903	5.089	.0743	.0134	.0755	10.24
.90	.9705	.1242	.9784	7.294	.1111	.0293	.1149	14.79
.91	.9641	.1355	.9736	7.999	.1224	.0357	.1275	16.27
.92	.9554	.1489	.9670	8.856	.1358	.0444	.1429	18.10
.93	.9434	.1648	.9576	9.912	.1519	.0565	.1621	20.40
.94	.9260	.1840	.9440	11.24	.1711	.0739	.1863	23.36
.95	.8999	.2064	.9233	12.92	.1936	.0999	.2179	27.30
.96	.8595	.2311	.8900	15.05	.2183	.1404	.2596	32.74
.97	.7950	.2522	.8341	17.60	.2396	.2048	.3152	40.53
.98	.6950	.2502	.7387	19.80	.2376	.3048	.3865	52.06
.99	.5689	.1787	.5963	17.44	.1661	.4310	.4619	68.92
1.00	.4999	.0062	.5000	.7162	-.0062	.4999	.5000	90.72

APPENDIX III

PERFORMANCE CALCULATIONS FOR SELECTED VALUES OF THE PARAMETER RATIOS OF THE MACHINE

Graphs are given in the last 3 chapters of the thesis to illustrate various features in the performance of the machine. These are plotted from the results of calculations which are based on selected values of the parameter ratios; specimen calculations are given in this appendix, and the results of further calculations are summarized in Tables A3.1, A3.2, A3.3.

A3.1 Parameter ratios and values

Fixed ratios: $X_{1d}X_2/X_d^2 = 1.1$, $X_2/X_d = 1.05$; hence $X_{1d}/X_d = 1.048$.

Variable ratios: $X_2/R_2 = 5, 10, 20,$ or 40.

Speed: 1.00, 0.99, ... 0.90, 0.80, 0.70, 0.

In sections A3.2 to A3.5 of this appendix:

(i) $R_{2f} = R_{2b} = R_2$, $X_{2f} = X_{2b} = X_2$, and $X_2/R_2 = 20$.

(ii) $S = 0.96$, and $R_{1d} = 0$.

A3.1.1 Scale factors

The use of parameter ratios leads to 'scale factors' in

many of the calculations:

(i) current, factor V_{1d}/X_{1d} (amps)

(ii) power, factor V_{1d}^2/X_{1d} (watts) (also used for torque)

In this thesis, the scale factors are replaced by unity.

A3.2 Winding currents

The supply voltage is taken as the reference vector, but for convenience, the arguments of the rotor currents are quoted as

$$-180^\circ + \text{(calculated value)}.$$

A3.2.1 Stator current

Using equation (3.14), $I_{1d} = V_{1d} \Big/ \left\{ jX_{1d} \left[1 - \frac{1}{2} \frac{X_d^2}{X_{1d} X_{2f}} \xi_{2f} - \frac{1}{2} \frac{X_d^2}{X_{1d} X_{2b}} \xi_{2b} \right] \right\}$

Substitution for ξ_{2f}, ξ_{2b} from sheet 3, Table A2.1 (p. 170) for S = 0.96, gives

$$I_{1d} = 1.227 - j1.937 = 2.293 \angle -57.65^\circ \quad \text{(amps)} \qquad \text{(A3.1)}$$

$$\text{power factor} = \cos(-57.65^\circ) = 0.535 \ \text{(lag)} \qquad \text{(A3.2)}$$

In tables A3.1, A3.2 the power factor (p.f.) is understood to lag the supply voltage.

A3.2.2 Rotor currents

A3.2.2.1 Rotating-field theory

Using equation (3.13), $\underline{I}^{f}_{2d} = -\frac{X_d}{X_{2f}}\,\underline{\xi}_{2f}\,\underline{I}_{1d}$, and $\underline{I}^{b}_{2d} = -\frac{X_d}{X_{2b}}\,\underline{\xi}_{2b}\,\underline{I}_{1d}$

Substitution for $\underline{\xi}_{2f}$, and I_{1d} (equation (A3.1)) gives

$$I^{f}_{2d} = -1.356 + j0.150 = 1.364\angle -6.31^{\circ} \quad (\text{amps}), \qquad (A3.3)$$

similarly $$I^{b}_{2d} = -1.215 + j1.814 = 2.183\angle -56.19^{\circ} \quad (\text{amps}). \qquad (A3.4)$$

A3.2.2.2 Cross-field theory

Using the inverse of equation (2.21),

$$\underline{I}_{2d} = \tfrac{1}{2}(\underline{I}^{f}_{2d} + \underline{I}^{b}_{2d}), \qquad \underline{I}_{2q} = -\tfrac{1}{2}j(\underline{I}^{f}_{2d} - \underline{I}^{b}_{2d})$$

Substitution for I^{f}_{2d} and I^{b}_{2d} (equations (A3.3), (A3.4)) gives

$$I_{2d} = -1.286 + j0.982 = 1.618\angle -37.38^{\circ} \quad (\text{amps}), \qquad (A3.5)$$

$$I_{2q} = -0.832 + j0.071 = 0.835\angle -4.85^{\circ} \quad (\text{amps}). \qquad (A3.6)$$

A3.3 Power-balance

Power in = $|V_{1d}||I_{1d}| \cos\phi = 1.227$ (watts) (A3.7)

Rotor copper-loss (forward field) $= \frac{1}{2}|\underline{I}^{f}_{2d}|^2 X_{1d} \frac{X_{2f}}{X_{1d}} \frac{R_{2f}}{X_{2f}}$

$= 0.047$ (watts) (A3.8)

Rotor copper-loss (backward field) $= \frac{1}{2}|\underline{I}^{b}_{2d}|^2 X_{1d} \frac{X_{2b}}{X_{1d}} \frac{R_{2b}}{X_{2b}}$

$= 0.120$ (watts) (A3.9)

Total rotor copper-loss = (A3.8)+(A3.9) = 0.167 (watts) (A3.10)

Power out = (A3.7) - (A3.10) = 1.06 (watts) (A3.11)

Efficiency % = 100 x ((A3.11)/(A3.7)) = 86.5 (A3.12)

A3.4 Output/loss ratio

The ratio of power output to rotor copper-loss is used in Appendix IV.

output/loss = (A3.11)/(A3.10) = 6.39 (A3.13)

A3.5 Developed torque

Using equation (3.11):

Forward torque = (A3.8)/(1-S) = 1.166 (watts) (A3.14)

Backward torque = (A3.9)/(1+S) = 0.061 (watts) (A3.15)

Net torque = (A3.14) - (A3.15) = 1.105 (watts) (A3.16)

A3.6 Explanation of the tables

In general, units are omitted from the tables.

A3.6.1 Table A3.1

Values of the terminal conditions and rotor currents are tabulated for 4 values of the ratio X_2/R_2, over the speed range $0.9 \leq S \leq 1.0$. Two sets of values are given for each speed: the first corresponds

to the normal operation and is calculated as shown above; in the second (shown *), skin effect is allowed for by putting $R_{2b} = 2R_{2f}$.

A3.6.2 Table A3.2

The terminal conditions are modified more by skin effect at lower values of speed and this is illustrated in Table A3.2 for 3 values of speed. Although the values chosen are outside the normal operating range, the information is important in an assessment of the overload capacity of the machine. Skin effect is allowed for by putting $R_{2b} = \beta R_{2f}$, where $\beta = 2$ or $(1+S)$. A set of values for $\beta = 1$, is also included for comparison.

A3.6.3 Table A3.3

This table gives values of the stator current obtained when performance calculations for a cage rotor machine are based on the cross-field theory. Two calculations are made for each value of speed: in the first, skin effect is allowed for by putting

$$R_{2b} = (1+S)R_{2f} \quad \text{and} \quad X_2/R_{2f} = \delta \ ;$$

in the second, $R_{2b} = 2R_{2f}$ so that the value of the X_2/R_2 ratio used in the cross-field theory calculation (v. equation (2.20a))

is deduced from

$$\frac{R_2}{X_2} = \frac{1}{2}\left[\frac{R_{2f}}{X_{2f}} + \frac{R_{2b}}{X_{2b}}\right] = \frac{3}{2}\frac{R_{2f}}{X_2} \qquad \text{i.e., } \frac{X_2}{R_2} = 0.6\,\delta \qquad \text{(A3.17)}$$

Different allowances are made for skin effect in order that the currents in each case have circular loci.

TABLE A3.1

sheet 1

$X_2/R_2 = 5$

S	I_{1d}		power in	power out	rotor copper loss	effy %	output /loss ratio	torque
	mod	p.f.						
.90	1.947	.4462	.8690	.4591	.4100	52.83	1.120	.5101
*	1.828	.4998	.9136	.2712	.6425	29.68	.4221	.3013
.91	1.919	.4167	.7994	.4120	.3873	51.55	1.064	.4528
*	1.806	.4720	.8527	.2343	.6184	27.48	.3789	.2575
.92	1.892	.3853	.7291	.3621	.3670	49.66	.9867	.3936
*	1.788	.4424	.7909	.1940	.5969	24.53	.3250	.2109
.93	1.869	.3521	.6582	.3092	.3490	46.97	.8859	.3324
*	1.772	.4111	.7283	.1500	.5783	20.60	.2595	.1613
.94	1.850	.3172	.5867	.2532	.3335	43.16	.7594	.2694
*	1.758	.3781	.6649	.1023	.5625	15.39	.1819	.1089
.95	1.834	.2807	.5147	.1942	.3204	37.74	.6062	.2045
*	1.749	.3435	.6006	.0508	.5499	8.452	.0923	.0534
.96	1.821	.2428	.4422	.1322	.3100	29.89	.4263	.1377
*	1.742	.3075	.5357	-.0048	.5405	-.8936	-.0089	-.0050
.97	1.813	.2037	.3692	.0670	.3023	18.13	.2215	.0690
*	1.740	.2319	.4701	-.0645	.5345	-13.71	-.1206	-.0665
.98	1.808	.1636	.2958	-.0014	.2972	-.4826	-.0048	-.0015
*	1.741	.2319	.4038	-.1284	.5321	-31.79	-.2412	-.1310
.99	1.808	.1228	.2220	-.0730	.2950	-32.89	-.2475	-.0737
*	1.746	.1929	.3368	-.1966	.5335	-58.37	-.3686	-.1986
1.00	1.812	.0816	.1478	-.1478	.2956	-100.0	-.5000	-.1478
*	1.755	.1534	.2693	-.2693	.5387	-100.0	-.5000	-.2693

S	I^f_{2d}		I^b_{2d}		I_{2d}		I_{2q}	
	mod	arg	mod	arg	mod	arg	mod	arg
.90	.8295	-.0621	1.845	-57.49	1.198	-40.52	.7815	5.947
*	.7785	3.424	1.704	-48.12	1.136	-32.55	.6816	15.31
.91	.7498	.3962	1.817	-59.40	1.144	-42.95	.7895	6.374
*	.7060	3.938	1.684	-50.01	1.088	-34.80	.6955	15.77
.92	.6694	.8583	1.793	-61.39	1.093	-45.67	.7975	6.805
*	.6323	4.458	1.667	-51.97	1.042	-37.33	.7093	16.23
.93	.5882	1.324	1.771	-63.47	1.045	-48.72	.8054	7.240
*	.5574	4.984	1.652	-54.02	.9986	-40.18	.7231	16.69
.94	.5062	1.793	1.752	-65.62	1.001	-52.12	.8133	7.679
*	.4812	5.516	1.640	-56.13	.9581	-43.37	.7369	17.17
.95	.4235	2.266	1.737	-67.84	.9615	-55.89	8210	8.122
*	.4039	6.053	1.631	-58.32	.9212	-46.92	.7508	17.65
.96	.3402	2.742	1.726	-70.12	.9272	-60.03	.8287	8.568
*	.3254	6.596	1.626	-60.56	.8888	-50.85	.7646	18.13
.97	.2561	3.221	1.718	-72.45	.8991	-64.52	.8364	9.018
*	.2458	7.146	1.624	-62.85	.8617	-55.14	.7784	18.62
.98	.1714	3.704	1.714	-74.82	.8778	-69.33	.8439	9.472
*	.1650	7.700	1.625	-65.17	.8405	-59.79	.7922	19.12
.99	.0860	4.189	1.713	-77.21	.8642	-74.39	.8513	9.929
*	.0830	8.261	1.630	-67.51	.8263	-64.72	.8059	19.63
1.00	.0000	4.683	1.717	-79.61	.8587	-79.61	.8587	10.39
*	.0000	8.825	1.639	-69.86	.8197	-69.86	.8197	20.14

* including skin effect

TABLE A3.1

sheet 2

$X_2/R_2 = 10$

S	I_{1d} mod	I_{1d} p.f.	power in	power out	rotor copper loss	effy %	output /loss ratio	torque
.90	2.461	.6180	1.521	1.109	.4122	72.90	2.690	1.232
*	2.358	.6475	1.527	.9006	.6263	58.98	1.438	1.001
.91	2.356	.5883	1.386	1.021	.3644	73.70	2.803	1.122
*	2.265	.6185	1.401	.8352	.5655	59.62	1.477	.9178
.92	2.255	.5534	1.248	.9272	.3208	74.29	2.890	1.008
*	2.176	.5844	1.272	.7618	.5098	59.91	1.494	.8280
.93	2.162	.5125	1.108	.8262	.2818	74.57	2.932	.8883
*	2.093	.5444	1.139	.6800	.4594	59.68	1.480	.7312
.94	2.077	.4650	.9655	.7182	.2474	74.38	2.903	.7640
*	2.017	.4980	1.005	.5896	.4149	58.69	1.421	.6272
.95	2.001	.4103	.8211	.6032	.2179	73.46	2.768	.6349
*	1.950	.4446	.8671	.4903	.3768	56.55	1.301	.5161
.96	1.937	.3484	.6748	.4812	.1936	71.31	2.485	.5013
*	1.894	.3839	.7272	.3818	.3454	52.51	1.106	.3977
.97	1.886	.2794	.5269	.3523	.1746	66.86	2.017	.3632
*	1.851	.3161	.5851	.2640	.3211	45.11	.8220	.2721
.98	1.850	.2041	.3776	.2164	.1612	57.31	1.343	.2208
*	1.822	.2421	.4410	.1365	.3045	30.95	.4483	.1393
.99	1.830	.1241	.2271	.0737	.1534	32.45	.4804	.0744
*	1.809	.1632	.2951	-.0007	.2959	-.2432	-.0024	-.0007
1.00	1.828	.0414	.0758	-.0758	.1515	-100.0	-.5000	-.0758
*	1.812	.0816	.1478	-.1478	.2956	-100.0	-.5000	-.1478

S	I^f_{2d} mod	I^f_{2d} arg	I^b_{2d} mod	I^b_{2d} arg	I_{2d} mod	I_{2d} arg	I_{2q} mod	I_{2q} arg
.90	1.657	-6.827	2.341	-48.81	1.870	-31.57	.7840	-3.814
*	1.588	-4.645	2.233	-43.64	1.804	-27.56	.7065	1.364
.91	1.501	-5.950	2.240	-50.97	1.734	-33.14	.7934	-2.953
*	1.443	-3.781	2.145	-45.82	1.679	-29.10	.7221	2.197
.92	1.342	-5.062	2.145	-53.42	1.599	-35.15	.8026	-2.081
*	1.295	-2.901	2.061	-48.29	1.555	-31.06	.7377	3.046
.93	1.181	-4.164	2.056	-56.21	1.467	-37.71	.8117	-1.198
*	1.143	-2.006	1.983	-51.10	1.432	-33.55	.7532	3.911
.94	1.018	-3.256	1.975	-59.34	1.340	-40.97	.8206	-.3056
*	.9884	-1.095	1.911	-54.24	1.313	-36.71	.7686	4.791
.95	.8523	-2.339	1.903	-62.84	1.219	-45.13	.8293	.5968
*	.8307	-.1685	1.848	-57.75	1.199	-40.74	.7840	5.688
.96	.6851	-1.412	1.842	-66.69	1.109	-50.40	.8378	1.508
*	.6700	.7727	1.795	-61.60	1.094	-45.85	.7992	6.599
.97	.5162	-.4771	1.794	-70.87	1.013	-56.99	.8461	2.429
*	.5065	1.728	1.754	-65.78	1.002	-52.26	.8143	7.525
.98	.3456	.4662	1.760	-75.33	.9374	-65.04	.8541	3.358
*	.3403	2.698	1.726	-70.22	.9275	-60.12	.8293	8.466
.99	.1735	1.417	1.741	-80.00	.8876	-74.45	.8619	4.294
*	.1714	3.682	1.714	-74.87	.8780	-69.38	.8441	9.421
1.00	.0000	2.372	1.739	-84.76	.8694	-84.76	.8694	5.237
*	.0000	4.683	1.717	-79.61	.8587	-79.61	.8587	10.39

* including skin effect

TABLE A3.1

sheet 3

$X_2/R_2 = 20$

S	I_{1d} mod	I_{1d} p.f.	power in	power out	rotor copper loss	effy %	output /loss ratio	torque
.90	3.760	.7287	2.740	2.162	.5782	78.90	3.738	2.402
*	3.632	.7470	2.713	1.875	.8377	69.12	2.238	2.083
.91	3.506	.7183	2.519	2.026	.4927	80.44	4.111	2.226
*	3.396	.7359	2.499	1.776	.7231	71.07	2.456	1.952
.92	3.251	.7026	2.284	1.871	.4127	81.93	4.534	2.034
*	3.158	.7198	2.273	1.658	.6152	72.94	2.695	1.802
.93	2.997	.6796	2.037	1.698	.3392	83.35	5.005	1.825
*	2.921	.6965	2.034	1.519	.5151	74.68	2.949	1.633
.94	2.749	.6467	1.778	1.505	.2729	84.64	5.512	1.601
*	2.687	.6635	1.783	1.359	.4242	76.21	3.203	1.446
.95	2.512	.6001	1.507	1.292	.2150	85.74	6.011	1.360
*	2.464	.6172	1.521	1.176	.3441	77.37	3.418	1.238
.96	2.293	.5351	1.227	1.061	.1661	86.46	6.388	1.105
*	2.257	.5527	1.247	.9712	.2761	77.86	3.517	1.012
.97	2.104	.4461	.9385	.8114	.1271	86.45	6.382	.8365
*	2.077	.4644	.9648	.7432	.2216	77.03	3.353	.7661
.98	1.955	.3289	.6429	.5441	.0988	84.63	5.508	.5552
*	1.937	.3480	.6742	.4923	.1819	73.02	2.706	.5023
.99	1.861	.1839	.3422	.2605	.0817	76.13	3.190	.2631
*	1.850	.2039	.3772	.2190	.1582	58.06	1.384	.2212
1.00	1.832	.0208	.0381	-.0381	.0762	-100.0	-.5000	-.0381
*	1.828	.0414	.0758	-.0758	.1515	-100.0	-.5000	-.0758

S	I^f_{2d} mod	I^f_{2d} arg	I^b_{2d} mod	I^b_{2d} arg	I_{2d} mod	I_{2d} arg	I_{2q} mod	I_{2q} arg
.90	3.203	-16.66	3.580	-41.72	3.311	-29.90	.7584	-15.15
*	3.094	-15.11	3.454	-38.66	3.205	-27.54	.6910	-12.09
.91	2.919	-15.03	3.338	-42.59	3.039	-29.75	.7724	-13.53
*	2.827	-13.56	3.230	-39.62	2.951	-27.47	.7104	-10.56
.92	2.625	-13.36	3.095	-43.87	2.760	-29.90	.7860	-11.87
*	2.551	-11.96	3.004	-40.98	2.689	-27.68	.7297	-8.979
.93	2.323	-11.65	2.853	-45.70	2.476	-30.48	.7992	-10.17
*	2.263	-10.32	2.778	-42.89	2.421	-28.31	.7487	-7.350
.94	2.011	-9.904	2.617	-48.23	2.188	-31.67	.8118	-8.428
*	1.966	-8.625	2.556	-45.48	2.147	-29.54	.7675	-5.674
.95	1.691	-8.123	2.391	-51.65	1.900	-33.80	.8238	-6.654
*	1.659	-6.889	2.343	-48.95	1.872	-31.68	.7860	-3.953
.96	1.364	-6.310	2.183	-56.19	1.618	-37.38	.8351	-4.849
*	1.343	-5.110	2.147	-53.53	1.600	-35.23	.8040	-2.190
.97	1.031	-4.469	2.003	-62.05	1.350	-43.25	.8457	-3.015
*	1.018	-3.292	1.976	-59.42	1.340	-41.04	.8214	-.3857
.98	.6915	-2.602	1.861	-69.35	1.113	-52.78	.8554	-1.155
*	.6852	-1.436	1.843	-66.74	1.109	-50.44	.8382	1.456
.99	.3475	-.7136	1.772	-77.96	.9395	-67.57	.8642	.7257
*	.3456	.4546	1.760	-75.36	.9374	-65.06	.8542	3.331
1.00	.0000	1.200	1.744	-87.38	.8721	-87.38	.8721	2.624
*	.0000	2.372	1.739	-84.76	.8694	-84.76	.8694	5.237

* including skin effect

TABLE A3.1

sheet 4

$X_2/R_2 = 40$

S	I_{1d} mod	I_{1d} p.f.	power in	power out	rotor copper loss	effy %	output /loss ratio	torque
.90	6.130	.6923	4.243	3.415	.8288	80.47	4.120	3.794
*	5.970	.7099	4.239	3.048	1.191	71.90	2.559	3.386
.91	5.732	.7060	4.047	3.327	.7200	82.21	4.621	3.656
*	5.591	.7218	4.036	2.996	1.040	74.24	2.882	3.292
.92	5.301	.7174	3.803	3.193	.6102	83.95	5.232	3.470
*	5.179	.7315	3.788	2.902	.8869	76.59	3.272	3.154
.93	4.837	.7249	3.507	3.005	.5017	85.69	5.990	3.231
*	4.735	.7375	3.492	2.757	.7352	78.95	3.750	2.964
.94	4.344	.7264	3.155	2.758	.3970	87.42	6.947	2.934
*	4.261	.7376	3.143	2.555	.5883	81.28	4.343	2.718
.95	3.827	.7180	2.748	2.448	.2995	89.10	8.175	2.577
*	3.764	.7281	2.740	2.290	.4505	83.56	5.083	2.411
.96	3.298	.6928	2.285	2.072	.2124	90.70	9.755	2.159
*	3.253	.7022	2.284	1.957	.3268	85.69	5.990	2.039
.97	2.779	.6373	1.771	1.632	.1396	92.12	11.69	1.682
*	2.750	.6464	1.777	1.555	.2224	87.49	6.991	1.603
.98	2.311	.5256	1.215	1.130	.0844	93.06	13.40	1.153
*	2.294	.5349	1.227	1.084	.1428	88.36	7.590	1.106
.99	1.963	.3189	.6260	.5762	.0498	92.04	11.56	.5820
*	1.955	.3288	.6428	.5500	.0928	85.56	5.925	.5555
1.00	1.833	.0104	.0191	-.0191	.0382	-100.0	-.5000	-.0191
*	1.832	.0208	.0381	-.0381	.0762	-100.0	-.5000	-.0381

S	I^f_{2d} mod	I^f_{2d} arg	I^b_{2d} mod	I^b_{2d} arg	I_{2d} mod	I_{2d} arg	I_{2q} mod	I_{2q} arg
.90	5.664	-32.15	5.837	-45.44	5.712	-38.90	.6706	-31.40
*	5.516	-30.74	5.684	-43.26	5.567	-37.09	.6167	-29.23
.91	5.260	-29.56	5.459	-44.34	5.315	-37.09	.6961	-28.81
*	5.130	-28.27	5.323	-42.29	5.188	-35.41	.6452	-26.77
.92	4.819	-26.81	5.048	-43.42	4.882	-35.31	.7215	-26.06
*	4.708	-25.64	4.931	-41.50	4.773	-33.75	.6741	-24.14
.93	4.338	-23.88	4.606	-42.80	4.412	-33.63	.7466	-23.14
*	4.247	-22.83	4.508	-41.00	4.323	-32.19	.7031	-21.35
.94	3.819	-20.79	4.136	-42.68	3.905	-32.18	.7709	-20.06
*	3.746	-19.85	4.057	-41.00	3.836	-30.85	.7320	-18.38
.95	3.260	-17.54	3.644	-43.37	3.365	-31.19	.7939	-16.81
*	3.206	-16.70	3.583	-41.80	3.314	-29.96	.7602	-15.24
.96	2.663	-14.14	3.140	-45.42	2.795	-31.10	.8152	-13.41
*	2.627	-13.39	3.097	-43.94	2.762	-29.95	.7872	-11.93
.97	2.033	-10.60	2.647	-49.68	2.208	-32.80	.8343	-9.875
*	2.012	-9.925	2.618	-48.28	2.189	-31.71	.8124	-8.471
.98	1.375	-6.949	2.201	-57.57	1.626	-38.49	.8505	-6.225
*	1.365	-6.323	2.184	-56.22	1.618	-37.40	.8354	-4.876
.99	.6943	-3.206	1.869	-70.68	1.115	-53.97	.8635	-2.486
*	.6915	-2.608	1.861	-69.37	1.113	-52.79	.8555	-1.169
1.00	.0000	.6000	1.746	-88.69	.8728	-88.69	.8728	1.313
*	.0000	1.200	1.744	-87.38	.8721	-87.38	.8721	2.624

* including skin effect

TABLE A3.2

Terminal conditions at 3 values of speed in the region of pull-out, showing the modifications due to skin effect.

	X_2/R_{2f}	20			40		
	β	S			S		
		.90	.80	.70	.90	.80	.70
Stator current	1	3.760	5.953	7.390	6.130	8.614	9.611
	2	3.632	5.623	6.893	5.970	8.347	9.318
	(1+S)	3.645	5.688	7.041	5.986	8.401	9.409
Power factor	1	.7287	.7118	.6434	.6923	.5363	.4258
	2	.7470	.7429	.6918	.7099	.5723	.4750
	(1+S)	.7453	.7373	.6786	.7082	.5654	.4608
Power in	1	2.740	4.237	4.755	4.243	4.619	4.092
	2	2.713	4.177	4.768	4.239	4.776	4.426
	(1+S)	2.716	4.193	4.778	4.240	4.750	4.335
Power out	1	2.162	2.674	2.307	3.415	2.946	2.000
	2	1.875	2.068	1.565	3.048	2.415	1.475
	(1+S)	1.902	2.181	1.771	3.083	2.517	1.627
Efficiency %	1	78.90	63.12	48.52	80.47	63.78	48.88
	2	69.12	49.51	32.83	71.90	50.56	33.31
	(1+S)	70.04	52.02	37.07	72.72	53.00	37.54
Torque	1	2.402	3.343	3.296	3.794	3.683	2.858
	2	2.083	2.585	2.236	3.386	3.018	2.107
	(1+S)	2.114	2.727	2.530	3.426	3.147	2.325

notation:- $R_{2b} = \beta R_{2f}$, where β is equal to 1, 2, or (1+S)

TABLE A3.3

Values of stator current appropriate to Fig. 5.9 (p. 139)

$\lvert I_{1d} \rvert$							
		S					
X_2/R_{2f}		1.00	.95	.90	.80	.70	0
5	(a)	1.755	1.753	1.840	2.173	2.582	4.642
	(b)	1.787	1.780	1.814	1.980	2.218	3.331
10	(a)	1.812	1.953	2.369	3.407	4.355	7.436
	(b)	1.821	1.883	2.099	2.754	3.461	5.765
20	(a)	1.828	2.466	3.645	5.688	7.041	9.650
	(b)	1.830	2.148	2.876	4.465	5.757	8.509
40	(a)	1.832	3.767	5.986	8.401	9.409	10.61
	(b)	1.833	2.931	4.626	7.111	8.458	10.18

phase angle°							
		S					
X_2/R_{2f}		1.00	.95	.90	.80	.70	0
5	(a)	-81.17	-70.08	-60.30	-46.85	-39.87	-35.75
	(b)	-83.15	-75.36	-68.01	-55.85	-47.41	-33.56
10	(a)	-85.32	-63.71	-49.84	-39.40	-37.84	-47.98
	(b)	-86.46	-71.20	-58.99	-45.21	-39.90	-39.75
20	(a)	-87.62	-51.95	-41.82	-42.50	-47.27	-64.05
	(b)	-88.21	-60.78	-47.23	-41.27	-43.03	-54.77
40	(a)	-88.81	-43.31	-44.91	-55.57	-62.56	-76.06
	(b)	-89.11	-48.30	-42.89	-49.25	-56.09	-69.73

notation:- (a) rotating-field theory, $R_{2b} = (1+S)R_{2f}$, $X_2/R_{2f} = \delta$

(b) cross-field theory, $R_{2b} = R_{2f}$, $X_2/R_2 = 0.6^{\circ}\delta$

APPENDIX IV

THE ROTOR COPPER-LOSS

The rotor winding copper-loss of a two-phase machine can be determined from the output provided that the speed is known. In the single-phase machine, however, it is also necessary to know the value of the X_2/R_2 ratio.

Let $\propto$ = (rotor output)/(rotor copper-loss)

Then
$$\propto = \left[|I_{2d}^{f}|^2 \left(\frac{S}{1-S}\right) R_{2f} - |I_{2d}^{b}|^2 \left(\frac{S}{1+S}\right) R_{2b} \right] \Big/ \left[|I_{2d}^{f}|^2 R_{2f} + |I_{2d}^{b}|^2 R_{2b} \right]$$

$$= \left[|\xi_{2f}|^2 \left(\frac{S}{1-S}\right) \frac{R_{2f}}{X_2} - |\xi_{2b}|^2 \left(\frac{S}{1+S}\right) \frac{R_{2b}}{X_2} \right] \Big/ \left[|\xi_{2f}|^2 \frac{R_{2f}}{X_2} + |\xi_{2b}|^2 \frac{R_{2b}}{X_2} \right]$$

$$= \frac{1}{1+K} \quad \frac{S}{1-S} \qquad \text{(A4.1)}$$

.. where $K = \frac{2}{1-S} \quad \frac{1}{\beta - 1}$ and $\beta = \mathcal{I}_m \xi_{2f} \Big/ \mathcal{I}_m \xi_{2b}$.

The factor K is a function of the speed and the reactance/resistance ratios of the rotor. If K were zero then equation (A4.1) would represent the value of $\propto$ for a two-phase machine.

A4.1 The wound rotor machine

When skin effect is neglected so that $R_{2b} = R_{2f} = R_2$, equation (A4.1) can be simplified to

$$\propto = \frac{1}{1+K_1} \quad \frac{S^2}{1-S^2} \qquad \text{where} \quad K_1 = 2 \Big/ \left\{ (1-S^2) \left[(1-S^2) \left(\frac{X_2}{R_2}\right)^2 - 1 \right] \right\} .$$

Curves are given in Fig. A4.1 (overleaf), for the variation of $\propto$ over the limited speed range $0.9 \leqslant S \leqslant 1.0$ for 4 values of the ratio X_2/R_2. The values of $\propto$ are tabulated in Table A3.1 (Appendix III). Similar curves for a wider range of values of X_2/R_2 are given by Veinott [1].

(1) The curves are similar in form to both the torque/speed and the power output/speed characteristics; in particular, the ratio $\propto$ is zero at a speed corresponding with the no-load speed of the motor.

(2) At synchronous speed, $\propto = -\frac{1}{2}$ for all finite values of X_2/R_2.

(3) In the limit as $X_2/R_2 \rightarrow \infty$, $\propto \rightarrow S^2/(1-S^2)$.

This represents the maximum theoretical value of $\propto$ for the single-phase machine. In the absence of all losses except the rotor copper-loss, the per-unit efficiency is $\propto/(1+\propto)$ - in a two-phase machine this is equal to S, while for a single-phase machine the maximum attainable value is S^2: e.g., at a full-load speed of 0.96, the efficiencies of the respective machines are 96% and 92%. In other words the single-phase induction motor is inherently less efficient than the two-phase machine. This is because each phase of the two-phase machine contributes both to the rotor copper-loss and to the output, whereas in the single-phase machine the

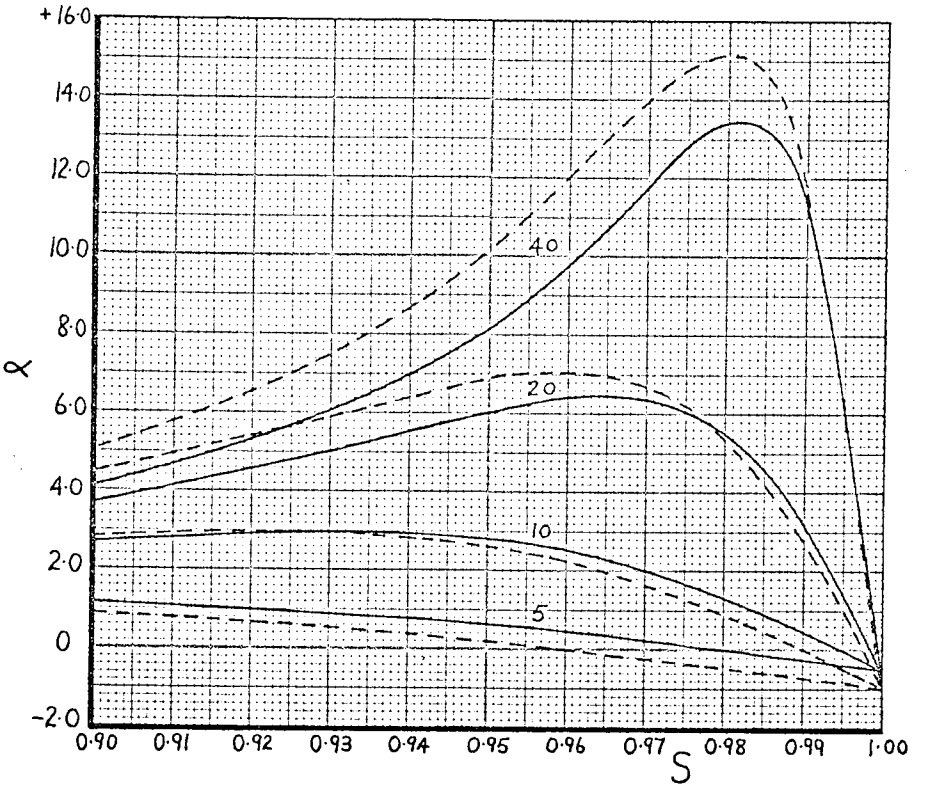

——————— $R_{2f} = R_{2b} = R_2$

- - - - - - $R_{2f} = R_2$

$R_{2b} = 2R_2$

(scale x $\frac{1}{2}$, i.e., $-1 \leqslant \alpha \leqslant +8$)

Fig. A4.1 The variation of the output/loss ratio for 4 values of X_2/R_2

output is obtained from one phase which also supplies the losses in two rotor axes.

A4.2 The cage rotor machine

When skin effect is considered, the general expression for $\propto$ (equation (A4.1)) cannot be simplified. However if tables of the ξ functions are available, the computation presents little difficulty. Curves are included on Fig. A4.1 (p. 186) to illustrate the manner in which $\propto$ is modified by skin effect ($R_{2b} = 2R_{2f}$) and the corresponding values are given in Table A3.1 (Appendix III).

(1) The form of the curves is not modified by skin effect, although the magnitudes for given values of speed and the no-load speed are reduced.

(2) At synchronous speed $\propto = -\frac{1}{2}$. Exactly the same result is obtained with the wound rotor machine, because at this speed the forward rotor current I^{f}_{2d} is zero and half of the rotor copper-loss is supplied as reconverted mechanical energy.

(3) For a given value of speed in the normal operating range: the increase in the backward resistance due to skin effect causes

an increase in the net rotor copper-loss (there is a slight decrease in the forward rotor copper-loss), and a decrease in the power output; the power input is only slightly affected and typical values of $\propto$ are approximately half those for a similar wound rotor machine.

Let $X_2/R_2 \rightarrow \infty$, then $|\xi_{2f}| = 1$, $|\xi_{2b}| = 1$ ($0.9 \leq S \leq 1.0$),

and $$\propto(s) = \left[1 - \frac{1}{3S}\right] \frac{S^2}{1 - S^2}$$

For the same conditions without skin effect $\propto = \frac{S^2}{1 - S^2}$

Hence $\frac{\propto(s)}{\propto} = \left[1 - \frac{1}{3S}\right]$ i.e., for $S = 0.96$, $\frac{\propto(s)}{\propto} = 0.6875$.

Therefore skin effect tends to reduce the maximum attainable efficiency still further; for the example given above, the efficiency would be reduced to 89%.

LIST OF

ABBREVIATIONS AND SYMBOLS

A	velocity coefficient of friction	eqn. (2. 5) *
e_{2a}, e_{2b}	rotor induced e.m.f.'s	eqn. (3. 1)
e^{+}_{2a}, e^{-}_{2a}	rotor induced e.m.f.'s	eqn. (3. 2)
e^{f}_{2d}, e^{b}_{2d}	rotor induced e.m.f.'s	eqn. (3. 3)
e_{2d}	rotor induced e.m.f.	eqn. (4. 5)
e_{2q}	rotor induced e.m.f.	eqn. (4. 6)
$E^{t}_{n}, E^{tm}_{n}, E^{r}_{n}, E^{rm}_{n}$	e.m.f. phasors (n = 1d, 2d, 2q)	p. 97 note
f	line frequency	
f_{1d}, F_{1d}	stator m.m.f.	eqn. (3. 4)
f_{2d}, f_{2q}	rotor m.m.f.'s	fig. 5. 1
F_{2d}, F_{2q}	rotor m.m.f.'s	fig. 4. 1
F^{f}_{2d}, F^{b}_{2d}	rotor m.m.f.'s	eqn. (5. 1)
F_{d}, F_{q}	d, q axis resultant m.m.f.'s	p. 89
F_{f}, F_{b}, F_{m}	resultant m.m.f.'s	fig. 5. 1
i_{1d}, I_{1d}	stator current	fig. 2. 1
I^{f}_{1d}, I^{b}_{1d}	stator currents	p. 62
I^{nl}_{1d}	stator current, no-load value	eqn. (4. 18)

---

* suitable definition or illustrated use

I_{1d}^{nL} (mag.)	stator current, no-load value	eqn. (4.19)
i_{2a}, i_{2b}	rotor currents	fig. 2.1
$i_{2af}, i_{2ab}, i_{2bf}, i_{2bb}$	component rotor currents	eqn. (2.1)
$i_{2df}, i_{2db}, i_{2qf}, i_{2qb}$	rotor currents	eqn. (2.10)
$I_{2df}, I_{2db}, I_{2qf}, I_{2qb}$	rotor currents	eqn. (2.12a)
I_{2d}^{f}, I_{2d}^{b}	rotor currents	eqn. (2.14)
I_{2d}, I_{2q}	rotor currents	eqn. (2.18)
J	moment of inertia	eqn. (2.4)
L_{1d}	stator winding inductance	fig. 2.1
L_2	rotor winding inductance	p. 38
L_{2a}, L_{2b}	rotor winding inductances	fig. 2.1
$L_{2af}, L_{2ab}, L_{2bf}, L_{2bb}$	rotor winding inductances	eqn. (2.4)
L_{2f}, L_{2b}	rotor winding inductances	eqn. (2.7a)
M_d	mutual inductance, stator/rotor	eqn. (2.4)
p	d/dt operator	
p.f.	power factor	
R	total effective motor resistance	eqn. (4.16)
R	resistance, d.c. value	p. 161
R_{ac}	resistance, apparent value	p. 160
R_d, R_{df}, R_{db}	iron loss 'resistors'	fig. 5.6
R_{1d}	stator winding resistance	fig. 2.1

R_2	rotor winding resistance	p. 38
R_{2a}, R_{2b}	rotor winding resistances	fig. 2.1
R_{2af}, R_{2ab} R_{2bf}, R_{2bb}	rotor winding resistances	eqn. (2.5)
R_{2f}, R_{2b}	rotor winding resistances	eqn. (2.7a)
S	per-unit speed (synchronous: S=1)	
S_o, S^{nL}	per-unit speed, no-load value	eqn. (4.17)
t	time	
T_E	developed torque	eqn. (2.12a)
T_L	load torque	eqn. (2.7b)
T_f, T_b	component developed torques	sec. 3.6.2
X	total motor reactance	eqn. (4.16)
X	reactance, neglecting skin effect	p. 161
X_{ac}	apparent cross-slot reactance	p. 160
X_d	mutual reactance, stator/rotor	eqn. (2.12a)
$X_{n\ell}$	leakage component of X_n (n = 1d, 2, 2f, 2b)	fig. 3.4 fig. 4.6
X_2	rotor winding reactance	eqn. (2.22)
X_{2f}, X_{2b}	rotor winding reactances	eqn. (2.12a)
v_{1d}, V_{1d}	supply voltage	fig. 2.1
V^f_{1d}, V^b_{1d}	'supply' voltages	fig. 3.4
V^f_{2d}, V^b_{2d}	rotor voltages	eqn. (2.14)

V_{2d}, V_{2q}	rotor voltages	eqn. (2.19b)
Z'_{2f}, Z'_{2b}	rotor impedances	eqn. (2.20a)

α	rotor output/loss ratio	p. 151
α	rotor resistance/reactance ratio	p. 164
Δ	value of a determinant	eqn. (3.12) eqn. (4.12)
$\epsilon, \epsilon_p, \epsilon_q, \epsilon_f, \epsilon_b$	differences due to skin effect	p. 75, p. 145
η	efficiency	
θ	rotor angular position	fig. 2.1
$\dot{\theta}$	rotor angular velocity	fig. 2.1
ξ_n	Xi functions, (n=2f, 2b, 2d, 2q)	App. II
ϕ, ϕ_l	phase angles	p. 47
ϕ_f, ϕ_b	phase angles	fig. 3.6

REFERENCES

CHAPTER I

1 Heyland, A.: 'Theory and calculations of asynchronous alternate current motors, Pt. II ', Electrician 1896, 36, p. 753.

2 Thompson, S. P.: Polyphase electric currents (Spon, 1900), p. 440.

Arno, G.: 'A simple method of starting alternating single-phase induction motors', Electl, Rev. Lond., 1897, 41, p. 753.

3 Brown, C. E. L.: correspondence, Electrician 1891, 28, p. 698.

Brown, C. E. L.: 'Non-synchronous motor for ordinary alternate currents', Electrician 1893, 30, p. 358.

Boyd, A.: 'The starting of the Heyland single-phase induction motor', Electrician 1904, 53, p. 912.

Lauper, F. A.: 'The starting of single-phase induction motors', Proc. Instn, elect. Engrs, 1927, 65, p. 160.

4 Hobart, H. M.: Electric motors (Whittaker, 1910), p. 605.

5 'The Langdon-Davies alternate current motor', Electrician 1896, 37, p. 247.

Weber, C. A. M.: 'Winding small single-phase induction motors', Elect. (Cl.) J., 1917, 14, p. 189, and 1924, 21, p. 377.

Dellenbaugh, F. S.: 'Split-phase motor starting switches', Elect. (Cl.) J., 1917, 14, p. 198.

6 Saunders, N. F. T.: 'The design of fractional horse-power induction motors', J. Instn, elect. Engrs, 1939, 85, p. 161. (Based on the Steinmetz form of the cross-field theory - M. J. J.)

Kuhlmann, J. H.: Design of electrical apparatus (Wiley, 3rd., Ed. 1957), p. 356.

7 Behrend, B. A.: The induction motor (McGraw Hill, 1921), p. 211.

8 Lamme, B. G.: Electrical engineering papers (Westinghouse, 1919), pps. 554, 556.

9 Maccall, W. T.: Alternating current electrical engineering (University tutorial press, 1924), p. 286.

10 Veinott, C. G.: 'Segregation of losses in single-phase induction motors', Trans. Amer. Inst. elect. Engrs, 1935, 54, p. 1302.

11 Behrend, B. A.: op. cit., p. 204.

Suhr, F. W.: 'Symmetrical components as applied to the single-phase induction motor', Trans. Amer. Inst. elect. Engrs, 1945, 64, p. 651.

Dooley, H.: 'An analysis of the single-phase induction motor by symmetrical-components', Thesis M. Sc(Eng.), Nottingham University 1951.

12 Arnold, E., and LaCour, J. L.: Die wechselstromtechnik, Vol. 5 Pt. I (Die induktionsmaschinen), (Springer, 1909), p. 152.

Karapetoff, V.: 'On the equivalence of the two theories of the single-phase induction motor', J. Amer. Inst. elect. Engrs, 1921, 40, p. 640.

Bretch, E.: 'The Steinmetz conception of the single-phase squirrel-cage motor', Trans. Amer. Inst. elect. Engrs, 1958, 77(III), p. 1041.

Alger, P. L.: 'The dilemma of single-phase induction motor theory', Trans. Amer. Inst. elect. Engrs, 1958, 77(III), p. 1045.

13 Ingram, W. H.: 'The dynamical theory of alternating current machinery and the problem of stability of power systems', J. Franklin Inst., 1930, 210, p. 327.

Kron, G.: 'Non-Riemannian dynamics of rotating electric machinery', J. Math. Phys., 1934, 13, p. 103.

14 Kron, G.: Tensors for circuits (Dover, 1959), p. 118.

15 Ferraris, G.:'A method for the treatment of rotating or alternating vectors', Electrician 1894, 33, pps 152, 184.

16 Thomälen, A.:Electrical engineering (Arnold, 1920), p. 429.

17 Weber, C. A. M.:'Interpretation of test data', Elect. (Cl.) J., 1916, 13, p. 381.

18 Liu, C.:'Rotor currents and rotor copper-losses in a single-phase squirrel cage induction motor', Thesis M. Sc., Birmingham University 1948.

19 Alger, P. L.:The nature of induction machines (Gordon and Breach, 1965), p. 265.

CHAPTER II

1 Wells, D. A.:'Application of the Lagrange equation to electric circuits', J. appl. Phys., 1938, 9, p. 312.

Gibbs, W. J.:'Limitations of Lagrangian methods in electrical machine theory', B. T. H. Technical Monograph, TMS 754.

2 Kron, G.:Tensors for circuits (Dover, 1959), p. 67.

3 Kron, G.:The application of tensors to the analysis of rotating electrical machinery (G. E. Rev., 1942), p. 201.

CHAPTER III

1 Adkins, B.:The general theory of electrical machines (Chapman and Hall, 1959), p. 14.

2 Bretch, E.:(discussion), Trans. Amer. Inst. elect. Engrs, 1954, 73(III), p. 292.

3 Andronow, A., and Chaikin, S.: Theory of oscillations (Princeton, 1949), Ch. 4.

4 Puchstein, A. F., Lloyd, T. C., and Conrad, A. G.: Alternating current machines (Wiley, 3rd., Ed., 1960), p. 367.

CHAPTER IV

1 Jevons, M.: 'The dependence diagram - a teaching aid in the presentation of electrical machine theory', Quart. J. Tensor Soc., 1964, 14, p. 116.
(This paper is bound in at the end of the thesis.)

2 Beach, R.: 'A physical conception of single-phase induction motor operation', Elect. Engng, N.Y., 1944, 63, p. 254.

3 Puchstein, A. F., and Lloyd, T. C.: 'Single-phase induction motor performance', Elect. Engng, N.Y., 1937, 56, p. 1277.

CHAPTER V

1 Button, C. T.: 'Single-phase motor theory - a correlation of the cross-field and revolving-field concepts', Trans. Amer. Inst. elect. Engrs, 1941, 60, p. 507.

2 Lamb, H.: Infinitesimal calculus (Cambridge 3rd., Ed., 1919) p. 305.

3 Veinott, C. G.: v. reference 10, Chapter I .

APPENDIX IV

1 Veinott, C.G.: v. reference 10, Chapter I.

ACKNOWLEDGEMENTS

The author acknowledges with gratitude the advice and encouragement given by

Dr. E. J. Davies,

Reader in electrical engineering (heavy current) at the University and supervisor of this research.

The author also aknowledges with gratitude the painstaking care exercised by

Mr. J. T. Whittle,

of the University library, in the production of Xerox copies of the thesis.

REPRINTS OF THE AUTHOR'S PAPERS

1 'The dependence diagram - A teaching aid in the presentation of electrical machine theory',

Quart. J. Tensor Soc., 1964, 14, p.116.

2 'A versatile resistance-network analogue',

Int. J. elect. Engng, Educ., 1966, 4, p. --.
(To be published)

3 British Patent Specification 1,035,113 'Electrical Machines' Published July 1966

(This describes the use of an electrical machine as a relaxation oscillator)

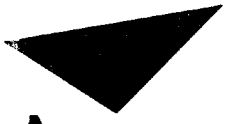

Aston University